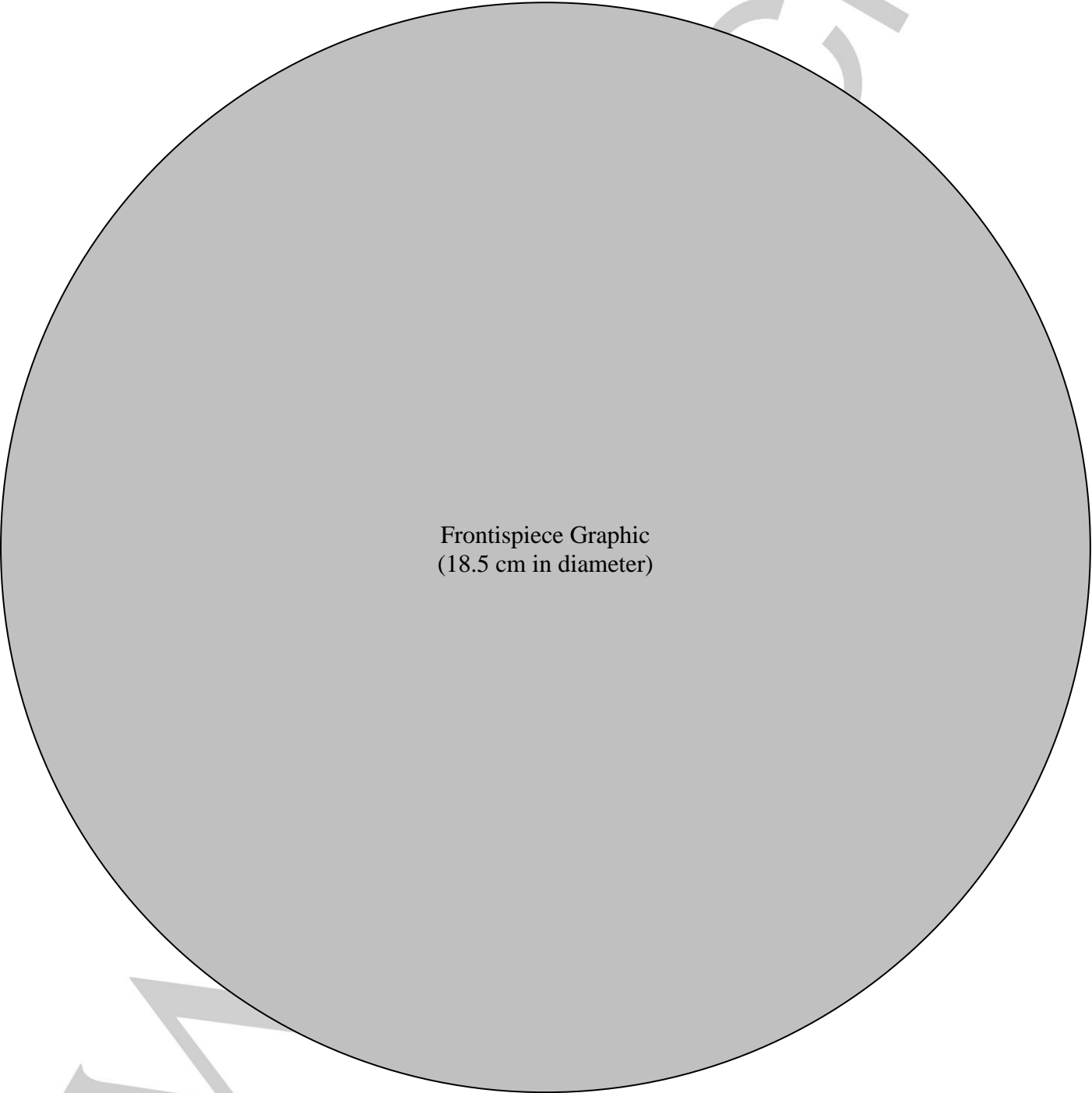# State of the art and perspectives of hierarchical zeolites: practical overview of synthesis methods and use in catalysis

Dorien Kerstens,[a] Brent Smeyers,[a] Jonathan Van Waeyenberg,[a] Qiang Zhang,[b] Jihong Yu,[b] and Bert F. Sels*[a]

Frontispiece Graphic
(18.5 cm in diameter)

[a]   D. Kerstens, B. Smeyers, J. Van Waeyenberg and prof. dr. B. F. Sels
       Centre for Sustainable Catalysis and Engineering
       KU Leuven
       Celestijnenlaan 200f, 3001 Leuven
       E-mail: bert.sels@kuleuven.be
[b]   Dr. Q. Zhang and Prof. J. Yu
       State Key Laboratory of Inorganic Synthesis and Preparative Chemistry
       College of Chemistry
       International Centre of Future Science
       Jilin University
       Changchun 130012, P. R. China

       Supporting information for this article is given via a link at the end of the document.

Abstract: Microporous zeolites have proven to be of great importance in many chemical processes. Yet, they often suffer from diffusion limitations causing inefficient use of the available catalytically active sites. To address this problem, hierarchical zeolites have been developed which extensively improve the catalytic performance. There is a multitude of recent literature describing synthesis of and catalysis with these hierarchical zeolites. This review attempts to organize and overview this literature (of the last 5 years), with emphasis on the most important advances with regard to synthesis and application of such zeolites. Special attention is paid to the most common and important 10- and 12-membered ring zeolites (MTT, TON, FER, MFI, MOR, FAU and *BEA). In contrast to previous reviews, this review brings together and discusses the research per zeolite topology. This allows the reader to instantly find the best synthesis method in accordance to the desired zeolite properties. A summarizing graph is made available to enable the reader to select suitable synthesis procedures based on zeolite acidity and mesoporosity, the two most important tunable properties.

1.   Introduction

Bert F. Sels (1972), currently full professor at KU Leuven, obtained his PhD in 2000 in the field of heterogeneous oxidation catalysis. He was director of the Centre for Surface Chemistry and Catalysis (COK, 2015-2018), and started in 2019 at KU Leuven a new division called 'Centre for Sustainable Catalysis and Engineering, CSCE'. His research activities encompass the design of heterogeneous catalysts for the future challenges in industrial organic and environmental catalysis. His expertise includes heterogeneous catalysis in biorefineries and biofactories, design of hierarchically structured materials such as zeolites and carbons for catalysis, and identification of catalytically active sites for small molecule activation using spectroscopy and kinetics.

Zeolites are highly crystalline aluminosilicates with well-defined pores that are constructed of SiO_2 and AlO_4 tetrahedra. These tetrahedra can be linked together in different unique ways to form various materials with a specific topology.[1] According to the International Zeolite Association (IZA), more than 250 different topologies, which are all assigned with a three-letter code, have been identified.[2] The micropores in zeolites are typically constructed from 8, 10 or 12 tetrahedral atoms (T-atoms) and form rings with pore sizes less than 2 nm in diameter. According to their pore size, they can be classified into small-, medium- and large pore zeolites.[3] Zeolites can be found in nature or can be synthesized either industrially or on lab-scale. Large-scale production of synthetic zeolites began in the 1950s, when the use and discovery of new zeolites revolutionized the petrochemical and chemical industries. Zeolites are used in many heterogeneous catalytic applications such as catalytic cracking, alkylations and isomerizations, thanks to their unique properties such as the presence of strong acid sites, large specific areas, high ion exchange capacities (with the ability to introduce strong acid sites), and moderate to high thermal and hydrothermal stability (with different impacts of gaseous steam and condensed hot liquid water).[4] Moreover, because of the presence of micropores, zeolites possess the ability to be shape selective on the level of (I) the reactant, (II) the transition state, and (III) the product, meaning that zeolites can act as very selective catalysts in chemical reactions.[5,6]

Despite their numerous advantages and contributions to chemical processes, zeolites also have limitations. The major problem is the inaccessibility of active sites when the reactants have similar or larger dimensions than the micropores, causing diffusion limitations. Consequently, a rapid drop of molecular diffusivity in the zeolite occurs from "intercrystalline" (i.e. diffusion of molecules outside the catalyst) to "Knudsen" (i.e. diffusion dominant in mesopores) to "configurational" (i.e. diffusion in micropores). The slow transport of molecules in the zeolite crystal particularly advantaging shape selectivity (I) and (III), may also facilitate (usually unwanted) secondary reactions, which can result in lower selectivity and the formation of coke precursors leading to micropore blocking and subsequent deactivation of the catalyst. In addition, diffusion limitation causes a poor use of the zeolite crystal since only the outer shell is effectively used and the interior remains largely catalytically inactive.[6,7]
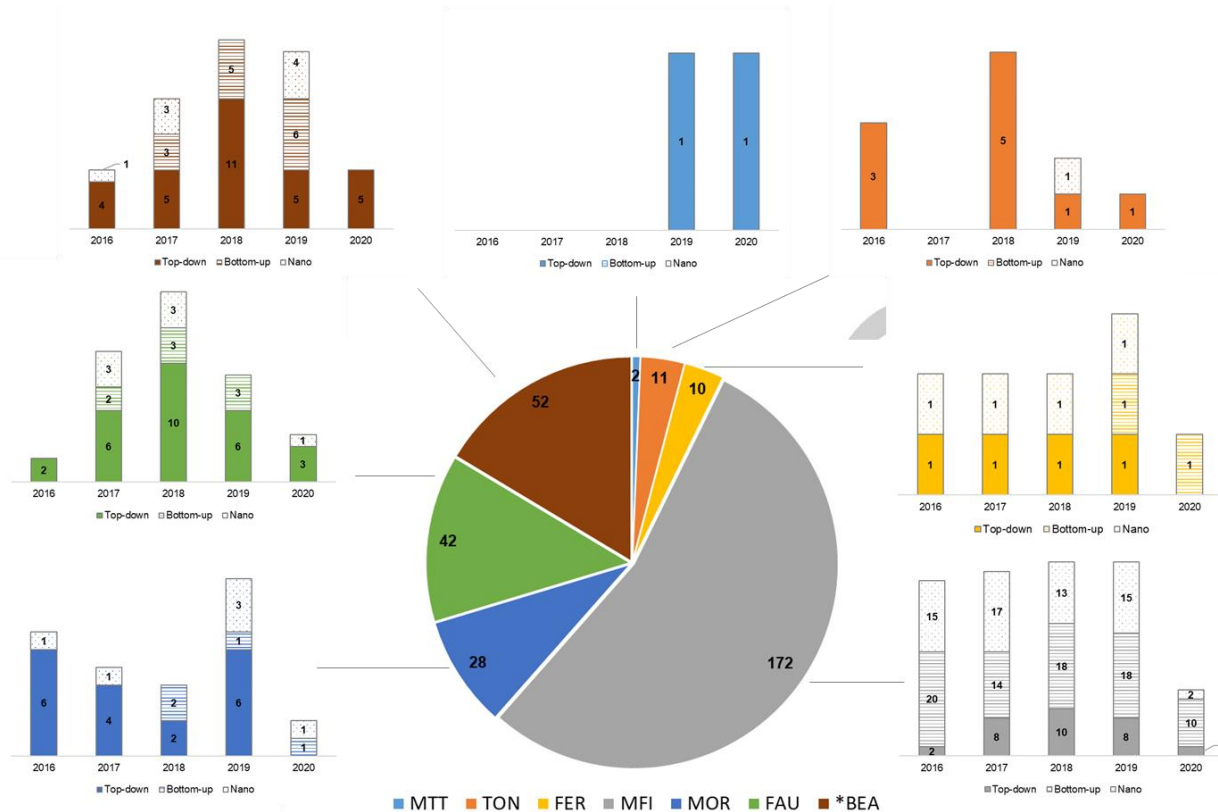
Figure 1. Overview of the amount of new open publications per year since 2016 regarding new hierarchization synthesis techniques for zeolites that were taken into account for this review. A distinction is made between the different papers based on the topology and the hierarchization procedure used.

In order to alleviate these problems, different strategies have been elaborated. A first strategy is the development of "ordered mesoporous materials". Typical structures are MCM-41, HMS, KIT and SBA among others.[8] These materials have attracted research interest for their use as solid acid catalysts and adsorbents. However, their structure is amorphous, which causes them to have a lower hydrothermal stability, and generally a lower acidity, and as such all this limits their applications. A second strategy is the synthesis of zeolites with larger pore sizes (> 12-membered rings). Such extra-large pore zeolites have been made using complex organic compounds as structure-directing agents (SDA's) and germanium as framework atoms. Unfortunately, these materials show lower acidity, high production costs and poor (hydro)thermal stabilities.[9] A third strategy is reducing the crystal size to a nanometer scale. While making nanozeolites, the external surface area increases rapidly and the diffusion path is significantly reduced. As such, nanozeolites provide an effective way to improve the diffusion rate of molecules and the conversion of bulky molecules. Despite these promising properties, nanozeolites have some drawbacks such as a difficult separation from the reaction products and more tedious synthesis protocols.[10]

Another strategy to alleviate these problems is the production of hierarchical zeolites. Hierarchical zeolites refer to zeolites with an additional porous network on top of and interconnecting with the micropores, which can be mesoporous (2-50 nm) and/or macroporous (> 50 nm). These additional pore networks increase the diffusivity and may be formed in the crystal (i.e. intracrystalline porosity) or between crystal particles (i.e. intercrystalline porosity).[7,11] Different strategies have been developed to obtain hierarchical zeolites, and they can be divided into three main groups: (I) top-down strategies, (II) bottom-up strategies, and (III) assembly of nanozeolites. More details about these strategies will be given in the next section.

Ample studies have shown that the use of hierarchical zeolites can result in improved catalytic performances. An example can be found in a study from Venkatesha et al., where a hierarchical *BEA zeolite was synthesized after dealumination with phenoldisulfonic acid (PDSA), and tested for the condensation of glycerol with acetone. It was shown that an increase in pore volume could rise the dioxalane selectivity up to 100 %. Herein, the influence of the acidity was cancelled out by employing the so called "volume space acidity". The improved performance of the hierarchical zeolite could thus be attributed to the increase in pore volume.[12] The creation of hierarchical zeolites, however, can influence other characteristics of the crystal as well. One of the most important properties is the acidity of the zeolite. Depending on the modification strategy this can be changed, influencing the catalytic performance. This means that caution has to be taken when changes in catalytic performance are ascribed to the mesopore system. An example is given by Jamil et al. who used a diluted HF-solution to introduce mesopores in a self-prepared ZSM-22 zeolite. The obtained hierarchical catalyst showed a higher initial conversion in the steam catalytic cracking (SCC) of *n*-hexane, an effect that is assigned to the enhanced acidity of the zeolites rather than the increased mesoporosity.[13] Similarly, Liao et al. demonstrated that hierarchical ZSM-5 was an excellent catalyst for the monomolecular dealkylation of 4-propylphenol, due to the creation of more active Lewis acid sites, rather than the increased porosity.[14]

3

In this work, the hierarchization of a selection of industrially relevant zeolites is critically reviewed. Here, ZSM-23 (MTT), ZSM-22 (TON), ferrierite (FER), ZSM-5 (MFI), mordenite (MOR), X, Y and USY (FAU), and beta (*BEA) are taken into account. For this review, only the new synthesis procedures from 2016 to February 2020 are mostly discussed. For earlier literature the reader is referred elsewhere.[15–17] Figure 1 overviews the number of new publications per year regarding any new synthesis techniques for hierarchization that were taken into account in this review. Among them, we have distinguished the top-down, bottom-up and assembly of nanozeolite synthesis approaches. A clear difference in number between the selected catalysts can be observed showing the following order: ZSM-5 (MFI) > Beta (*BEA) > X, Y and USY (FAU) > Mordenite (MOR) > ZSM-22 (TON) > Ferrierite (FER) > ZSM-23 (MTT). This difference can reflect the ease or study interest of each strategy on the used zeolite. However, this does not exclude that the distribution might be different upon investigating older literature.

2. Synthesis of hierarchical zeolites

A diversity of methods has been developed the last decades to create hierarchical zeolites. In general, these methods can be subdivided in two main groups: (I) the top-down and (II) the bottom-up methods. Top-down methods are used when zeolites, synthesized in advance or commercially available, are used to create a hierarchical zeolite system upon post-treatment procedures. By etching away a part of the zeolite, and in some cases recrystallizing it again, mesopores can be created. These methods are thus considered as destructive. When the hierarchical system is created during the zeolite synthesis, one can speak of bottom-up methods. These methods are not considered as destructive. A third class of hierarchical systems that will be discussed in this review are nanozeolites and their assemblies. These can be produced using both top-down and bottom-up methods. Some general aspects typical of the different methods are discussed below.

2.1. Top-down methods

Dealumination
Dealumination is the oldest technique used to introduce mesopores in a zeolite. It is used industrially since mid-1960 to increase the (steam hydro)stability of high alumina microporous zeolites, as by removing Al from the zeolite framework the acidity and Si/Al ratio are altered. Nowadays, the technique is industrially mainly used for the production of USY, which can be used for fluid catalytic cracking (FCC) and hydrocracking. Next to the increased stability, the dealuminated zeolites also appeared to have an increased mesoporosity. In general, dealumination can be performed by means of steam, acid or heat treatment.[5,18–20]

Steam treatments are traditionally performed at temperatures higher than 500 °C in a water vapor atmosphere causing Al-O-Si bonds to break and defects to be formed. The released Al will remain on the zeolite surface and in the pores as extra-framework Al (EFAl), while less stable Si will move to the Al depleted regions creating Si rich domains. As such, a part of the amorphous structure generated during dealumination is recovered while creating mesopores. The entire mechanism is however not completely understood yet.[5,18,20–24] The use of steam during the treatment causes an improved mobility of Al and Si compared to heat treatments without the use of the steam. Steam treatments themselves don't cause a change in Si/Al ratio as Al remains on (in) the zeolite as debris. A mild acid treatment, also called 'acid wash', is often performed after the steam treatment to remove this debris and to open the previously formed mesopores. For instance, depending on the temperature of steaming and the number of acids washes, USY zeolites with different pore volumes and acidity can be obtained from a parent Y zeolite.[5,18,22,24]

In contrast to mild acid treatments, severe acid treatments are used to hydrolyze Si-O-Al bonds. In this case, the Al is immediately extracted from the framework causing the Si/Al ratio to increase and mesopores to be formed without the extra need of an acid wash. The performance of the acid treatment depends on the zeolite, type of acid used and the pH of the acid solution.[5,18,22,24] The acid dealumination can also be performed in combination with microwave irradiation as the heating method. This method can reduce the energy-intensive and time-consuming heating as in conventional heating methods. A short overview is given in the following source.[25]

However, the use of dealumination techniques to introduce mesopores in a zeolite comes with a few important disadvantages. A partial amorphization of the zeolite occurs, causing the relative crystallinity to drop. Often, the formed cavities and mesopores are not connected or lie within the zeolite framework, i.e. they are not connected to the surface and therefore not really optimal for fastening molecule transport in the crystal. Moreover, the pore size distribution of the formed mesopores is wide.[5,6,18,24]

Desilication
When contacting the zeolite with an alkaline solution, e.g. diluted NaOH, Si-O-Si bonds are selectively hydrolyzed causing the preferential removal of Si from the zeolite framework and the formation of mesopores.[6,19,20] The process is preferentially initiated at the boundaries of the zeolite crystal or at structural defects. Thus, the morphology of the zeolite crystal has an important impact on the desilication process.[15,20,23] Moreover, the framework Al is an important factor during desilication, and as such the Si/Al ratio of the parent zeolite, as the charge of the framework Al prevents the extraction of nearby Si species.[5,6,18,24] Often Al is also considered as a pore-directing agent during desilication. Al is leached from the framework, but precipitates again on the zeolite surface forming an amorphous layer blocking the micropores of the zeolite. This Al debris can be removed with a mild acid wash, opening the micropores again.[20]

Both inorganic and organic bases can be used during desilication. As the latter are less reactive than the former, higher temperatures and longer reaction times are needed to create a significant amount of mesopores. Also more Al is removed from the zeolite framework, causing higher Si/Al ratios for the treated zeolites, compared to purely inorganic treatments. However, the desilication can be better controlled. When used alone or in combination with inorganic bases, the micropores are better retained. Furthermore, after desilication a protonic zeolite can be easily obtained by calcining the zeolite, meaning no additional ion-exchange is necessary.[19,20,23] Sometimes, SDA's like

tetraalkylammonium salts are used during desilication in combination with a base. In this case, they are often called pore-directing agents and protect the zeolite during desilication by interacting preferentially with the surface of the zeolite crystal and preventing the attack of OH⁻ ions at the zeolite.[20,23]

During desilication, interconnected mesopores can be formed while the zeolite (largely) retains its microporous character. However, when using too concentrated alkaline solutions, a lot of zeolite material can be lost and the microporosity could decrease drastically.[19,20] Reporting of material yields, which is often ignored, should be done here. Moreover, it is difficult to obtain abundant mesopores in large zeolite crystals.[5,18]

Dissolution-recrystallization
A third top-down method used to create hierarchical zeolites is based on the recrystallization of a partially dissolved zeolite. The method comprises two main steps. In a first step, a part of the zeolite is dissolved, usually using an alkaline solution. Alternatively, structure depolymerization with glycerol has also been reported in the first step. In a second step, the dissolved zeolite is recrystallized by reassembling the dissolved and dispersed species into a mesoporous phase. This recrystallization takes place during a hydrothermal treatment in the presence of a surfactant. Depending on the level of dissolution and recrystallization, different types of hierarchical zeolites can be prepared as depicted in Figure 2. RZEO-1 consists of the same zeolitic phase as the parent material and is coated by a thin film of mesoporous material. RZEO-2 is a composite material consisting of both a zeolitic and a mesoporous phase. This mesoporous phase can be amorphous or ordered (usually MCM-41). Finally, RZEO-3 is a material that has been completely recrystallized and as such only contains a mesoporous phase, usually MCM-41.[26] With this technique, it is also possible to synthesize hollow ZSM-5 single crystal, as was shown by Dai et al.[27]
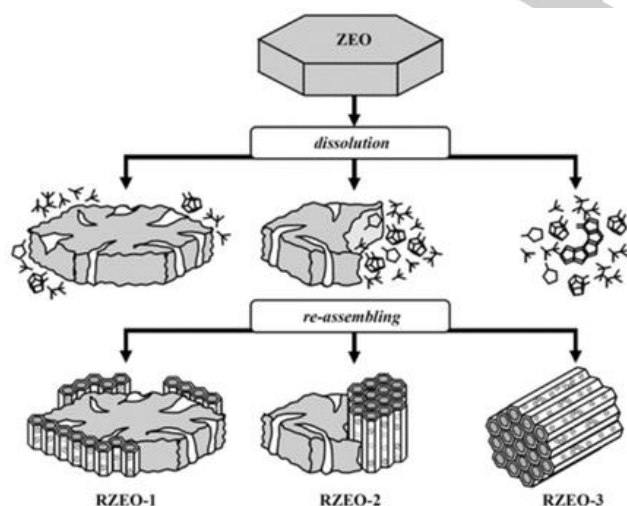
Figure 2. Schematic representation of the recrystallization procedure leading to different types of material.[26] Reproduced with permission of The Royal Society of Chemistry.

2.2. Bottom-up methods

Bottom-up methods are based on the fact that the mesopores are created during the synthesis of the zeolite. Often, a mesoporogen is added to create the mesopores, but template-free methods also exist.

Soft templating
During zeolite synthesis, an SDA as well as a mesoporogen can be added. In this case, one can category this method as a dual-template method. The SDA is responsible for the formation of micropores in the zeolite, whereas the mesoporogen vouches for the creation of mesopores. Mesoporogens like surfactants, polymers or organosilanes are considered as soft templates.[5,18,20–22,28] Alternatively, hard templates can also be used; they are discussed in the next paragraph. The soft templates can act as a physical scaffold by for instance forming micelles, around which the mesopores can be formed, but they also can interact chemically with the formed zeolite phase.[20] After zeolite synthesis, the mesoporogens can easily be removed through calcination, after which mesopores are created at the locations of the mesoporogen.[5,18,29] Interestingly, a wide variety in soft templates is possible. Given they can be tailored, the size of the mesopores can be readily controlled.[20–22] One point of importance is to select mesoporogens that are hydrothermally stable during zeolite synthesis.[21] Caution is advised as amorphous mesoporous materials might be formed instead of crystalline hierarchical zeolites. Moreover, defect sites can be created during synthesis, lowering the hydrothermal stability of the zeolite. Aside from the creativity and the beauty of controlling pore architectures of zeolites, the use of soft-templates comes with a higher economic cost (as the templates are often expensive), making them less suitable for industrial applications. Finally, toxic gasses can be formed during the removal of the soft-templates.[5,18]

Instead of using two different templates (one SDA and one mesoporogen) during the synthesis of hierarchical zeolites, one can also use two-in-one templates. These two-in-one templates consist of a hydrophobic alkyl chain on one side and a hydrophilic quaternary ammonium group on the other side. Both are separated from each other by means of short alkyl linkers. The hydrophobic tail will take part in the formation of micelles and is thus responsible for the formation of the mesopores. The hydrophilic head will participate in the formation of the micropores of the zeolite.[5,18,20]

Hard templating
Hard templates can also be used in combination with SDA's for the synthesis of hierarchical zeolites. Hard templates are solid materials with a relatively rigid structure, such as carbon materials, polymers and biological materials. When added during zeolite synthesis, they will act as a template around which the microporous zeolite is synthesized. After synthesis, the template is removed by means of calcination or dissolution. This creates meso- or macropores at the locations of the hard templates.[5,6,18–20] Hard templates are divers and chemically inert. Moreover, they enable the control of the mesopore size. They are also easy to remove after synthesis, but they often require quite high temperatures to do so, risking loss of product. Due to their more hydrophobic character, applications are limited. Hierarchical zeolites synthesized using hard templates are often

hydrothermally and mechanically less stable. Furthermore, the interconnectivity of the formed mesopores is rather low.[5,18,20,21]

Template free
Template free methods don't require the use of a mesoporogen to create hierarchical zeolites. As such, these methods might be a more cost-effective and green way to produce them.[5] A possible route is seed-assisted synthesis. These seeds are small proto-zeolitic units from early stages of zeolite crystallization and can be added to a synthesis gel. By using them, an improved crystallinity is obtained and the mesoporosity can be tuned. However, the synthesis is mechanistically not fully understood. Seed-assisted synthesis can also be used in combination with an SDA.[5,18]

Hierarchical zeolites can also be synthesized without templates by regulation of the crystallization process, meaning that nucleation and growth are strictly controlled. As such, hierarchical zeolites with controllable mesopores can be obtained, wherein the distribution and state of the active sites can be controlled.[5,16]

2.3. Nanozeolites and their assembly

Nanozeolites, which are defined as zeolite crystals with crystal sizes in the nanometer range, are of great interest in catalytic applications as they offer some interesting advantages compared to traditional zeolites. Due to their small crystal size, they have a high external surface area and short diffusion path lengths. They have a high external/internal atom number ratio and a high number of accessible active sites.[6,20,21] Thanks to these properties, they show improved activity, better performance and a longer lifetime in catalytic applications.[21] Nanozeolites can be synthesized in many different ways: with or without the use of SDA's, seed-induced, via milling and recrystallization, via confining the space growth or by using more alternative techniques like microwaves or ultrasonic irradiation.[20,21] By controlling the kinetics of the nucleation and growth, the zeolite size can be limited to nanosized zeolite crystals.[30,31]

By assembling the synthesized nanozeolites into larger ordered structures, one can obtain a hierarchical structure containing inter(nano)crystalline mesopores. These mesopores can be tuned by the size of the nanocrystals. The assembled nanozeolites show enhanced properties compared to traditional zeolites, combining the superior properties of nanozeolites as stated above and the presence of mesopores. Thanks to these mesopores, reagents and products can be faster transported in and out the zeolite system.[6,20,22]

The next part of this review will discuss in very detail the progress and advancements made since 2016 with regard to the hierarchization of the most important 10- and 12-membered ring (MR) zeolite topologies. 8-membered ring zeolites are not within the scope of this review.

3. Synthesis of hierarchical 10-MR zeolites

3.1. ZSM-23

ZSM-23 (MTT) is a unidimensional 10-MR zeolite. The crystals of the zeolite are needle or rod shaped with teardrop shaped pore channels (0.45 x 0.52 nm) running parallel to the longest dimension of the crystal. ZSM-23 is a promising zeolite in cracking, dewaxing and isomerization reactions.[32,33] In analogy with ZSM-22, the use of zeolite crystals having a high aspect ratio (i.e. crystal length over crystal width ratio) causes increased diffusion path lengths and as such pore diffusion limitations. Efforts have been made to improve the mass transfer in the zeolite by reducing the aspect ratio of the crystals and by developing hierarchical pore systems.[34] For many other zeolite topologies bottom-up techniques are used to do this. However, zeolites like ZSM-23 and ZSM-22 seem to be unaffected by the presence of additives as these zeolites grow as needle or rod-like crystals. Top-down methods such as desilication are thus used to overcome these issues.[35]

Top-down methods

Desilication
The literature with respect to hierarchical ZSM-23 is limited, as only a few papers have been published so far. Silva et al. synthesized ZSM-23 using four different SDA's: (I) isopropylamine (IPA), (II) ethylene glycol (ETG), (III) pyrrolidine (PYR) and (IV) N,N-dimethylformamide (DMF). They looked at their influence and at that of a post-synthetic alkaline treatment followed by an acid wash on the resulting structure and catalytic properties. The obtained hierarchical zeolites maintained their MTT structure after post-synthetic treatment, with an increased external surface area and pore volume compared to the parent zeolites. The Si/Al ratio decreased, clearly indicating the leaching of Si atoms from the zeolite structure. Moreover, a decrease was observed in the weak acid site density due to leaching of extra-framework Al. Instead, the total and strong acid site density of the hierarchical zeolites depended on the SDA that was used during the synthesis. In addition, the SDA not only had an influence on the purity, crystallinity and structure of the zeolite phase, but also on the effect of the alkaline treatment. Nevertheless, the data presented by Silva et al. show that the introduction of mesoporosity in ZSM-23 is difficult, which can be attributed to the crystal morphology and the unidimensional pore system.[34,36] The performance of the hierarchical zeolites was tested and compared to their microporous analogues for the catalytic cracking of n-heptane[36] and polyethylene.[34] In both cases, the observed activity was higher and the amount of cokes formed was lower for the hierarchical zeolites. These effects can be clearly attributed to the more open porous structure of the hierarchical zeolites in comparison to their microporous analogues. This makes it easier for reagents and products to respectively enter and leave the zeolite. The lower external surface acidity restricts the formation of cokes.[34,36]

3.2. ZSM-22

ZSM-22 (TON topology) is a unidimensional 10-MR zeolite with needle or rod shaped crystals. The pores of the zeolite (0.46 x 0.57 nm) run parallel to the longest dimension of the needle shaped crystals.[37] ZSM-22 is of high interest for use in cracking, hydroisomerization, methanol to olefin (MTO) and methanol to hydrocarbon (MTH) reactions.[37–41] As explained earlier for ZSM-23, ZSM-22 also suffers from diffusion limitations due to the high

aspect ratio of the zeolite crystals. Rapid deactivation, caused by pore blocking as a result of coke deposition, is also reported as a major issue.[13] In contrast to other zeolite topologies for which bottom-up techniques are frequently used to introduce mesopores in the zeolite crystal, this technique is difficult to apply for ZSM-22 as impurities can be easily brought into the zeolite crystal. This is why top-down strategies like desilication are preferentially chosen.[37,38] However, given the surface of ZSM-22 is rich in Al, vigorous alkaline treatments are necessary to introduce mesopores. The formation of mesopores, though, is limited due to the shape and size of the zeolite crystals, making it difficult to introduce proper mesoporosity in the zeolite crystal without destroying it.[38]

Top-down methods

Dealumination

A dealumination procedure was performed by Jamil et al., who used an aqueous HF-solution to introduce mesopores in a self-prepared ZSM-22. When treating the zeolite with a very diluted HF-solution (0.7 and 1.0 wt%), Al was preferentially leached from the zeolite framework. When more concentrated HF-solutions, viz. 1.5 wt%, were applied, Si was preferentially leached. While performing the treatment, the structure of the zeolite was maintained but the crystallinity decreased. Moreover, the crystals seemed to be less agglomerated. When using the most concentrated HF-solution (1.5 wt%), the highest mesopore volume was created. This sample also showed the most retained micropore volume. Nevertheless, all dealuminated samples had a lower BET surface area and external surface area compared to the parent zeolite. The dealuminated zeolites were hydrothermally more stable and possessed a lower Brønsted acidity compared to the parent zeolite. They were tested for their suitability in the steam catalytic cracking (SCC) of n-hexane. The zeolites treated with low concentrations of HF were more active, yielding higher initial conversions. This can be explained by the enhanced acidity of the zeolites. Additionally, no difference was noticed for the deactivation rate. The zeolite treated with a higher concentration of HF (1.5 wt%) showed a lower initial conversion and showed more cokes formation at the end of the reaction.[13]

Desilication

Desilication is a method that has been frequently used the past few years to introduce mesopores in the ZSM-22 zeolite crystals. Dyballa et al. studied the influence of different alkaline treatments, based on NaOH or KOH, followed by an acid wash on the properties of ZSM-22. During the desilication and acid wash, the crystallinity of the zeolites was largely maintained, indicating the reduced susceptibility of unidimensional zeolites like ZSM-22 and ZSM-23 to desilication.[37,39] Nevertheless, an increased BET surface area and mesopore volume was created in comparison to the parent material. This increase was higher when KOH or more concentrated alkaline solutions were used. The Brønsted acid strength remained unchanged. However, the acid site density (or the amount of acid sites) was lowered due to the alkaline treatment. The obtained hierarchical zeolites were tested for the MTO conversion. The results indicated that an improved catalyst lifetime was not only achieved when there is an increased mesopore volume, but that an optimized Brønsted acid site density is also crucial in this type of reaction. Moreover, the shape selectivity of the 10-MR pores was maintained.[39]

Del Campo et al. looked at the influence of three different desilication procedures, (I) NaOH, (II) surfactant-assisted NaOH treatment with cetyltrimethylammonium bromide (CTAB), and (III) NaOH and tetrabutylammonium hydroxide (TBAOH), followed by an acid wash on a commercial and a self-prepared ZSM-22. Their research showed that the influence of the desilication procedure depends strongly on the morphology of the crystal, wherein the commercial ZSM-22 is more rod shaped while the self-prepared ZSM-22 is needle shaped. As such, intra-mesoporosity was generated more efficiently in the rod shaped crystals, while the needle shaped crystals got more fragmented, leading to a higher external surface area with less intra-mesopore creation. del Campo et al. also demonstrated that the employed desilication method had an influence on the pores formed. Using only NaOH during alkaline treatment gave rise to non-uniform mesopores and a roughening of the crystal surface, while the use of CTAB or TBAOH during desilication formed more well-defined mesopores. Thanks to the use of an acid wash after the alkaline treatment, the micropore volume was restored by removing the EFAl, formed during desilication. The Brønsted acidity of the zeolite did not seem to be modified because of desilication, although the amount of surface hydroxyls decreased.[40] The different hierarchical ZSM-22 zeolites of del Campo et al. were tested in the MTH conversion. The obtained results indicated that the catalyst lifetime could be increased dramatically when using a hierarchical ZSM-22. This could be explained by a combination of the enhanced accessibility to the acid sites and increased adsorption and transport properties. However, the parent material of the hierarchical zeolite was decisive here as the effect of the post-synthetic treatments differed depending on the starting zeolite.[41]

Silva et al. also used an alkaline solution based on NaOH to desilicate three differently self-prepared ZSM-22 samples. Thanks to the desilication, a significantly increased surface area and mesopore volume was achieved while mainly maintaining the micropore volume. The more concentrated the alkaline solution, the higher the observed mesopore volume of the zeolites.[42] This effect was also observed by Dyballa et al.[39] Importantly, the type of precursor that was used during synthesis of the parent material had an influence on the amount of mesoporosity in the zeolite.[42] This finding was also observed by the same group for ZSM-23.[36] The best results were obtained when an organosilane, viz. trimethoxyphenylsilane, was used during zeolite synthesis.[42]

According to Li et al., the use of a desilicated ZSM-22 zeolite is also beneficial for the hydroisomerization of n-hexane, since the conversion and selectivity were higher compared to untreated ZSM-22. As for the previous discussed cases, the performance of the zeolite was determined by both the acidity and the pore structure of the zeolite. To obtain these superior zeolites, the researchers performed an alkaline treatment on a commercial ZSM-22. They also showed that during treatment, the topological structure was maintained, but the relative crystallinity of the samples was strongly influenced by the concentration of the alkaline solution. A reduction of the length of the needle shaped crystals was observed as well. During the alkaline treatment, mesopores were created while largely retaining the micropores of the zeolite. This is in contrast with previous papers wherein an extra acid wash was performed to obtain this result. However, during the ion-exchange of the zeolite, a small amount of acid was added to the NH$_4$Cl solution, which might have the same effect.

Nevertheless, no further details were given about the procedure. A decreased acidity was observed, which can be mainly attributed to a decrease of the Lewis acid sites.[43]

Taking into account the difficulties that come along during the desilication of ZSM-22, Wang et al. looked at the possibilities of performing a desilication while protecting the zeolite crystals. To do so, they detemplated the rod-shaped zeolite only partially before desilication and added CTAB to the desilication mixture. By partially detemplating the zeolite before desilication, the region and degree of mesopore formation can be tailored since only desilication will occur in zeolite crystal parts free of template. As such, the crystals were protected against heavy destruction. By adding CTAB, the size of the generated mesopores was centered and below the width of the crystals, avoiding them to crack. In addition, it reduces the blockage of the micropores. As such, a higher desilication efficiency (i.e. the amount of external surface area developed per % of weight loss) could be obtained and the Brønsted acid sites were more accessible. The obtained catalyst was superior compared to its parent material for the hydroisomerization of *n*-dodecane, showing indeed a higher isomer yield and less cracking.[38]

Dissolution-recrystallization
Another approach to obtain hierarchical zeolites is by simultaneously dissolving a part of the zeolite in an alkaline solution and recrystallizing it on the remaining zeolite in the presence of a surfactant. Liu et al. used this technique and obtained a microporous ZSM-22 zeolite with a well-developed MCM-41 mesoporous surface coating with 3 nm mesopores. CTAB was used as surfactant assisting the formation of the mesoporous phase. The obtained material had an increased amount of weak acid sites but a lower total acid site content. The acid sites were situated at the pore mouths, in the micropores and on the mesopore surface. During the hydroisomerization of *n*-heptane, *n*-dodecane and *n*-hexadecane, cracking reactions were suppressed while the selectivity towards multi-branched compounds increased when compared to microporous ZSM-22. The latter was caused by the presence of Brønsted acid sites in the mesoporous structure.[44,45]

Nanozeolites and their assembly

Finally, Wang et al. reported ZSM-22 nanozeolites assembled into hollow-spheres. Therefore, a two-step hydrothermal synthesis was performed. In a first crystallization step, ZSM-22 nanorods were synthesized, while the second crystallization step included the self-assembly of these nanorods in the presence of CTAB and KF to form hollow-spheres. As such, a zeolite system was created having micropores in the ZSM-22 nanorods and inter(nano)crystalline mesopores in the hollow-spheres self-assembly. The obtained catalysts were not tested for their performance in catalysis.[46]

3.3. Ferrierite

Ferrierite (FER) is a two-dimensional zeolite with intersecting 10- and 8-MR channels (0.42 x 0.54 nm and 0.35 x 0.48 nm respectively). At the intersection of the 8-MR channel and the 6-MR channel, a spherical ferrierite cage is formed which is accessible via the 8-MR channel. Ferrierite shows a good thermal, hydrothermal and chemical stability and is currently used in many applications such as the hydroisomerization of *n*-alkanes, isomerization of *n*-alkenes, cracking of *n*-paraffins, NO_x reduction, styrene epoxidation, N_2O decomposition, etc.[47–49] The main industrial application of ferrierite is the isomerization of 1-butene.[50]

Top-down methods

Dealumination/desilication
Dealumination and desilication have been reported multiple times to introduce mesopores in ferrierite. Brylewska et al. combined a dealumination and desilication procedure on two ferrierite zeolites having different Si/Al ratios. Zeolites were created with an increased mesopore volume and surface area, while preserving the micropore structure and the crystallinity of the zeolites. Additionally, the acid site density also increased. This might be attributed to an enhanced accessibility of the acid sites. The hierarchical zeolites were tested in the dehydration of ethanol. The data indicated that for this reaction the best results were obtained when the catalyst had a high concentration of acid sites and a well-defined microporous structure. Meaning that in this case the introduction of mesopores not necessarily provided a more effective catalyst.[47]

Pereira et al. only used a desilication procedure with NaOH to introduce mesopores in ferrierite. Compared to the parent ferrierite, an increased mesopore area was observed while the micropore volume slightly decreased. The catalyst also lost crystallinity. The obtained catalysts were tested in the conversion of propylene to light olefins. The results showed a positive correlation of the initial activity with the mesopore area, indicating higher site accessibility. Furthermore, a different product selectivity was detected, yielding more products in the gasoline range.[50]

Finally, Catizzone et al. used a sequence of three different post-synthetic treatments proposed by Verboekend et al. to obtain a hierarchical ferrierite and used it for the dehydration of methanol. First, the ferrierite zeolite was treated with $NaAlO_2$, creating mesopores in the zeolite structure. Meanwhile, Al debris blocking the micropores and Si nanocrystals were formed. Then, the zeolite was treated with HCl to remove the Al debris and restore the microporosity of the zeolite crystals. Finally, an alkaline wash with NaOH was performed to remove the Si nanocrystals. In the paper, special attention was paid to the influence of the first $NaAlO_2$ treatment on the properties of the zeolite. The results indicated that a higher concentration of $NaAlO_2$ or a higher contact time gave higher mesoporosity. Despite these textural changes, the Si/Al ratio and acidity were preserved after the treatment sequence. The obtained hierarchical zeolites showed a higher activity in the dehydration of methanol. However, a lower selectivity to dimethyl ether was observed due to the presence of the mesopores.[51,52]

Dissolution-recrystallization
To the best of our knowledge, only one paper was published since 2016 describing the one-step desilication and recrystallization of ferrierite. In this paper by Cheng et al.*,* an alkaline treatment with NaOH in the presence of cetyltrimethylammonium bromide (CTAB) was used to create a ferrierite with a hierarchical pore system. The obtained intracrystalline mesopores were parallelepiped-shaped and in the direction of the 10-MR pores.

The CTAB can also be inserted between the layers of the ferrierite crystals, leading to the partial delamination of layered crystals in addition to the formation of occluded mesopores. When more severe process conditions were applied, other zeolite phases like GIS and SOD were formed.[49]

Bottom-up methods

Soft templating

While some researchers focus on the use of top-down techniques to obtain hierarchical ferrierite, others use bottom-up techniques. One possible option uses the dual templating technique. Here a SDA's is responsible for the common zeolite formation in combination with a mesoporogen that directs the formation of mesopores. Bolshakov et al. used this technique twice to create hierarchical ferrierite. In a first paper, they synthesized mesoporous ferrierite in presence of N-methylpyrrolidine (NMP) (as SDA) and N,N-methyl-hexadecylpyrrolidinium bromide (C_{16}NMP) (as mesoporogen). Thanks to the presence of the mesoporogen, highly crystalline and acidic ferrierite was obtained having both micro- and mesopores. The hierarchical ferrierite was subsequently tested in the dehydration-isomerization of 1-butanol to isobutene. Despite a somewhat lower conversion rate compared to that of the non-mesoporous ferrierite, the deactivation rate of mesoporous ferrierite was substantially lower.[53]

A second paper of Bolshakov et al. describes a hierarchical ferrierite synthesis through transformation of a FAU precursor in the presence of NMP (as SDA) and the amphiphile mesoporogen 1,2-dimethyl-3-hexadecyl-1H-imidazol-3-ium bromide (C_{16}dMImz). A strongly crystalline ferrierite zeolite was presented with high mesoporosity and small crystal size. Compared to the previously discussed dual templating technique, this mesoporous ferrierite has a higher acid site density. The hierarchical zeolite showed an improved activity in the isomerization of unsaturated fatty acids to branched fatty acids thanks to the better mass transport and appropriate acidity.[54]

Nanozeolites and their assembly

Crystal size reduction to nanoscale is an alternative option to improve mass transport in zeolites. Chu et al. synthesized in the presence of pyrrolidine (as SDA) rod-shaped nano-ferrierite appearing as aggregates.[55] A very similar approach was used by Liu et al., showing comparable nanomaterials. They both looked in more detail into the synthesis parameters that determine the crystallinity and intercrystalline mesoporosity of high quality nano-sized ferrierite crystals. These data led to optimal synthesis conditions (i.e. synthesis temperature, alkalinity, crystallization time, SDA concentration). Both research groups tested the nano-ferrierite aggregates in the skeletal isomerization of n-butene and found improvements of selectivity and stability.[55,56]

Margarit et al. used two SDA's (piperidine (Pip) and cetylmethylpiperidinium bromide (C_{16}MPip)) to synthesize nano-ferrierite crystals. The first SDA initiates the crystallization process, while the second SDA restricts crystal growth. This procedure led to very small nano-sized ferrierite crystals, viz. 10 x 10 nm dimension, of excellent crystallinity quality. Thus, the microporous structure is maintained and large external surface and intercrystalline mesoporosity are present. This nano catalyst showed a very high 1-pentene oligomerization activity with high diesel selectivity and a longer life time, explained by the short diffusion path lengths in the zeolite crystals.[48]

Finally, Wuamprakhon et al. assembled nanosheets of ferrierite into a ball-shaped morphology during a direct hydrothermal synthesis in the presence of dimethyloctadecyl[3-(trimethoxysilyl)propyl]ammonium chloride (TPOAC) as SDA. As such, a hierarchical ferrierite system with high crystallinity and microporosity was acquired. The acid strength of the hierarchical ferrierite was similar to that of the microporous analogue, but acid density (and in particular the very strong ones) was lower. Potential benefits were screened for the benzylation of toluene with benzyl chloride. The catalytic data showed higher activity without compromising selectivity.[57]

3.4. ZSM-5

ZSM-5 (Zeolite Socony Mobil-5) is one of the most widely studied and used catalysts. ZSM-5 has an MFI topology and 10-MR openings, which make zig-zag channels along the [100] axis (0.51 x 0.55 nm). Besides this, the zeolite also has straight intersecting channels along the [010] axis (0.53 x 0.56 nm).[58] Due to its controlled acidity, high hydrothermal stability and unique pore structure, ZSM-5 is one of the most important shape-selective catalysts. The catalyst is widely used in industry, for example in alkylation, isomerization and cracking reactions.[59]

This part collects and discusses the recent literature of mesoporous MFI zeolites with focus on ZSM-5. Because of the vast amount of literature concerning ZSM-5, rather an analysis of the methods instead of a comprehensive review of individual work will be presented. No systematic evaluation of silicalite-1 is done unless when used as seed material. The following thus contains emerging synthesis methods for pure ZSM-5 zeolites excluding composites with other materials/topologies and surface functionalization.

**Top-down methods**

Dealumination

Dealumination of ZSM-5 zeolites is generally done by steaming, acid treatment or leaching with complexing agents. It often results in poor mesopore formation, and decreases the Al content and thus the zeolite acidity. In this way, Al-rich MFI zeolites are made more susceptible for a subsequent desilication treatment.[60] Some recent studies where dealumination is used in a first step to create mesopores are discussed below.

Recent studies suggested the successive steaming-alkaline leaching of ZSM-5.[61–63] Wang et al. used this consecutive treatment to create mesoporous ZSM-5 with intracrystalline mesopores around 2-4 nm. In this process, steaming extracted EFAl from the outer surface of the zeolite, reducing the acid density and strength of the parent zeolite. The additional alkaline-treatment partially restored the acid density and strength. This can be explained by considering realumination of EFAl in the outer shell of the zeolite, preventing further excessive desilication in the alkaline treatment. This two-step approach results in pores with a smaller aperture in comparison with a sole desilication treatment. Reversibly, a successive alkaline-steaming treatment causes a structural collapse.[62] Yang et al. also used this steaming-alkaline treatment in an Al-rich ZSM-5 zeolite. Here, the researchers were

able to regulate the acid quantity by altering the concentration of the base in the alkaline treatment.[63]

The influence of the Al coordination was further studied by Li et al. Different Al coordinations resulted in different zeolite structures when different treatments were applied on Al-zoned ZSM-5 crystals, as can be seen in Figure 3. A conventional desilication with NaOH leaches framework Si without disturbing much of the framework Al. The use of a tetrapropylammonium hydroxide (TPAOH) treatment resulted in a desilication-recrystallization process (vide infra). In contrast, prior steaming or fluorination treatments largely disturbed the Al coordination. A subsequent NaOH or TPAOH treatment was able to redistribute Al, ultimately resulting in higher mesoporosity with narrow and uniform pores.[64] Similarly, Li et al. produced ZSM-5 zeolites with an Al-rich exterior and a defective silicious interior. This enabled a hollow structure formation upon selective base leaching/desilication of the crystal inside. However, this catalyst was not found to be more stable than the parent zeolite in the methanol to propylene (MTP) reaction. The instability was related to the highly acidic shell and the closed hollow structure, leading to quick coke deposition on the external surface. When the parent ZSM-5 with discontinuous composition along the crystal radius was first treated with NH_4F, the interior Si-defects were repaired and the Al in the outer shell distorted. In a subsequent alkaline treatment, most Al in the shell was leached out and slowly redeposited on the zeolite surface, acting as an external pore directing agent (PDA). This series of treatments ultimately resulted in a higher solid yield and an open mesoporous structure with uniform 13 nm pore size. This catalyst showed a long lifetime and high propylene formation activity in the MTP process, when compared to the parent zeolite.[65]
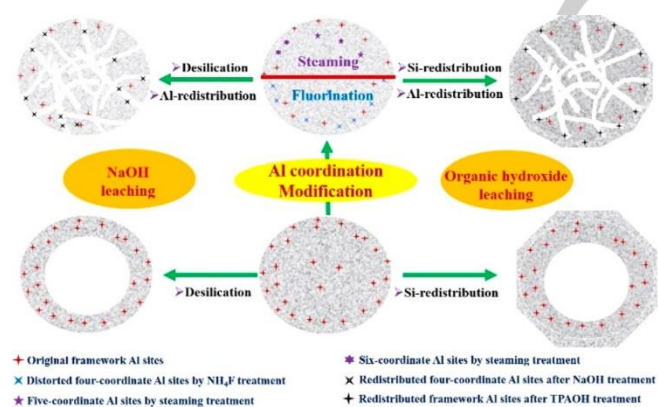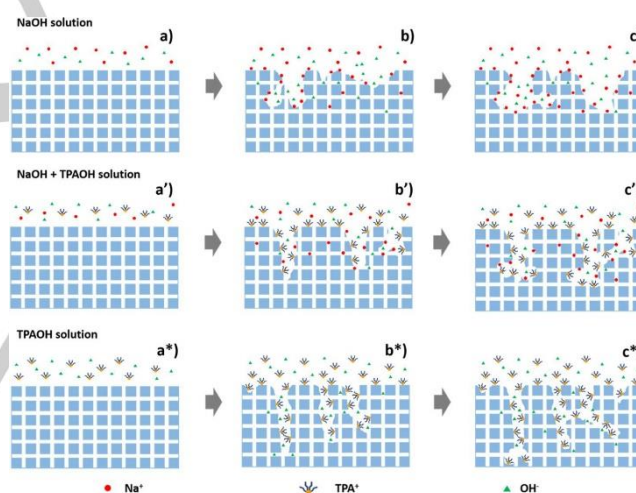

Figure 3. The effect of different treatments and the Al-coordination in the zeolite structure.[64] Reproduced with permission. Copyright 2018 American Chemical Society.

Desilication

Desilication of parent ZSM-5 zeolites with aqueous NaOH is one of the most popular methods to prepare mesoporous ZSM-5.[66–68] Comprehensive studies on top-down mesoporization were done by Groen et al. They noted the importance of framework Al during desilication with NaOH and concluded that the optimal Si/Al ratio ranged from 25 to 50. At higher Si/Al ratios, non-selective and excessive extraction of framework Si occurs, whereas minor extraction and limited mesoporosity formation takes place for low Si/Al ratios.[60] That is, Al rich ZSM-5 samples are more difficult to mesoporize, whereas Al poor samples are

very sensitive to complete dissolution. Verboekend et al. were able to extend this 25-50 range limitation by using PDA's which also enabled the modification of siliceous ZSM-5. These PDA's protect the framework from excessive dissolution resulting in higher crystallinity and solid synthesis yield. The use of a sequential acid wash can be used for zeolites with lower Si/Al ratios. As seen before, another method to modify Al-rich zeolites is to perform a dealumination before desilication. However, some Al-rich framework may be completely lost with this treatment, resulting in a low material yield.[69]

Recently, various adaptations to the NaOH treatments have been performed to desilicate ZSM-5. It is known that the addition of certain additives to the NaOH solution can increase mesoporosity. The co-effect of for instance Na^+ and TPA^+ was investigated in a NaOH desilication process by Wan et al. High concentrations of TPA^+ did not result in high mesoporosity, however, it had a protective role against desilication. In contrast, Na^+ shows a positive effect on the mesoporization process. The latter approach enabled synthesis of highly mesoporous ZSM-5, containing small-sized mesopores that are evenly distributed over the crystal. An example is shown in Figure 4. This catalyst showed a superior methanol to hydrocarbon (MTH) lifetime compared to the ZSM-5 catalyst that was treated according to the traditional NaOH treatment.[70]

Figure 4. The desilication mechanism in different alkaline solutions. Reproduced with permission.[70] Copyright 2016 American Chemical Society.

Smail et al. investigated the effect of a NaOH treatment with and without the presence of other additives, i.e. (I) NaOH, (II) cetyltrimethylammonium bromide (CTAB) with NaOH, (III) TPAOH with NaOH and (IV) and CTAB/TPAOH with NaOH. The organic additives positively affected the desilication process regarding the creation of uniform pores. The treatment with NaOH resulted in the smallest mesopores (ca. 3.7 nm), followed by TPAOH with NaOH (ca. 11.1 nm), CTAB with NaOH (ca. 14.9 nm), and CTAB/TPAOH with NaOH (ca. 15.2 nm).[71]

Feng et al. compared an alkaline (NaOH) with an acid (citric acid, EDTA-2Na, and combination thereof) mesoporization treatment. Citric acid was able to remove EFAl species, which resulted in an increase in micropore surface area. The use of EDTA-2Na promoted desilication and simultaneously transformed the removed Al-species into EFAl. By consequence, the Lewis acid

site density increased. The use of these three agents created an effective hierarchical zeolite with high Brønsted and Lewis acid site density. The material showed significant improvement in the catalytic cracking of n-heptane.[72] Another variation of the classic NaOH desilication procedure suggested the use of ultrasound. Upon using rice husk ash as the silica source, the authors demonstrated the formation of mesopores as a result of ultrasound utilization in a NaOH alkaline treatment process. The higher catalytic cracking activity of light naphtha was related with the obtained higher mesoporosity compared to a classically NaOH modified zeolite.[73]

The desilication of ZSM-5 can also be executed with other bases than NaOH. Feng et al. focused on the effect of weak bases such as $NaHCO_3$, Na_2CO_3 and $NH_3 \cdot H_2O$. Treatment with $NaHCO_3$ and Na_2CO_3 sharply reduced the Brønsted/Lewis (B/L) acid site ratio, whereas the use of $NH_3 \cdot H_2O$ showed a slight increase of this ratio. The $NH_3 \cdot H_2O$ treatment yielded a highly stable catalyst for the methanol to aromatics (MTA) reaction and this was explained by a combination of the appropriate B/L ratio, large pore volume and surface area. Interestingly, the ZSM-5 catalyst also showed a higher selectivity towards benzene-toluene-xylene (BTX).[74] Zhang et al. systematically studied desilication with different alkali-metal hydroxides such as LiOH, NaOH, KOH and CsOH. All of them effectively created mesoporosity. The hierarchical ZSM-5 modified with CsOH showed the best results during butene oligomerization. Overall, this catalyst contained a high L/B acidity ratio, had interconnected open mesopores, and showed the smallest crystal size.[75]

$NaAlO_2$ can also be used in the desilication process of ZSM-5. Gorzin et al. studied the use of different amounts of $NaAlO_2$ and TPAOH for the desilication of highly-silicious ZSM-5 zeolites (Si/Al = 200). The use of TPAOH protected the zeolite against severe base leaching of the framework. When using the appropriate $NaAlO_2$/TPAOH ratio and performing a subsequent an acid wash, uniform and narrow mesopores were created without significantly changing the original Si/Al ratio. A successful improvement of the catalytic performance was demonstrated for the MTP reaction. The catalyst showed an increased lifetime compared to the parent catalyst, which may be explained by its lower acid strength and higher mesoporosity.[76]

The use of alkaline media can also produce internal cavities in the crystal rather than recognizable mesopores. This can be achieved in different ways. Hollow ZSM-5 crystals were made by ammonia leaching by Xu et al. With this method, hollow structures with a shell-thickness of 40 nm were obtained.[77] Fu et al. used a two-step method to similarly treat 100 nm ZSM-5 zeolites, producing hollow ZSM-5 zeolites with a mesoporous shell. They first dissolved internal silica using NaOH, transforming the crystals to hollow objects. The next step attempted the formation of mesoporosity in the remaining shell using a protective leaching concept with NaOH/TPAOH. The obtained catalyst showed improvements regarding its service time in the MTH reaction.[78,79] Similarly, Xu et al. reported hollow ZSM-5 with a mesoporous shell using NaOH/TPAOH. They further tuned the mesopore size by addition of Na^+. As such, mesopore sizes of 7.9 to 20.5 nm can be obtained. As generally accepted, TPA^+ plays a protective role in the synthesis, limiting crystal growth and fusion of the growing pores. However, the addition of Na^+ induced a competitive adsorption to fine tune growth and protection processes. Clearly,

large framework dissolution was noticed in absence of TPA^+. When mixed with $Fe_3O_4@MnO_2$, this zeolite was an excellent catalyst for the gasoline production from syngas in the Fischer-Tropsch synthesis. Here, an unprecedented C_{5-11} selectivity was reported with substantial suppressing of C_{2-4}. This can be explained by a reduction of hydrocracking as a result of the limited residence time of the molecules in the zeolite.[80]
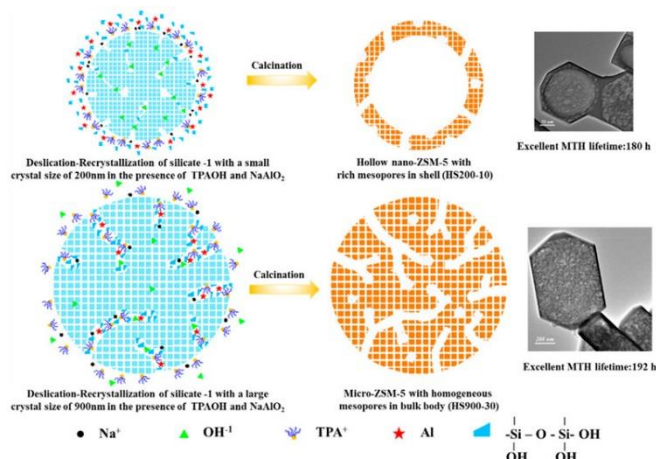
Dissolution-recrystallization
Different organics can be used for the dissolution-recrystallization approach to create mesopores in ZSM-5 zeolites. Among them, TPAOH is the most familiar candidate. It is known that this dissolution-recrystallization mechanism can produce hollow zeolites, while additional mesoporosity in the remaining shell will benefit crystal diffusion. Mesopores around 2-4 nm were for instance created in the shell by Niu et al. Here, TPAOH was used with an Al source and added to silicalite-1 zeolite. The produced hierarchical hollow zeolite was deposited with Pt, and the Pt/ZSM-5 showed superior catalytic activity in the hydrodeoxygenation of guaiacol, compared to conventional Pt/ZSM-5. This can be explained by the synergetic effect of the hollow structure and the enhanced Pt dispersion due to the interaction of the Pt particles with the generated strong acidic centers.[81] Lin et al. were also able to produce similar hollow ZSM-5 by using TPAOH and by regulating the kinetics of the dissolution-recrystallization process (e.g. temperature control). They showed the formation of open box-like ZSM-5 zeolites which showed higher catalytic performance in a benzyl alcohol self-etherification reaction, compared to a conventional ZSM-5 or hollow ZSM-5.[82] Similarly, Jiao et al. also produced box-like mesoporous ZSM-5. Here, parent zeolites containing tetrahedral extra-framework Al were produced via a rapid ageing procedure, and further consequently converted into Al-enriched mesoporous ZSM-5 with box-like morphologies using a TPAOH post-treatment. The improved diffusion and strong acidity of the produced catalyst resulted in improved catalytic performance in the cracking of n-octane and cumene.[83] Also Ma et al. produced hollow ZSM-5 and highly mesoporous micro-ZSM-5 by starting with two differently sized silicalite-1 crystals (200 and 900 nm, respectively), as can be seen in Figure 5. A desilication-recrystallization process was applied with $NaAlO_2$ as Al source and TPAOH as template. TPA^+ played the protective role in the desilication process, while the presence of Na^+ directed the formation of mesopores during the recrystallization process. The smaller silicalite-1 zeolites were transformed into hollow ZSM-5 with mesopores around 23 nm, while the larger ones transformed into highly mesoporous ZSM-5 with mesopores of approximately 15 nm. Both catalysts showed excellent MTH activity with higher service times in comparison to the conventional ZSM-5.[84] A similar study of the TPAOH desilication-recrystallization method with 200 nm sized silicalite-1 and $NaAlO_2$ investigated the influence of the Si/Al ratio. A high ratio led to hollow ZSM-5, whereas a mesoporous shell was observed at a low Si/Al ratio. By adjusting the porosity and acidity in the synthesis process, long catalytic lifetimes and high selectivities could be obtained in the MTH reaction.[85] Luo et al. used a modified TPAOH dissolution-recrystallization technique in which different morphologies (e.g. microporous, mesoporous and core-shell mesoporous) were noticed upon adjusting the detemplation of the parent zeolite.[86]

Besides TPAOH, other organic bases have been tested as well. Tetraethylammonium hydroxide (TEAOH) for instance strongly resembles TPAOH during post-synthetic treatment.[87] Zhang et al. used TEAOH during treatment of highly silicious ZSM-5, and tested the mesoporous ZSM-5, containing 2-3 nm sized pores, for the MTP reaction. They found substantial improvement of the service time.[88] CTAB with NaOH is another alternative that can be used during dissolution and recrystallization.[89] It was used by Subhan et al., showing the formation of meso-structures similar to Al-MCM-41, with enhanced adsorptive desulfurization properties.[90]

Figure 5. The proposed mechanism of the desilication-recrystallization of 200 nm (S200) and 900 nm (S900) silicalite-1.[84] Reproduced with permission. Copyright 2019 American Chemical Society.

The dissolution-recrystallization approach can also be combined with other synthesis techniques. A first study described the desilication of ZSM-5 zeolite with NaOH, followed by recrystallization treatment with TEAOH wherein oxidized lignin was added to the mixture. This combined treatment resulted in mesoporous ZSM-5 with a broad pore size distribution. The material showed enhanced CO_2 physisorption capacity compared to conventional ZSM-5.[91] Another combination of techniques was proposed by Lin et al. Here, the use of polyethylene glycol (PEG) directed the synthesis to mesopores in the steam-assisted crystallization (SAC) process. The following dissolution-recrystallization process was carried out with TPAOH and created the expected core shell-like zeolite. This method ensured surfacing of the mesopores. Addition of Na^+ competed with the adsorption of TPA^+ and enabled tailoring the porosity. Acetylation catalysis of cyclohexanone with these materials showed promising enhancement of the catalytic activity.[92]

Recently, the dissolution-recrystallization was also applied in the presence of a binder. Zhou et al. created a full-zeolitic hierarchical monolytic ZSM-5. Addition of n-butylamine (as SDA) and a binder to cylindrical shaped ZSM-5 pellets under steam conditions induced binder crystallization. In addition, mesopores were formed due to a recrystallization process (Figure 6). This catalyst showed superior catalytic activity in the MTH process when compared to the commercial catalyst.[93]

Bottom-up methods

Soft templating

Organic compounds can be used as mesoporogen templates in the synthesis mixture to induce intracrystalline and/or intercrystalline mesopores. Different templates such as polymers, organosilanes, amines and organic ammonium salts, can be used. Direct synthesis routes with surfactant-based templates often result in a random stacking of nanosheets or an agglomeration of nanozeolites. The catalysts that are clearly assembled of particles in the nano-range are described in the section 'Nanozeolites and their assemblies'. The recent soft templating reports for hierarchical microporous zeolites are summarized here.
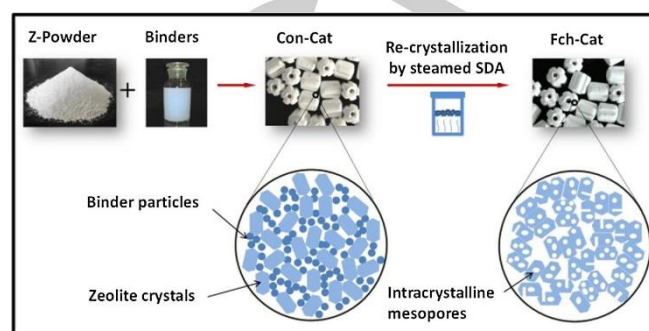
Figure 6. Schematic representation of the preparation of full-zeolitic hierarchical ZSM-5 monoliths.[93] Reproduced with permission of Elsevier.

Templates with ammonium groups are popular given their strong electrostatic interaction with the zeolite framework. Zhang et al. used a surfactant with a hydrophobic alkene chain and a multi-quaternary ammonium head group. The mesoporous zeolite was synthesized according to a sol-gel method in a tumbling autoclave. New core-shell structured ZSM-5 zeolites were obtained with a micro-macroporous core and a mesoporous shell.[94]

The higher economic cost of customized soft templates is often a drawback for catalytic applications. Meng et al. were able to produce mesoporous ZSM-5 using a cheap mono-quaternary ammonium surfactant ($C_{16}H_{33}$-[N^+-methylpiperidine]) and diethyl amine (DEA). This catalyst resulted in similar catalytic performances when it was compared to a catalyst that was synthesized with an expensive di-quaternary ammonium surfactant.[95]

Most surfactant soft-templating techniques result in disruptive mesopore formation along the b-axis. In this aspect, the group of Zhang et al. was able to produce a single-crystalline mesoporous MFI zeolite with sheet-like mesopores along the a- and b-axis. They used a triply branched surfactant with diquaternary ammonium groups, connected to 1,3,5-triphenylbenzene by a six- and eight-carbon alkyl chain. These surfactants were able to self-assemble and gave a highly ordered orientation due to π-π stacking.[96] In another study, Tian et al. used a non-surfactant dual functional polymer-based template. They synthesized a cationic non-surfactant polymer that enabled the synthesis of ZSM-5 with open, interconnected mesopores in a 3D single-crystalline zeolite. This material contained a mesoporous shell and a conventional zeolite core.[97] Sadrara et al. produced mesoporous ZSM-5 crystals by using decyltrimethylammonium bromide as mesoporogen and tetramethylammonium hydroxide as SDA. Certain ratios of these templates allowed the formation zeolites with well-developed 4 to 10 nm mesopores, with preservation of the crystal structure and acidity.[98] Hollow ZSM-5 with intracrystalline mesopores have also been synthesized with

soft templates containing ammonium groups. In this aspect, a gemini-type quaternary ammonium cation surfactant together with tetrapropylammonium bromide (TPABr) can be used in a hydrothermal synthesis. The Fe-substituted hollow catalyst was tested for the hydroxylation of phenol with H_2O_2 to form dihydroxybenzenes wherein the highest activity was observed for the mesoporous catalyst.[99]

A popular quaternary alkylammonium template is CTA^+. Meng et al. used KOH in a cetyltrimethylammonium hydroxide (CTAOH) templated one-pot synthesis. The use of these cations influenced the dissolution rate. As an example, KOH led to a faster dissolution of the silica species.[100] The same group used CTAOH as template, which functioned as a bifunctional template in a RbOH-based alkaline synthesis gel. The use of Rb cations influenced the dissolution rate in such a way that the mesoporous texture of the amorphous precursor is retained to some extent, resulting in a zeolite with uniform mesopores. This stands in contrast to the use of KOH where the KOH disturbs the formation of micellar rods, leading to less ordered mesopores compared to the use of RbOH. Catalysis testing was performed for MTH, and better results were obtained when compared to conventional ZSM-5 zeolite.[101] The use of different alkali metals in combination with CTA^+ was further studied by Meng et al. They produced mesoporous ZSM-5 with CTA^+ as a sole template in a one-pot synthesis. Here, the mesoporous silica-alumina precursor is transformed in a dissolution-recrystallization mechanism. In this study, LiOH, NaOH, KOH, RbOH and CsOH were investigated. The use of KOH and RbOH led to a mesoporous ZSM-5, whereas NaOH, LiOH and CsOH led to an amorphous material.[102]

A careful use of soft *versus* hard templates is crucial. Zhou et al. synthesized different mesoporous ZSM-5 zeolites depending on the template used (CTAB and distearyl dimethyl ammonium chloride as soft templates, and carbon nanotubes as hard template). The synthesis in presence of carbon nanotubes resulted in ZSM-5 with well-preserved strong acid sites and a well-connected micro-mesopore network, which was not observed when the soft templates were used. This difference in pore architecture led to better catalytic results for the MTH reaction in case of the hard templated ZSM-5, as reflected in the higher BTX yield and lower carbon deposition rate.[103]

Other ways to induce mesopores are the use of organosilane or organosiloxane templates. Mesoporous high-silica ZSM-5 was for instance synthesized in the presence of dimethylhexadecyl [3-(trimethoxysilyl)propyl] ammonium chloride (TPHAC) in a seed-induced method, and contained intracrystalline mesopores of approximately 2-10 nm, which is in accordance with the micellar size of TPHAC.[104] A new organosilane, 1,6-bis(diethyl(3-trimethoxysilylpropyl)ammonium) hexane bromide, possessing a gemini-type structure, was synthesized by Zhu et al. and used as mesoporogen together with TPAOH (SDA). Tuning of the irregular mesoporosity was demonstrated by variation of the organosilane/TEOS ratio.[105] Other researchers have shown the formation of core-shell ZSM-5 with trimodal mesopores, of which the size gradually reduced from surface to core, in the presence of organosilyl components. This zeolite was produced in a one-pot approach with controlled orthogonal self-assembly, and was the result of the specific nanoscale phase separation between the dimethyloctadecyl[3-(trimethoxysilyl)propyl]ammonium chloride

(TPOAC) organosilane supramolecular assembly and the zeolite framework. Variation of the amount of organosilane enabled control over the mesopores in the core, shell and intermediate boundary.[106] The same TPOAC, but now in combination with TPAOH, was studied by Shen et al., who showed different morphologies by adjusting the composition of the synthesis mixture, in this way catalysts with nanorod morphologies and worm-like intracrystalline mesopores were created.[107] In another study, Xing et al. used an acid treated kaolin clay as an Al and Si source in combination with organosilanes. Hexadecyltrimethoxysilane was added as a mesoporogen in a SAC method. This catalyst showed better performances in the MTA reaction compared to a commercial ZSM-5.[108] Several other authors studied the use of similar templates, such as an organosilane quaternary ammonium salt with double-oxycarbonyl carbon chains (resulting in mesopores of 4 nm),[109] triethoxyvinylsilane (resulting in mesopores of 2.7 nm),[110] organosiloxane-polyether amine (resulting in mesopores of 6 -15 nm),[111] an organosiloxane ($C_{24}H_{57}O_{12}NSi_3$) (resulting in mesopores of 3-6 nm),[112] and phenylaminopropyltrimethoxysilane (PATMOS) (resulting in mesopores of 3-6 nm).[113]

Soluble polymers are another popular soft template. Polyacrylic acid was used as a mesoporogen by Guo et al. Small amounts of TPOAC were responsible for enhancing the connection between the growing crystal domains and the polymer. In this way, single-crystalline zeolites with mesopores around 5-20 nm were formed.[114] Liu et al. produced cuplike ZSM-5 agglomerates by using an MFI precursor seed solution as nucleation promotor and polyacrylamide for the crystal growth restriction. At lower temperatures monolithic nanocrystal agglomerates with a large number of intercrystalline mesopores were formed. Synthesis at higher temperatures led to a cuplike morphology with walls that were composed of monolayers of highly crystalline ZSM-5 (thickness < 200 nm). This catalyst showed excellent activity in the LDPE (low-density polyethylene) cracking due to its highly accessible acid sites and high acid strength.[115] Another synthetic, inexpensive polymer, namely polyvinyl alcohol (PVA), was used as mesoporous template by Miyake et al. This template gave rise to uniform mesopores of 15 nm.[116]

Polymers can also result in the construction of hollow hierarchical zeolites. Niu et al. were able to produce such structures by using polyvinylpyrrolidone as template in a one-pot hydrothermal synthesis method (Figure 7). The hydrophilic polymer resulted in intense interaction between polymer and framework. The amount of template is a way to control the particle dimensions. By incorporation of Mn, excellent activities were obtained for the oxidation of cyclohexane to cyclohexanol. This can be attributed to the good accessibility of the active sites and fast mass transfer in the hollow structure with nano- and mesochannels.[117]

Besides the common templates, other molecules have also been used as mesoporogen. A new anionic soft template, hexadecanesulfonic acid sodium salt was used to produce small mesoporous ZSM-5 crystals of around 100-400 nm.[118] Tian et al. produced mesoporous ZSM-5 by adding imidazole to the synthesis mixture. This mesoporous catalyst showed better selectivity and higher catalytic lifetime in the MTA reaction, compared to a conventional ZSM-5.[119]
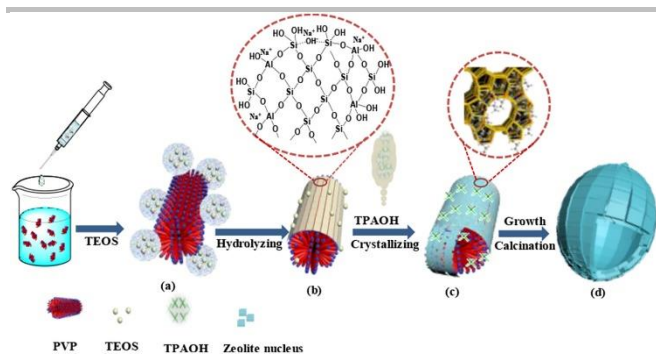
Figure 7. Imaginative scheme for the morphology evolution of hierarchical hollow ZSM-5.[117] Reproduced with permission of Elsevier.

Given the trend towards green and sustainable synthesis, bio-derived molecules were also screened for their template potential. The group of Chen et al. used gelatin where the pores in the hydrogel served as a microreactor. They were able to affect the zeolite porosity by adjusting the gelatin/H_2O ratio. When using a specific ratio, mesopores around 15 nm were formed inside the crystals.[120] Carbohydrates are another cheap option to be used as bio-templates. For instance, soluble starch was used as a bio-template for the synthesis of mesoporous ZSM-5. The introduction of mesopores was found effective given the higher activity of the mesoporous zeolites in the esterification of acetic acid with benzyl alcohol.[121] Disaccharides such as sucrose can also act as soft mesoporogen. Their use generates mesoporous ZSM-5 with reduced acid site density and increased mesoporosity with 4 nm mesopores. The catalyst showed an increased lifetime and decreased coking rate in the methanol to gasoline (MTG) reaction.[122] Jin et al. used sucrose as a template to create a chainlike structure by using high sucrose contents. The materials typically have a high mesoporosity and surface area with nm sized mesopores.[123] Monosaccharides such as glucose can also assist in mesopore creation. Feng et al. used glucose in a precrystallization step to form semi-crystalline amorphous species. A second crystallization step transforms this into fully-crystalline mesoporous ZSM-5. This two-step method gave a lower number of acid sites and weaker acid strength compared to a conventional one-step crystallized ZSM-5.[124] It is the group of Che et al. who made a comparative study of different green templates. Sucrose, starch and cellulose with different molecular sizes were used as soft template. The addition of 10 % starch resulted in superior acidity and porosity, compared to the other prepared catalysts, and this mesoporous ZSM-5 gave the highest BTX yield in the catalytic pyrolysis of biomass.[125] Functionalized carbohydrates such as carboxymethyl cellulose was used as a mesoporogen by another group. The obtained mesoporous ZSM-5 showed superior activity for the acetalization of cyclohexanone with methanol.[126] Fibrous mesoporous ZSM-5 was synthesized with the aid of another bio-template, namely sodium alignate. Here, the carboxyl and hydroxyl groups of the polymer induced a self-stacking of the growing ZSM-5 nanocrystals along the direction of the *b*-axis.[127] In a last soft templating study with bio-derived molecules, Zhang et al. produced hierarchical ZSM-5 in the presence of L-lysine during a kinetic-modulated crystallization. The use of L-lysine induced oriented aggregation of protozoic nanoparticles. A subsequent intraparticle ripening of the crystals delivered nicely interconnected mesopores.[128]

Hard templating

Jacobsen et al. was one of the first to prepare mesoporous ZSM-5 crystals with hard templates.[129] Excess of zeolite gel with carbon particles allowed zeolite crystal growth around the carbon particles. Controlled combustion removed the carbon particles leaving mesoporous ZSM-5 crystals. Later, many other studies were performed on the creation of mesoporous MFI crystals with hard templates. For example, carbon nanotubes (CNTs) and nanofibers,[130,131] ordered mesoporous carbons,[132,133] non-ordered carbon aerogels or mesoporous carbons,[134–136] pyrolyzed wood or carbonized rice husk,[137,138] $CaCO_3$ nanoparticles[139] and polystyrene (and other polymeric) microspheres.[18,140–142] These have been complemented in the last 5 years with other hard templates and template synthesis methods. Similarly, there is a tendency to use bio-derived hard templates as a cheaper and greener alternative.

One of these modified templates is hydrophilic carbon black. Commercial hydrophobic carbon black was oxidized using a sodium hypochloride solution. A mix of hard template and synthetic precursor is crystallized and calcined, leading to mesoporous single crystal-like aggregates of approximately 2 μm with a narrow pore size distribution, viz. 5-18 nm. The hydrophilic nature of carbon was essential to allow high dispersion of the template in the synthesis. Previous attempts have shown formation of aggregates resulting in wider mesopore size distribution. The amount of hydrophilic carbon black controls the textural characteristics and acidity of the final zeolites. The uniform mesopores resulted in an enhanced mass transfer which resulted in enhanced catalytic performances in the toluene disproportionation, compared with conventional ZSM-5.[143,144] Zhao et al. also selected hydrophilic carbon nanoparticles to avoid phase separation issues. In this case, the hydrophilic carbon is prepared by carbonizing polyethylene oxide mixed with urea. Hard templating gave mesoporous ZSM-5 with large 12.5 to 34.5 nm pores, depending on the size of the carbon nanoparticles. The presence of surface -C-O-C- and -C-O-H groups is proposed to promote the synthesis of mesoporous ZSM-5 with preference of aluminum in the framework. The high Brønsted acidity in the mesoporous pore architecture led to a high ethanol to olefin reaction stability (on stream) and the highest conversion rate in the sterically demanding benzylation of mesitylene with benzyl alcohol.[145]

Additional modification of popular templates was for instance suggested by Zhang et al. They used tetrabutylammonium bromide (TBABr) grafted multiwall carbon nanotubes (MWCNTs) as bifunctional hard template to synthesize mesoporous ZSM-5. They controlled morphology and acid properties by varying the amount of TPABr. Grafting of MWCNTs clearly led to more effective utilization of the hard template. The mesoporous ZSM-5 had highly interconnected mesopores of 20-30 nm, identical to the MWCNTs diameter.[146] Flores et al. also focused on the use of modified CNT's as hard template. Here, a mesoporous Co/ZSM-5 was synthesized by using CNTs impregnated with cobalt. When pristine CNTs followed by a Co impregnation step were used, the sample surface area and pore volume was significantly reduced. One of the reasons for this effect was plugging of the pores by Co_3O_4. In contrast, samples prepared with Co/CNTs showed surface areas and microporous volumes similar to the pure zeolites, but with a three to fourfold mesopore volume. The use of pristine *vs.* Co/CNTs also determines high contents of Lewis and

14

Brønsted acidity respectively. These Co/CNTs prepared ZSM-5 zeolites showed to have an up to eightfold higher reaction rate in Fischer-Tropsch synthesis (normalized by reducible Co) compared to a catalyst that was prepared by conventional impregnation. In addition, a higher selectivity towards isomerized branched hydrocarbons was also noticed.[147] A similar CNT hard template but with Ga was proposed by Chen et al. The researchers synthesized Ga/ZSM-5 using the Ga-immobilized CNTs hard template in the classic SAC method. Similarly, the use of Ga/CNTs instead of pure CNTs followed by Ga impregnation, was more effective to generate mesoporous ZSM-5. Moderate mesoporosity with a high surface concentration of (GaO)$^+$/Brønsted acid sites was obtained. The mesoporous Ga/ZSM-5 proofed to be beneficial for methanol aromatization.[148] The effect of (I) CNTs, (II) carbon nanofibers and (III) graphene oxide as hard templates was studied for the synthesis mesoporous ZSM-5 in presence of TPAOH as SDA. In analogy with the mesoporization of FAU zeolites (see Section 4.2), the use of graphene oxide results in the highest mesoporosity and largest pore size. This mesoporous ZSM-5 showed the highest selectivity towards propylene in the MTO reaction among the tested catalysts.[149,150]

The crystallization method in hard template synthesis can be different and impact the material's properties. The use of MWCNTs during a (I) hydrothermal or (II) SAC synthesis was for instance compared by Qiu et al. The SAC method is clearly preferred for CNTs hard templates because of less phase-separation issues, and thus higher mesoporosity.[151]

Other carbon structures can also function as hard templates. Activated carbon is a first example, but a comparative study with CNTs revealed a higher amount of amorphous phase and inaccessible large gaps between the crystals, whereas CNTs create extra channels inside the crystal. Different catalytic results were associated to the pore architecture. As an example, CNTs assisted synthesis of mesoporous ZSM-5 zeolites outperformed amorphous carbon assisted zeolites in the catalytic cracking of LPG to ethylene and propylene.[152] Liu et al. also used activated carbon, but in a solvent free one-pot synthesis with mechanical mixing of the solid raw materials prior to a heat treatment. With this method, a highly crystalline ZSM-5 zeolite with macro and mesopores of respectively 68 and 2.6 nm was obtained. This mesoporous ZSM-5 was very active in the MTG reaction.[153] Abildstrøm et al. used metal nanoparticles instead of carbon to synthesize mesoporous ZSM-5. They added Ni nanoparticles to the silica gel. Coke carbon templates were grown on the metal clusters via a chemical vapor deposition. After crystallization and calcination, ZSM-5 with mesopores of approximately 17 nm were formed. This zeolite showed higher isomerization and cracking activity of n-octane in comparison with the conventional zeolite.[154]

In another strategy, silica-carbon composite materials are fabricated prior to crystallization. Hierarchical ZSM-5 was for instance produced using a polyurethane sponge. In a first step, the sponge was contacted with a silica and alumina precursor solution, followed by a SAC hydrothermal treatment with an ammonium hydroxide aqueous solution. After three repeating cycles, the material was impregnated with TPAOH, followed by another SAC with water. After calcination, a ZSM-5 product with the shape of the original sponge was obtained.[155] Liu et al. used

a SiO$_2$/carbon composite as a silica source and template in a hydrothermal synthesis method. The structure of the composite significantly affected the pore structure, and ZSM-5 with intercrystalline meso- and macropores was created.[156] Silica composites were also used by Peng et al. They produced a hierarchical ZSM-5 in accordance to Murray's law (i.e., the cubes of the radii of the parent vessel should equal the sum of the cubes of the radii of the daughter vessels). They used amorphous nano-silica spheres coated with porous carbon and impregnated them with a mix of an aluminum source and TPAOH. A SAC method was used to obtain crystalline mesoporous ZSM-5. Calcination of the composite material recovered pure mesoporous ZSM-5 (Figure 8). This catalyst showed a much higher conversion rate in the cracking of isopropylbenzene, compared to prepared nano-ZSM-5.[157]
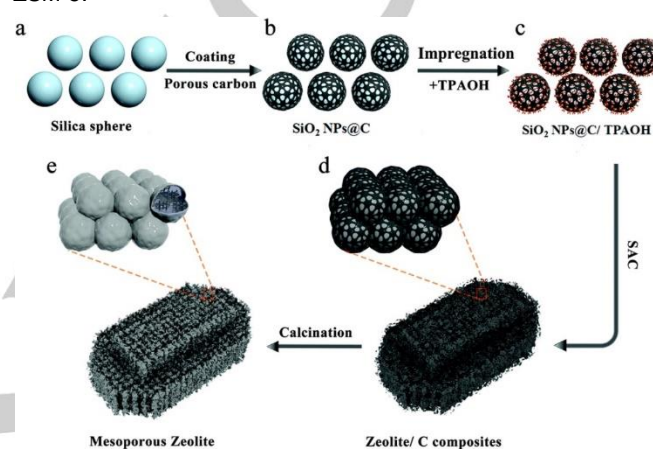
Figure 8. Schematic representation of the crystallization process of mesoporous zeolite crystals. (a) Original nanosized silica sphere. (b) SiO$_2$NPs@C composites. (c) SiO$_2$NPs@C composites impregnated with a TPAOH solution. (d) Formation of zeolite/C composites after SAC treatment. (e) Final mesoporous zeolite crystals after calcination.[157] Reproduced with permission of The Royal Society of Chemistry.

Bio-based hard templates also gained interest in recent years. Such templates are mostly cheap and may result in more sustainable mesoporization synthesis routes, especially when obtained from waste streams. Corn and sorghum stem piths, composed of cellulose, hemicellulose and lignin, were for instance evaluated as sacrificial hard template. This bio-organic material is spongy in nature and has interconnected macropores. Given the surface of the pith is negatively charged at the used pH, dipping of the organic material into poly (diallyldimethylammonium chloride) facilitates adsorption of the negatively charged silica prior to a classic SAC method. After calcination, a hierarchical ZSM-5 material with connected micro-, meso- and macropores was recovered. Higher conversion rates compared to the conventional ZSM-5, mesoporous ZSM-5 (prepared via alkaline treatment) and Al-SBA-15 was observed in the presence of the bio-templated ZSM-5 for the esterification of benzyl alcohol with hexanoic acid.[158] Zhang et al. used soluble-starch as an in-situ bio-template for mesoporous ZSM-5 synthesis. Here, a precursor solution with the soluble starch was first heated, resulting in carbonized starch. Hereafter, the solution was hydrothermally treated, resulting in the mesoporous catalyst. They found unordered pores with non-uniform pores of different sizes. The material showed excellent thermal and hydrothermal stability, but catalysis was not performed.[159] In-situ hydrothermal carbonization of sucrose in a SAC method (with ethylene diamine

instead of NaOH) was developed by Zang et al. to create mesoporous ZSM-5 with SiO_2/Al_2O_3 ratios as low as 30. A comparative study with soft templating methods using P123 and PEG revealed poor mesoporization because of dissolution of the soft templates out of the precursor gel in the alkaline environment.[160] Another study used sucrose as a hard template with pre-crystallization and dry gel methods, showing that pre-crystallization led to a higher crystallinity and BET surface area.[161] Nanocrystalline cellulose is an alternate hard template to synthesize mesoporous ZSM-5. Tailoring of the pore structure and acidic sites was demonstrated by playing with the template/precursor ratio. After modification with metallic Ni, this catalyst was successfully tested in the reductive splitting of cellulose into hexitols.[162] Furthermore, chitin (the exoskeleton of insects and crustaceans) is an interesting low-cost hard bio-template for the synthesis of mesoporous ZSM-5.[163,164] The obtained material with 15-50 nm mesopores successfully adsorbs crystal violet dye, and obtained a much higher capacity than conventional ZSM-5.[163] Bacterial cellulose converted into active carbon also gave promise to a sustainable synthesis of mesoporous ZSM-5. Due to the improved mass transfer performance, the authors showed an exceptionally high adsorption rate of formaldehyde.[165] Instead of carbonizing bacterial cellulose, it can also be coated with aluminosilicates and TPAOH as a precursor scaffold. Vapor treatment of this structure resulted in self-assembled three-dimensional b-oriented MFI superstructures with meso- and macroporosity.[166] To conclude, Gomes et al. used sugar cane bagasse and biomass-derived compounds by hydrolysis of the sugar cane. This approach yielded mesoporous zeolites with particular morphologies and broad differences regarding external surface areas (between 51 and 153 m² g⁻¹), Si/Al ratio (between 8 and 29) and zeolite crystal size (between 0.3 and 13 μm). The catalysts were tested in the cracking of n-hexane, and the MTH reaction. A positive correlation was found between activity and high Al content for n-hexane cracking. Mesoporous ZSM-5 with a high external surface area and Si/Al ratio converted methanol mainly into light olefins, whereas a lower external surface area and Si/Al ratio yielded gasoline precursors, in line with the mechanism of the MTH reaction.[167]

Template free

Different methods for the bottom-up synthesis of zeolites without hard or soft mesoporogen templates can be distinguished. One uses physical methods to create mesopores.[168–170] This can be the use of an ultrasound treatment to assist the formation of mesoporous ZSM-5 (Figure 9),[168,169] or the use of mechanical pressing and high-temperature treatment of zeolite particles into stacked catalysts.[170]

The template free synthesis of mesoporous ZSM-5 often relies on the SAC method. He et al. synthesized mesoporous ZSM-5 with Si/Al ratios ranging from 30 to 150. This was done by varying the TPAOH concentration, as higher Al-doping resulted in a higher need of TPAOH.[171] Ge et al. succeeded in the synthesis of single-crystalline mesoporous ZSM-5 having an abundant 3D interconnected network based on the SAC method using small amounts of TPAOH.[172] The method was also applicable for high-silica crystals.[173] Similarly, Rilyanti et al. also used a TPA⁺ lean SAC, and found that the presence of mesopores is attributed to the presence of severe defect sites.[174]

Zeolitization of mesoporous material with SAC often only results in a partial conversion, causing composite materials. However, transformation of Al-SBA-16 to fully crystalline mesoporous ZSM-5 was successfully demonstrated. This ZSM-5 catalyst showed promising activity in the benzylation of mesitylene and performed better than the commercial ZSM-5.[175] Other hierarchical ZSM-5 zeolites were produced by a dry gel conversion-SAC method using different Si/TPA⁺ ratios. High ratios led to hierarchical ZSM-5 with intracrystalline mesopores, whereas low ratios gave zeolite assemblies with intercrystalline mesoporosity.[176] Two-step mesoporous ZSM-5 syntheses were also reported. A carbonaceous SBA-15 was formed by an in-situ carbonization of an SBA-15/P123 composite, followed by SAC after impregnation with TPAOH. A wormlike morphology, similar to the SBA-15, was obtained. In another sample, 1,3,5-trimetylbenzene was added as swelling agent at the SBA-15/P123 stage, resulting in micro-spherical forms.[177] Similarly, Zhang et al. impregnated mesoporous silica spheres with a precursor solution to obtain hierarchical ZSM-5 using SAC, resulting in a porous ZSM-5 with 300 to 500 nm macropores interconnected with 50-90 nm pores.[178]
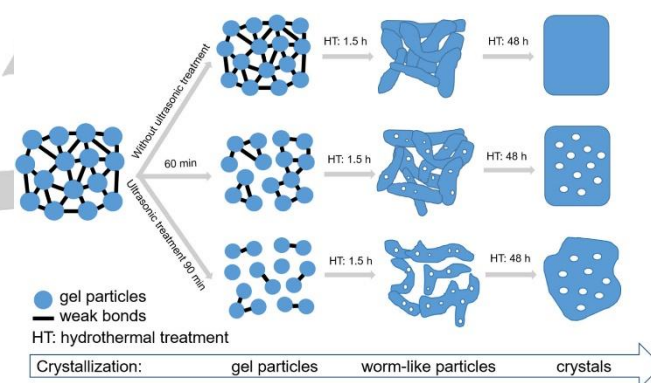
Figure 9. Schematic representation of the mesopore formation by ultrasonic treatment.[169] Reproduced with permission of Elsevier.

Adjustments of the classic hydrothermal synthesis conditions also allows mesoporization of ZSM-5 without templates. Hartanto et al. produced a mesoporous ZSM-5 in a seed-assisted synthesis. The group dispersed cheap kaolin in highly alkaline NaOH solution, inducing the formation of ZSM-5 zeolite. The excess NaOH acted as a desilicating agent forming mesopores in the formed zeolite crystals.[179] Other one-step template-free syntheses of mesoporous ZSM-5 followed a combination of two strategies: (I) the silicalite-1 seed-induced interface assembly and (II) the acidic co-hydrolysis/condensation of aluminosilicate species and alkali-earth metals.[180] Single crystalline mesoporous ZSM-5 was synthesized in a one-pot using sodium carbonate, yielding uniform crystals around 200 to 300 nm in size with high pore volume.[181] Kadja et al. were able to produce template-free a mesoporous ZSM-5 under 100 °C after systematic optimization of the Si/Al, TPA⁺/Si and H_2O/Si ratio.[182]

Other non-classical template-free crystallization methods are the solid-state crystallization and the crystallization with vapor phase transport. The latter was applied by Zhao et al. wherein a mesoporous ZSM-5 was synthesized by alkaline etching of shaped precursors using trimethylamine and ethylenediamine.[183] A solid-state crystallization was introduced by Wang et al. In a first step they produced aluminosilicate nanogels resulting in dried

nanoparticles. Next, transformation of the particles to zeolites relied on the intrinsic water content, and gave fused nanocrystals with stable mesoporosity.[184]

Template-free synthesis can also form hollow ZSM-5 spheres. A hollow sphere of stacked ZSM-5 crystals with inter- and intracrystalline mesopores was made by Wu et al. Here, ZSM-5 crystals, silica spheres and NH_4F were grinded together and subsequently crystallized during a solid-state crystallization. In this process, the pre-made ZSM-5 functions as a confined Al-source, whereas NH_4F is a mineralizer (Figure 10). The catalyst was tested with success in the MTG reaction.[185] Hollow ZSM-5 can also be obtained by adjustment of the hydrothermal synthesis. This can be done in a one-pot hydrothermal synthesis with a high concentration of SDA, and occurs through a dissolution-recrystallization process. The less dense Al-low and amorphous particle center preferably dissolves and recrystallizes on the outer layer of the zeolite crystals. Mesoporous hollow ZSM-5 crystals of 1.5 µm were produced with a shell thickness of around 200 nm.[186] Wang et al. produced a bayberry-shaped MFI zeolite, consisting of an hollow assembly of zeolites. Here silicalite-1 seeds with $NaAlO_2$ were contacted with silica microspheres of around 15 µm. The dried samples were crystallized in a SAC method. After 24 h, the amorphous phase was fully transformed into the MFI phase and a hollow bayberry-shaped morphology was produced. This catalyst showed higher conversion and longer lifetime compared to non-hierarchical ZSM-5 zeolites in the MTA reaction.[187]

Figure 10. Proposed reaction mechanism for the creation of a hollow sphere with stacked ZSM-5 zeolites.[185] Reproduced with permission of Wiley-VCH Verlag GmbH & Co. KGaA.

Nanozeolites and their assembly

This section summarizes the recent publications related to zeolite nanostructures. New synthesis procedures of nanostructures, hierarchical nanoparticles and assemblies of nanostructures will be discussed. The term 'nanozeolite' is often used for zeolites with at least one dimension smaller than 100 nm. Frequently, methods or a combination of methods of the previous parts are used during synthesis.[188] New procedures for the synthesis of conventional non-mesoporous nanozeolite particles go beyond the scope of this review.

A common strategy to create hierarchical zeolites is the formation of nanozeolite assemblies. This is often accomplished with the aid of a nanozeolite seed-solution (ZSM-5 or silicalite-1). Addition of CTAB as mesoporogen in the seed-solution is a well-known strategy as well that leads to assembly of nanostructures, impeding crystal growth.[189–191]. For economic reasons, the use of a lower amount of CTAB has been studied. Chen et al. synthesized 400-600 nm aggregates of 20-50 nm ZSM-5 crystals

starting from silicate-1 seeds with no additional templates and trace amounts of CTAB.[192] Ultimately, $CTAB/SiO_2$ molar ratios as low as 0.008 were used to synthesize nano ZSM-5 aggregates from silicalite-1 seeds, of which the size of the crystals in the aggregates can be tuned, depending on the used ratio.[193] Seed-assisted synthesis with other mesoporogens than CTAB was studied as well. Nanocrystal agglomerates can be synthesized from a seed solution and polyacrylamide as mesoporogen. Upon removal of the template, inter- and intraparticle mesopores were formed.[194] Ultrafine and high silica ZSM-5 aggregates were also synthesized successfully from silicalite-1 seeds in the presence of hexatrimethylammonium bromide (HTAB) as mesoporogen in a solid state-like conversion. The finding of this work supports the occurrence of a kinetics-controlled dissolution/induction/ growth/aggregation mechanism.[195]

For economic and ecological reasons, seeding methods without use of organic mesoporogens have been proposed. Zhang et al. studied a seed-induced method in combination with a salt-aided route. They synthesized nanocrystallite-oriented self-assembled ZSM-5 and ZSM-5 with intracrystalline mesopores, and suggested that the seeds function both as micropore and mesopore template at the same time. Regulation of morphology is possible by playing with the amounts of KF and TPABr, or other SDA's. This regulation alters the kinetics of seed dissolution and seed-induced recrystallization.[196] Mesoporous bundle-like MFI crystals with a core-shell structure have also been reported in template-free seed induced conditions. Silicalite-1 seed acts as matrix to grow precursor particles, which crystallizes in epitaxial and anisotropic direction. This unique structure seems to be the result of the interplay of thermodynamics and kinetics.[197] Shen et al. were able to synthesize a meso-macroporous ZSM-5 using an additive-free, seed-assisted hydrothermal procedure in which they deliberately employed a low SDA/SiO_2 ratio. A mesoporous assembly of 20-50 nm nanorods was obtained. A Zn modified version was used to catalyze the MTA reaction, wherein a longer lifetime and higher selectivity towards total aromatics was observed in comparison to the conventional Zn/ZSM-5.[198] An assembly of (fairly aligned) Al-rich rod-like ZSM-5 nanocrystals was also obtained by Zhang et al. in template-free conditions with seeds. The resulting crystals were an assembly of rod-like nanocrystals. The inter-rod distance, responsible for mesopore volume, was around 10-30 nm. These rods showed beneficial catalytic properties during the catalytic cracking of cumene.[199] Nanocrystal agglomerates were synthesized from deionized silicalite-1 seeds (without mesoporogen) which reacted with ammonia to circumvent the time-consuming ion-exchange in further steps as the zeolite is already in the NH_4^+ form. With this method, zeolites with micro-, meso-, and macropores were obtained which showed great improvements in the catalytic lifetime during the dehydrogenation of glycerol to acrolein due to the enhanced resistance to coking.[200]

It may be also cost-effective and eco-friendly to synthesize ZSM-5 aggregates with low amount of SDA and using silicalite-1 seeds, but without combustion of the SDA. For instance, silicalite-1 seeds with a low concentration of TPAOH as SDA were synthesized and the formed mesoporous ZSM-5 aggregates were used as catalyst for LDPE cracking.[201]

Besides organics such as quaternary ammonia, the use of organosilanes is another common strategy to create mesoporous

nanoaggregates of ZSM-5. The reports often mention the use of a seed-solution. Li et al. for instance obtained hierarchical ZSM-5 powders from TPOAC and zeolite seeds in a rotation synthesis. The aggregates occur in a core-shell conformation, with loosely packed nanoparticles in the shell and mesopores of 4 to 22 nm and is produced by kinetic control through a nanoparticle oriented-aggregation mechanism.[202] Ahmadpour et al. also studied the effect TPOAC, but with addition of CTAB in a one-pot hydrothermal synthesis. To maximize mesoporosity (without compromising in microporosity), they found a 3:1 molar ratio of TPOAC:CTAB and a 0.02 molar ratio of (TPOAC + CTAB)/SiO$_2$ most suitable.[203] Liu et al. used other growth factors such as (3-aminopropyl)triethoxysilane and γ-chloropropyltriethoxysilane, leading to 1-2 µm sized spherical aggregates of nano-sized ZSM-5 zeolites with mesopores between 2-4 nm. The aggregates showed a higher CO$_2$ adsorption rate and capacity compared to conventional ZSM-5.[204] Similar CO$_2$ adsorption studies were done by Qian et al. who used organosilanes with different chain lengths: (I) trimethoxypropylsilane, (II) trimethoxyoctylsilane and (III) trimethoxydodecylsilane. The authors found the highest adsorption rate and capacity when the shortest organosilane was used in the synthesis. This could be attributed to the high mesopore volume and surface area.[205] Li et al. made mesoporous nano ZSM-5 aggregates with a similar short organosilane (3-aminopropyltrimethoxysilane), that effectively passivates and rapidly self-condensates. A high activity for the methanol to propylene reaction was observed.[206] The use of 3-glycidoxypropyltrimethoxysilane also led to a nanocrystalline self-assembly with ZSM-5 characteristics, but with 3 µm large spherical forms (Figure 11). Mesopores originated from the 2.1 nm intercrystalline distance between the 50-100 nm sized ZSM-5 crystals.[207] Hexadecyltrimethoxysilane was used as template in a hydrothermal synthesis method to generate hierarchical ZSM-5 with specifically nanocrystals on the surface of an intact ZSM-5 zeolite.[208]

The group of Serrano et al. tested the ability of sequential combinations to synthesize a mesoporous ZSM-5 zeolite. The crystallization process used silanized protozoic units, and was followed by a treatment with an alkaline surfactant/ammonia-containing solution. This enabled the reorganization of the irregular mesopores from the silanized protozeolitic units to more uniform 4 nm mesopores in the zeolite aggregate.[209]

Commercial organsilanes are very popular, but synthesis of tailor-made templates is a new trend. For instance, an organosilane with three alkyl chains and three silicon atoms on each chain, resulted in catalysts made up of 60-150 nm crystals.[210]

Nanoaggregates can also be synthesized using other diverse soft templates, such as nitrogen-containing organics. The group of Shen et al. aimed to synthesize ordered two-dimensional mesoporous MFI zeolites, and they achieved this by inserting azobenzene in the hydrophobic tail of the surfactant. Modification of the hydrophobic part is clearly a handle to tune morphological aspects of the nano-assemblies.[211] Another successful synthesis of mesoporous self-assembled ZSM-5 microspheres resulted from the intergrowth of primary nano-strips using *n*-hexylamine as template. The size of the primary particles, that can be altered by the alkalinity of the synthesis gel, controlled the mesopore size distribution. Advantages due to the mesoporosity were proposed for the catalytic cracking of LDPE.[212] Dual-functional N-containing templates were used by Barakov et al., showing

differences depending on the template used. The use of [C$_6$H$_{13}$-N$^+$(CH$_3$)$_2$-C$_6$H$_{12}$-N$^+$(CH$_3$)$_2$-C$_6$H$_{13}$](Br$^-$)$_2$ (C$_{6\text{-}6\text{-}6}$Br$_2$) or [C$_8$H$_{17}$-N$^+$(CH$_3$)$_2$-C$_6$H$_{12}$-N$^+$(CH$_3$)$_2$-C$_8$H$_{17}$](Br$^-$)$_2$ (C$_{8\text{-}6\text{-}8}$Br$_2$) resulted in an assembly of ZSM-5 nanoparticles, whereas the use of [C$_{16}$H$_{13}$-N$^+$(CH$_3$)$_2$-C$_6$H$_{12}$-N$^+$(CH$_3$)$_2$-C$_6$H$_{13}$](Br$^-$)$_2$ (C$_{16\text{-}6\text{-}6}$Br$_2$) resulted in an assembly of randomly oriented flake-like ZSM-5 zeolite particles. Smaller zeolite nanoparticles were obtained by combining CTAB with C$_{8\text{-}6\text{-}8}$Br$_2$, resulting in high specific surface area, high mesopore uniformity and better accessible Brønsted acid sites for sterically demanding molecules. A higher B/L acidity can be achieved by addition of TPAOH. Alternatively, the addition of CTAB to C$_{16\text{-}6\text{-}6}$Br$_2$ promoted the formation of the lamellar mesostructures, which became self-pillared (with higher specific surface area, higher mesopore uniformity and increased B/L acid site ratio) by adding TPAOH to the synthesis mixture. The select use of dual-functional templates, combined with TPAOH and CTAB, thus allows designing ZSM-5 mesoporous structures with different porosity and tunable acidity. The effect on catalysis is not reported.[213]
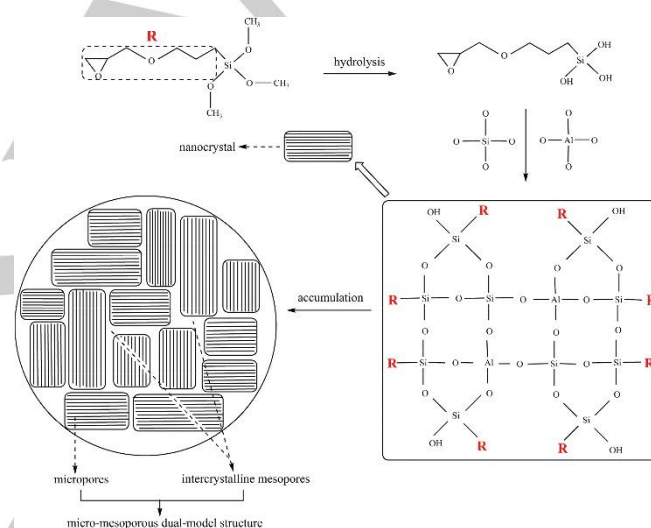
Figure 11. The formation mechanism of self-assembled hierarchical ZSM-5. Crystal growth is inhibited by the bond-blocking R-groups, resulting in nanocrystalline aggregates.[207] Reproduced with permission of Elsevier.

Polymers can also help in the formation of nanozeolite aggregates. An aggregate of 30 nm sized ZSM-5 crystals was synthesized using anionic polyacrylamide as template. The authors showed some control over the mesopore structure by varying the amount of template.[214] Dong et al. produced an assembly of ultrafine crystals wherein they varied the amount of SDAs on a cationic polymer. With this strategy, zeolites with a mean crystallite size as small as around 7 nm could be produced.[215]

Nano-assemblies can also be formed by chemical crosslinking. Shang et al. produced an assembly of nanozeolites using a suspension of nanozeolites and a soluble aluminosilicate. After a microfluidic jet spray drying step, particles from 70 to 108 µm with spherical, bowl-like or dimpled morphologies were formed, depending on the parameter conditions. In this process, soluble aluminosilicate act as stabilizer in the drying process and as cross-linker to chemically bind the preformed nanozeolites. This drying process enabled the synthesis of aggregates with uniform 6 nm sized mesopores.[216]

Synthesis of ZSM-5 nanoaggregates in absence of preformed MFI seeds and mesoporogens is possible. Li et al. demonstrated the formation of high-silica nano ZSM-5 aggregates that were built from 20-70 nm sized nano-crystallites by using an SDA-lean dry gel solid-like state in the SAC conversion method which is a kinetically-controlled nucleation/growth/aggregation process. Mesopore size control was done by alkalinity variation.[217] Sashkina et al. attempted changes in the H_2O/SiO_2 ratio of the precursor solution in a hydrothermal synthesis to get ZSM-5 nanocrystalline aggregates. They found a decrease of crystal size to nanometer scale and a wider crystal size distribution by increasing the ratio. The lower ratios (10 to 100) created aggregate-like mesoporous/hollow ellipsoid crystals, whereas a high ratio of 300 gave nano-pill-shaped crystal formation.[218] A Na-free hydrothermal synthesis was investigated and yielded ZSM-5 aggregates of 20 nm sized crystals with intercrystalline voids of 1 to 10 nm.[219] ZSM-5 nanoparticle aggregates were synthesized under low-solvent conditions by Shi et al. They converted Al-SBA-15 that was pre-synthesized with P123. Decomposition of P123 in the synthesis conditions created the confined mesoporous space surrounding the 20-40 nm sized nano-units. A type of interconversion or local dissolution/precipitation may be suggested given the aggregates closely resemble the size of the parent Al-SBA-15.[220] In another study, ZSM-5 aggregates were synthesized using 1,6-diaminohexane and CTAB as SDA and mesoporogen, respectively. In the crystallization process, mesoporous silica-alumina species were formed with the aid of CTAB, followed by a transformation to hierarchical ZSM-5 aggregates with the aid of 1,6-diaminohexane.[221]

Another common type of nanostructures is defined as nanosheets, and was mentioned sporadically above under particular conditions. These platelet structures can be formed with different methods. Fan et al. produced multi-lamellar ZSM-5 nanosheets using silicalite-1 as seed and TPOAC as organosilane. The zeolite nanosheets were stacked in a disordered manner forming mesoporous zeolite aggregates. The random house-of-cards-like (HCL) stacking, which was responsible for the interplate space, penetrated through the whole aggregate particle.[222] Moukahhal et al. developed a synthesis procedure to aggregate the ZSM-5 nanosheets in beads. The group used a pseudomorphic transformation of large amorphous mesoporous silica beads of 20, 50 and 75 μm. Mesopores with an average diameter of 3.9-4.7 nm were obtained.[223] In another study, Yan et al. used TPAOH and an ammonium surfactant, viz. $C_6H_5-C_6H_4-O-C_{10}H_{20}-N(CH_3)_2-C_6H_{13}$, in a dual templating synthesis method to create various bodies of ZSM-5 nanosheets (e.g. ultrathin ZSM-5 nanosheets, split-like nanosheets and condensed packing plates), depending on the precise ratios of the templates.[224] Other nanosheets were produced by using TPAOH in combination with octadecyltrimethylammonium chloride (C_{18}TMAC), CTAB or tetradecyltrimethylammonium bromide (C_{14}TMAB) in a hydrothermal synthesis.[225] An assembly of zeolite nanosheets was produced using a seed-assisted synthesis with a bolaform surfactant (an amphilic molecule with hydrophilic groups linked with a hydrophobic alkyl chain).[226] Higher Al content in the nanosheets changed the organization of the crystals in the aggregates from nanosheet stacks to HCL structures.[227] Another tetra-headgroup rigid bolaform quaternary ammonium surfactant was used to create a multi-lamellar

mesoporous ZSM-5. The dual-functional amphiphilic surfactants play a critical role for directing the structure with high mesoporosity.[228] Wei et al. were able to regulate the nanosheet stack size of mesoporous 2D MFI zeolites by changing the precursor cations and anions. They found that the following order was most suitable for the generation of inter-crystalline mesopores: $Na^+ > K^+ > Rb^+ > Cs^+$ and $SO_4^{2-} > NO_3^- > Cl^-$. The cations and anions did not influence the acidity of the zeolite, however, the hydrothermal stability was effected in accordance with the following order: $Na^+ < K^+ < Rb^+$ for cations and $SO_4^{2-} < Cl^- < NO_3^-$ for anions.[229] The thickness of nanosheets was modified in another study. A gradual change in the amount of Na^+ in a synthesis with C_{18-6-6}, controlled the thickness of the nanosheets over a range of 2.5 to 20 nm.[230] Seed-fused ZSM-5 nanosheets were produced by Shang et al. by adding ZSM-5 seeds in a hydrothermal synthesis with a $C_{18-6-6}Br_2$ template to reduce the extra-large external acidity that may cause rapid catalyst deactivation in for instance the methanol to propylene reaction. A 5 to 30 wt% increase of the seed amount shortened the crystallization time, decreased the particle size, and reduced the acid strength and external acidity, while the micropore volume increased with 50 %. Superior catalysis for the methanol to propylene reaction was reported.[231] Epitaxial growth of layered nanosheets over bulky ZSM-5 zeolites, obtained by adding conventional ZSM-5 to a synthesis solution of lamellar ZSM-5, yielded a hierarchical core-shell ZSM-5 structure.[232]

Self-pillared MFI nanosheets with Ni nanoclusters were synthesized by Gong et al. In the one-pot hydrothermal synthesis with the bifunctional surfactant $C_{18-6-6}Br_2$, MFI nanosheets were affected by the content of Ni as Ni nanoclusters prevented the adjacent nanosheets of forming new Si-O-Si bonds. Furthermore, the self-pillared structure protected the nanosheet against collapse during calcination.[233] In another report, sandwich-structured Pt between ZSM-5 nanosheets was produced by an intercalated wetness impregnation of zeolite nanosheets. The nanosheets were produced using $C_{22}H_{45}N^+(CH_3)_2C_6H_{12}N^+(CH_3)_2C_6H_{13}](Br^-)_2$ as SDA. Pt served as pillars stabilizing the mesopores between the nanosheets.[234] Another method to stabilize the mesopores in between ZSM-5 nanosheets suggested the intercalation of silicon precursors in the zeolite, protecting the nanosheets from collapse even after calcination.[235]

Techniques that are typically used in top-down methods were also used to produce nanosheets. Alkaline steaming with TBAOH and ethylenediamine was used in the presence of zeolite seeds. Here, nanosheet assemblies were formed with a layer space of approximately 10 nm and mesopores around 3.5 nm.[236] Qin et al. produced a single-crystalline ZSM-5 by using NH_4F-etching. This etching removed Si and Al at similar rates, and preferentially removed less-stable defects. The progressive etching to the core was less facile due to the limited amount of structural defects.[237] In another study, NH_4F-etching was applied on layered ZSM-5 zeolites. This etching step resulted in a de-pillaring of the zeolite and thus shortening of the interlayer d-spacing.[238]

Other nanostructures such as nanosponges, nanorods and nanofibers were also reported. Hierarchical zeolites with a tri-modal porosity were created by Wu et al. This group produced a ZSM-5 zeolite with 90° twin intergrowth nanofibers using 1,6-

bis(methylpiperidinium)hexyl dibromide as template. Using this template, large crystal sizes (10 μm x 10 μm) were obtained with an open marcroporous architecture and uniform Al distribution. A subsequent desilication step created mesopores of approximately 10 nm.[239] Another group used a diquaternary ammonium surfactant (e.g. $C_{18}H_{37}$-N$^+$(CH_3)$_2$-C_6H_{12}-N$^+$(CH_3)$_2$-C_4H_9) in a dry-gel synthesis of MFI zeolites, forming a nanosponge material composed of 2.5 nm thick MFI nanolayers with mesopores centered around a diameter of 4 nm.[240] Simone et al. also produced a nanosponge-like morphology, composed of unilamellar MFI nanosheets of 2.5 nm. This synthesis was done with $C_{22}H_{45}$−N$^+$(CH_3)$_2$−C_6H_{12}−N$^+$(CH_3)$_2$−C_6H_{13} as a template in a seed-assisted synthesis. The authors showed the benefits of the pore structure for the glycerol etherification with *tert*-butyl alcohol.[241] Different bolaform surfactants with an axial chiral binaphtyl core in the hydrophobic tail and various triquaternary ammonium heads were used by Zhang et al. Four to ten carbons in the alkyl chain between the triquaternary ammonium head group and the binaphtylgroup gave nanosponge-like MFI zeolites. In contrast, eleven and twelve carbons in the linker led to nanorod-constructed mesoporous MFI zeolites.[242] Shen et al. produced ultrathin ZSM-5 zeolites by performing a controlled crystal growth. A bifunctional template with quaternary ammonium groups and hydrophobic groups was used to control the crystal growth in the *a-c* plane and layer stacking along the *b*-axis. The spatial effect by using another template led to intergrown single-unit-cell nanowires, which showed promising catalytic results for the hydroxylation of phenol.[243] Agglomeration of uneven sized nanocrystals or nanoneedles can be obtained, using an inexpensive mono-quaternary ammonium *N*-cetyl-*N*-methylpyrrolidinium as a mesoporogen. The amount of mesoporogen and SDA controlled the morphology and structural properties.[53] Wool-ball-like structures and others, composed of 100-150 nm nanorods, were made without a mesoporogen. Here a high degree of supersaturation and self-assembly are at the basis of the formation of such structure, which performed better in the cracking of isopropylbenzene and *n*-octane.[244,245] A nanotube tri-modal network was used as a scaffold by Li et al. They were able to create hierarchical ZSM-5 zeolites with an inner nanotube diameter of 90 nm, mesopores of 2 nm and macropores of 700 nm, made up of nanocrystals. This catalyst showed superior catalytic performance in the MTH reaction compared to a conventional ZSM-5 catalyst.[246]

Hierarchical nanocrystals can also be produced with intracrystalline mesoporosity instead of intercrystalline mesoporosity. This can be created for example by controlling the nucleation-growth rate and engineering growth-defects,[247] by additional desilication of nanozeolites, creating mesopores or hollow zeolites.[248] In a last study, mesoporous nano-ZSM-5 crystals were produced by using a desilication-recrystallization process. Here silicalite-1 was added to a TPAOH solution in the presence of NaAlO$_2$. Here, mesopores or hollow zeolites were formed as well by adjusting the zeolite treatment procedure.[249]

4. Synthesis of hierarchical 12-MR zeolites

4.1. Mordenite

Zeolites with MOR topology consist of a framework that includes 12-MR channels in the [001] direction, which are interconnected by 8-MR channels.[250] According to IZA, zeolites with MOR topology contain a two-dimensional channel dimensionality. The 12-MR channels have dimensions of 0.65 x 0.70 nm, whereas the 8-MR channels are smaller with dimensions of 0.26 x 0.57 nm. The large 12-MR pores make this type of zeolites appropriate for applications in cracking or isomerization reactions.[251] Despite the relatively large 12-MR pores, MOR zeolites are susceptible to rapid deactivation due to the fact that reactant molecules cannot diffuse into smaller side channels.[252] It should be mentioned that there exist several material types with MOR topology, although, mordenite zeolites are most familiar and will be mainly discussed in following section.

Top-down methods

Dealumination
A first extensive screening of the dealumination process was done by the group of Wahono et al.[253] Herein, several dealumination procedures were performed on natural zeolite, which contained 48 % of a crystalline mordenite phase. Following parameters were examined: (I) HCl concentration, (II) zeolite/acid volume ratio, (III) treatment time, (IV) agitation, and (V) multi-stage dealumination. Afterwards, characterization data provided information about the improved Si/Al ratio, porosity, crystal structure, and engineering of surface functional groups. It was shown that a ten-stage dealumination could increase the Si/Al ratio from 3.9 up to 120 and the specific surface area from 25.95 up to 220 m² g^{-1}. This improvement indicates that such modified mordenite zeolites can be potentially used as hydrocarbon adsorbent or catalyst with hydrophobic surface. In contrast to the HCl concentration and single/multi-stage dealumination parameters, which all showed to have a significant influence on the framework composition and pore characteristics, zeolite/acid volume ratio, agitation and treatment time did not seem to affect the outcome of the dealumination significantly. However, the effect of treatment time was also investigated by Tamizhdurai et al.[252] and Nasser et al.[254] during the dealumination of mordenites in a HCl or HNO$_3$ reflux. Tamizhdurai et al. performed an acid treatment for 0.5 hour, 1 hour and 1.5 hours, whereas Nasser et al. applied a treatment time between 3 and 6 hours. A significant effect of treatment time was observed by the first group, wherein a treatment time of 1 hour in 6 N HCl (100 °C) resulted in high porosity, increased external surface area and improved total acidity compared to the parent mordenite without intensively destroying the microporosity. This was not the case for a treatment of 1.5 hour, which led to a loss of crystallinity of 37 %. It should be mentioned that an improved total acidity in this case corresponds to a decrease compared to the parent mordenite. This is because a lower total acidity tends to be beneficial in the isomerization of *n*-hexane, *n*-pentane and light naphtha, since higher acidities will lead to cracking.[252] The same improvement is true for the study of Nasser et al. wherein acidity decreased as well, compared to the parent zeolite. By consequence, the selectivity to light olefins increased in the conversion of dimethyl ether. Thus, a treatment time of 6 hours in 3 M HNO$_3$ (90 °C) seemed optimal to increase the surface area and pore volume.[254]

Multiple acids such as HCl, HNO$_3$ and oxalic acid were also applied in a study from Saxena et al., who concluded that an acid

treatment with HNO_3 resulted in a hierarchical mordenite that showed the highest increase in external surface area (from 20.81 to 39.40 m² g^{-1}) and mesopore volume (from 0.0191 to 0.0416 cm³ g^{-1}) compared to the untreated mordenite. In addition, the modified zeolites showed excellent reusability which makes them highly attractive for industrial applications, for example in the selective oxidation of benzyl alcohol to benzaldehyde.[255] Several other groups used HNO_3 as well in the acid treatment of mordenites.[254,256–258] In a study from Reule et al., the concentration of the HNO_3 solution, as well as the treatment temperature, was varied in order to study the effect on dealumination.[257] Both a higher HNO_3 concentration and a higher temperature resulted in an increase of external surface area, pore volume and average pore size. The treated mordenites were subsequently tested in the DME carbonylation to methylacetate.[257] Next to HNO_3 that was used in previous studies, there exist other mineral acids that can be employed as well for the dealumination of mordenites, such as HF[259,260] and NH_4F,[259] but also organic acids like oxalic acid[255] and citric acid[261] can be used. However, the effect of these acids on for instance the increase in mesopore volume was not as pronounced as was the case with HNO_3.

Desilication

Desilication of mordenites can be performed on its own, although, it should be noted that desilication is often preceded by a dealumination. A first extensive research regarding the combination of acid and alkaline treatment was done by Pastvova et al. This group performed following treatments in order to obtain hierarchical mordenite zeolites: (I) alkaline treatment, (II) alkaline-acid treatment, (III) acid-alkaline-acid treatment, and (IV) fluorination-alkaline-acid treatment. A schematic overview of these four strategies is shown in Figure 12.[262] Following paragraphs will discuss each strategy separately and comparable studies from other groups will be incorporated for each of them.

A pure alkaline treatment was performed by several groups.[262–268] Pastvova et al. treated a parent mordenite in a 0.2 M NaOH solution.[262] This concentration, however, was varied in another study from Huang et al. who concluded that extracting Si from the framework by an alkaline treatment could generate intracrystalline mesopores with diameters of 3-30 nm.[263] The same conclusion was made by Pastvova et al., who also mentioned that desilication preferably took place along crystal defects.[262] Furthermore, Tsai et al. performed desilication in a single-cycle, as well as in multiple cycles. It was concluded that a single-cycle treatment resulted in disordered mesopores of 8 nm, regardless of the alkaline-treating time. However, a multiple-cycle treatment tends to be most effective since mesopores of 8-14 nm were formed that were interconnected with silica-blocked 12-MR micropores. This last treatment showed to be most effective for enhancing the catalytic activity and stability.[265] A last (only) alkaline treatment from Issa et al. was assisted by pyridine, which showed dual action on textural and chemical properties. This approach yielded aggregates with smaller zeolite particles with a substantially higher amount of external silanols. In addition, pyridine in situ generated EFAl species during the final calcination step, which increased the acidity of the final hierarchical mordenite zeolite. Both smaller zeolite particles and higher acidity led to a considerable improvement of the catalytic properties in *n*-hexane cracking. Furthermore, it should be noted that desilication is a destructive approach in which material loss can be observed. For instance, in the pyridine-assisted desilication from Issa et al., a material yield of approximately 76 % was obtained.[266]

Another strategy is an alkaline treatment that is followed by an acid wash. This is done by several research groups.[258,262–264,267,268] Pastvova et al. performed an acid wash in 0.1 M oxalic acid or HNO_3 after an alkaline treatment in 0.2 M NaOH.[262] The combined alkaline and mild acid treatment resulted in a decrease of microporous volume (from 0.19 to 0.13 cm³ g^{-1}), and in an increase in mesoporous volume (from 0.05 to 0.12 cm³ g^{-1}) and
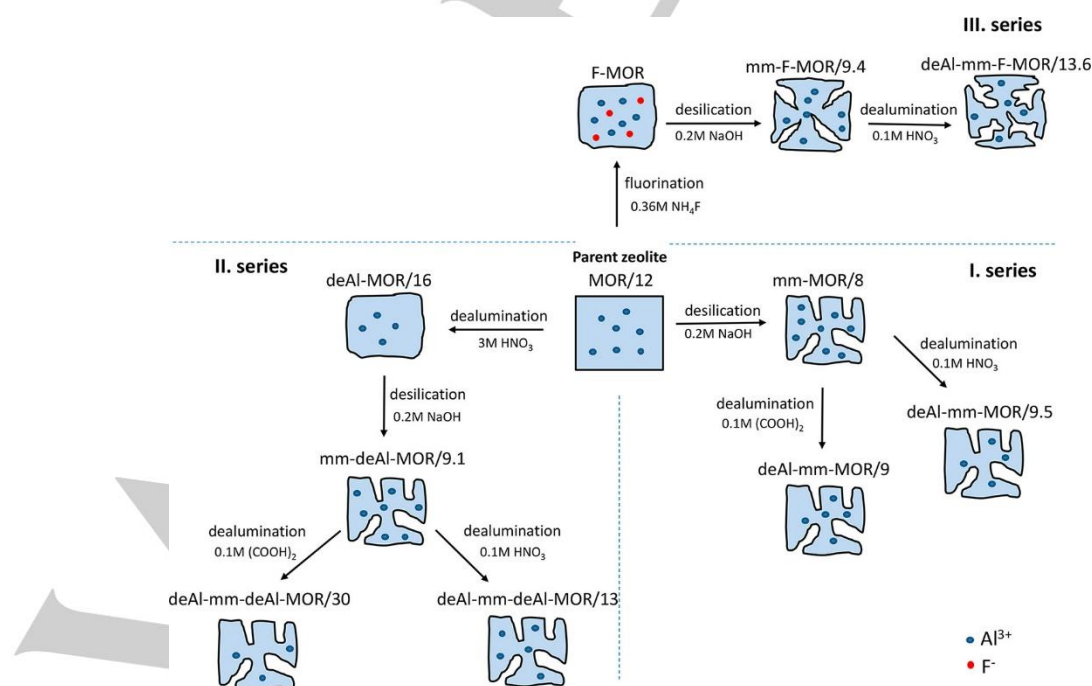
Figure 12. Scheme of the preparation of micro-mesoporous mordenite zeolites using post-synthesis alkaline−acid (series I), acid−alkaline−acid (series II), and fluorination−alkaline−acid (series III) leaching procedures.[262] Reproduced (adapted) with permission. Copyright 2017 American Chemical Society.

external surface area (from 42 to 114 m² g^{-1}) compared to the parent mordenite.[262]

To finish, Pastvova et al. performed a fluorination-alkaline-acid treatment wherein the fluorination step was executed in a 0.36 M NH$_4$F solution. Subsequent alkaline treatment resulted in the simultaneous removal of Si and Al. In this way, a micro-mesoporous mordenite was formed with a large number of unrestricted channels, as well as a large increase in accessibility of the OH-groups.[262]

Dissolution-recrystallization

A first recrystallization procedure that is discussed includes a hydrothermal recrystallization in the presence of cetyltrimethylammonium bromide (CTAB) as soft template. This was done by Ponomareva et al. who synthesized hierarchical Cs-mordenite for the production of isobutylene from acetone. Different NaOH concentrations were applied which led to various material types with different micropore and mesopore characteristics, which is illustrated in Figure 2 in section 2.1. As an example, an analogous method was employed by Lee et al. who opted for a NaOH concentration of 0.1 M. The resulting zeolite could then be described as a RZEO-1 type of material.[269] Back to Ponomareva, this group showed that a significant increase in mesopore volume from 0.08 to 0.77 cm³ g^{-1} improved the mass transfer to the active sites, which then led to an increase of the acetone conversion of 56.2 % (compared to 35.5 % for the untreated Cs-mordenite).[270]

Bottom-up methods

Soft templating

A first important factor in template assisted hydrothermal synthesis is the type of the soft template. Therefore, a first broad screening of mesoporogens was performed by Santos et al. This group performed a steam-assisted conversion (SAC) method in the presence of different soft templates: polyethylene glycol hexadecyl ether, pluronic P123, pluronic F127 and CTAB. The last template proved to successfully form a crystalline mordenite structure with preserved acidity and with significant mesoporosity (0.18 cm³ g^{-1}) compared to the parent. This led to a higher initial activity and lower deactivation rate in the catalytic cracking of *n*-heptane. However, it should be mentioned that a loss of crystallinity was observed when a high amount of CTAB was used.[271] In addition to previously tested mesoporogens, the group of Sheng et al. investigated the synthesis of hierarchical mordenites in the presence of *n*-butylamine or polyacrylamide.[272] It was shown that *n*-butylamine and polyacrylamide resulted in more framework aluminum and Brønsted acid sites in the 8 membered rings, which means that 12-MR pore channels contained less acid sites so that coke formation was suppressed. As a consequence, the carbonylation of DME showed a high DME conversion and high methylacetate selectivity.[272]

Nanozeolites and their assembly

A final class of synthesis procedures deals with the production of nano-assemblies of MOR zeolite crystals. Here, a distinction can be made between one-dimensional nanorods, and two-dimensional nanosheets. Several research groups have studied the formation of hierarchical mordenite nanorod bundles. The first group by Dai et al. used dimethyloctadecyl[3-(trimethoxysilyl)propyl]ammonium chloride (TPOAC) as an organosilane functioned fumed silica. This limits the growth of zeolite crystals into large crystals, such that nanorod assembled bundles are formed, of which the single nanorods have a diameter between 30 – 80 nm, external surface area of 148 m² g^{-1}, mesopore volume of 0.15 cm³ g^{-1} and mesopores of 2 – 8 nm. The hierarchical mordenite nanorod bundles showed good performance in the benzylation of mesitylene by benzyl chloride due to efficient diffusion and improved accessibility of the active sites.[273] Another group by Bolshakov et al. used an inexpensive mesoporogen, namely *N*-cetyl-*N*-methylpyrrolidinium. This proved to steer the synthesis towards 0.6–1 µm rod-like crystals with a mesopore volume of 0.12 cm³ and external surface area of 88.5 m² g^{-1}. Moreover, the mesoporogen tends to redistribute Al in the zeolite framework, which causes an increase of Brønsted acid sites in the 8-MR at the expense of acid sites in the 12-MR channels. This last decrease caused a better hydrocracking selectivity since 12-MR acid sites are otherwise involved in the conversion of alkene intermediates.[274]

In contrast to previous template-assisted methods, another synthesis strategy is possible, which falls under the concept of kinetic regulation. Herein, the hierarchical zeolite is synthesized without using a template, but by controlling the zeolite crystallization process so that a balance between nucleation and crystal growth is achieved. In this field, Singh et al. developed a template free facile synthesis method for mesoporous mordenite wherein small rod-shaped nanoparticles were transformed to 2 - 3 µm mordenite particles through self-assembly. The synthesis conditions were therefore carefully controlled, namely a 24 hour during crystallization process at 180 °C and a tumbling rate of 25 rpm. This created a rod-shaped mordenite nanoparticle-assembly wherein the nanoparticles contained mesopores with a diameter of 3 – 5 nm.[275] Another synthesis by kinetic regulation was done by Velaga et al. who used a seed-assisted method in which the influence of hydrothermal treatment and aging time was monitored. It was shown that an increase in treatment time resulted in an increase of crystallinity (up to 97 %), mesoporosity, and concentration of acid sites. The growth of the zeolite crystal involved several stages, starting from nano-spherical particles to nano-cylindrical particles, and finally micro-monolith mordenite particles which were used for (carbohydrate) biomass conversion to levulinic acid.[276]

Next to nanorods, nanosheets can be synthesized as well. This was done by Wang et al.[277] and Liu et al.[278] who both employed polyethylene glycol (PEG) as template in the hydrothermal synthesis, however, Liu et al. also used CTAB as an additional template. It was shown that the use of PEG dramatically increased the crystallinity compared to reference mordenites, that were synthesized without the addition of PEG. Moreover, the molecular weight of PEG showed to have an effect on the final properties of the material. An increase in molecular weight resulted in an increased stability of the catalytic activity in the carbonylation of DME, which was explained by an increase in specific surface area (from 487.1 to 567.4 m² g^{-1}), total pore volume (from 0.201 to 0.218 cm³ g^{-1}) and acid site strength compared to a mordenite that was synthesized without addition of PEG.[277] Next to relatively simple templates such as PEG and CTAB, more complex mesoporogens have been recently investigated, namely gemini-type amphiphilic surfactants. Such

templates were employed by Lu et al., who showed that the benzyl diquaternary ammonium cations structurally directed the crystallization towards the MOR topology, whereas a long hydrophobic hexadecyl tail prevented crystal growth along the *b*-axis (Figure 13). In this aspect, a hierarchical mordenite nanosheet was formed with a large external surface area that proved to be promising in the alkylation of anisole with benzyl alcohol. In addition, the material led to an extremely high ethylene selectivity in the methanol-to-olefin (MTO) reaction, compared to bulk mordenites.[279]

To finish, a different type of mesoporous nanostructures was developed through the formation of a cluster of nanodispersed mordenite crystals, as is shown in Figure 14. Such structures were prepared by Travkina et al., who crystallized these mesoporous mordenite granules, starting from a mixture of amorphous aluminosilicate, fumed silica and mordenite crystals. Depending on the proportion of the crystalline phase in the initial sample, two outcomes are possible. When 30 wt% of the initial sample is crystalline mordenite, a micro-macroporous system is formed (Figure 14a), whereas 60 wt% modernite crystals gives rise to a micro-mesoporous system (Figure 14b). These structures contain nanocrystals of 50 – 300 nm between the layers and were used as a bifunctional catalyst in the hydroisomerization of a model mixture of benzene-heptane after loading with 0.3 wt% Pt.[280]
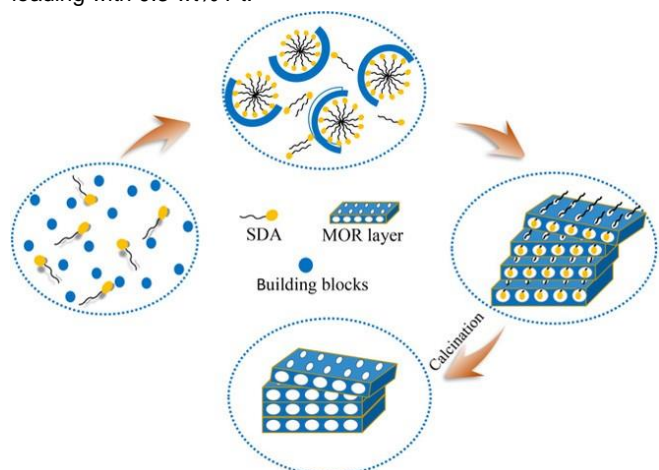
Figure 13. Graphic description for the formation of MOR nanosheet structures.[279] Reproduced with permission of Wiley-VCH Verlag GmbH & Co. KGaA.
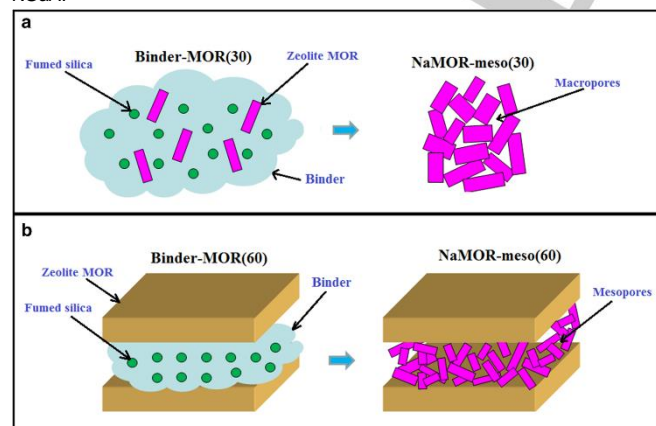
Figure 14. The mechanism of formation of a hierarchical porous structure: (a) crystalline seed content 30 %, only macropores are formed (NaMOR-meso (30)); (b) crystalline seed content 60 %, meso- and macropores are formed (NaMOR-meso (60)).[280] Reproduced with permission of Springer.

4.2. Faujasite

Faujasites (FAU) are one of the most industrially relevant zeolites. They are constructed of sodalite cages that are interconnected by their 6 membered rings. This creates a three-dimensional network of micropores made up of 12 membered rings (0.74 x 0.74 nm).[281] Next to these micropores, the crystal structure also contains supercages with a diameter of 1.124 nm. Altogether, this makes FAU zeolites belong to the group of large-pore zeolites.[282] The crystal in general consists of Si and Al atoms with relative amounts that can vary significantly. Three main types are commonly distinguished: (I) Zeolite X (Si/Al = 1-1.5), (II) Zeolite Y (Si/Al > 1.5), and (III) Ultra Stable Y zeolite or USY zeolite (Si/Al = 6 and higher).[283] Regarding the applications of FAU zeolites (mainly zeolite Y and USY), they are typically used in the process of Fluid Catalytic Cracking (FCC), which causes them to account for 95 % of the yearly consumption of the synthetic zeolites.[282] On the other hand, Zeolite X is more likely to be used in adsorptive applications. Most of recent research on mesoporization has been performed on zeolite Y and USY, and to a lesser extent on zeolite X. In following paragraphs, each type of FAU topology will be discussed, going from low Si/Al ratio (zeolite X), to high Si/Al ratio (USY).

Zeolite X

Top-down methods

Dealumination/desilication
Zeolite X is a zeolite with FAU topology that typically contains a high aluminum content, resulting in a low Si/Al ratio. Therefore, dealumination is a convenient first strategy to create a hierarchical pore structure in the crystalline material. Over the years, different strategies have been investigated to optimize the dealumination process. This ranges from template-free dealumination to dealumination in combination with a mesoporogen. In contrast, desilication is rather difficult or cannot be applied to zeolites with low Si/Al ratios since the framework Al generates a shielding effect that hinders attack by alkaline compounds.[284] Because of this aspect, desilication of zeolite X is always preceded by a dealumination step, which is why both treatments will be discussed together.
Only little amount of research has been performed on mesoporization of zeolite X. Al-Ani et al. demonstrated the synthesis of hierarchical zeolites X and Y by a two-step acid and alkaline treatment. This was done based on a method of Sachse et al., who tailored the intracrystalline mesoporosity through an alkaline treatment in a cetyltrimethylammonium bromide (CTAB) solution.[285] Al-Ani et al. subjected the parent zeolites (NaX and NaY) to a one hour acid treatment with 10% citric acid, followed by an alkaline treatment in a NaOH – CTAB solution for 24 hours. Catalytic tests of the synthesized hierarchical zeolites X and Y showed a declined activity in the transesterification of rapeseed oil after only a slight increase of the framework Si/Al ratio. This can be explained by a lower amount of framework Al which results in a lower ion-exchange capacity for electropositive cations (e.g. K^+, Cs^+) that are needed as basic sites. It can thus be concluded

that the accessibility is less important than the strength of the basic sites in the transesterification of triglycerides.[286]

Bottom-up methods

Soft templating
In addition to previous top-down approaches, several bottom-up approaches have been published in literature. Herein, temperature, crystallization time and the presence of a mesoporogen belong to the main variables. Starting with the mesoporogen, two research groups used different templates in the hydrothermal synthesis of hierarchical zeolite X. The first group by Gómez et al. used sodium dodecylbenzenesulfonate (SDBS), which is an anionic liquid. Important parameters that were examined are for instance the SDBS concentration, dissolution time of SDBS and aging time. It turned out that high SDBS concentrations (e.g., 3 times the Critical Micellar Concentration), long dissolution times (e.g., 24 hours) and long aging times (e.g., 48 hours) were necessary to obtain noteworthy mesoporosity in zeolite NaX..[287] Another mesoporogen, an organosilane named dimethyloctadecyl[3-(trimethoxysilyl)propyl]ammonium chloride (TPOAC), was used by Parsapur et al. By tailoring the zeolitization conditions, this group achieved a stable supramolecular self-assembly by consecutively performing (I) a homogeneous nucleation and (II) a multi-step crystallization, which are schematically shown in Figure 15. Therefore, the synthesis mixture was hydrothermally treated at two different temperatures apart from aging. In the initial step, the nucleation was encouraged over crystal growth by maintaining low-temperatures (50 °C), which is followed by complete zeolitization at higher temperatures (75-100 °C).[288] In both studies, the formed zeolites were tested as catalysts in the deoxygenation of benzyl acetate[287] and the tertiary butylation of phenol[288], respectively. The hierarchical zeolites showed remarkably higher conversions, product selectivity and excellent

lifetimes compared to their non-hierarchical analogs. Based on findings from Gómez et al., the higher catalytic lifetime was mainly attributed to a higher mesopore volume of 0.19 cm³ g⁻¹ (compared to 0.04 cm³ g⁻¹ for the pristine zeolite), since less pore blocking could occur and molecules had longer access to the active sites.

Template free
Koohsaryan et al. investigated the hydrothermal synthesis of highly crystalline mesoporous zeolite FAU in a template-free system. Instead, zeolite 13X and polyethylene glycol (PEG 400) were used as seed and polymeric solubilizer agent, respectively. The outcome of the template free synthesis were well-developed zeolite crystals with mesopore size distributions of 2–10 nm. Herein, zeolite 13X was indispensable to induce nucleation, while PEG was needed to enhance the crystallization of the synthesis gel since it provided a more basic medium, which is beneficial for the dissolution of the starting materials.[289]

Nanozeolites and their assembly

Nanozeolite assemblies of FAU type zeolite X under the form of nanoparticles, nanosheets or nanorods are also a new point of interest. In this aspect, layer-like zeolites are a recently developed type of structure which have already been discussed extensively in a review by Reiprich et al.[282] Layer-like zeolites, which are shown in Figure 16, consist of branched zeolite crystals and plates. Herein, branched zeolites are materials consisting of assemblies of intergrown two-dimensional zeolite crystals creating a house-of-cards-like structure (HCL). In contrast, plates are morphologies where the two-dimensional zeolites are not intergrown, they thus form separate plates. These type of structures can be seen as hierarchical structures as long as they are arranged in such a way that they create an additional pore system due to interlayer void spaces. Regarding the synthesis, such materials are usually formed in the presence of a growth
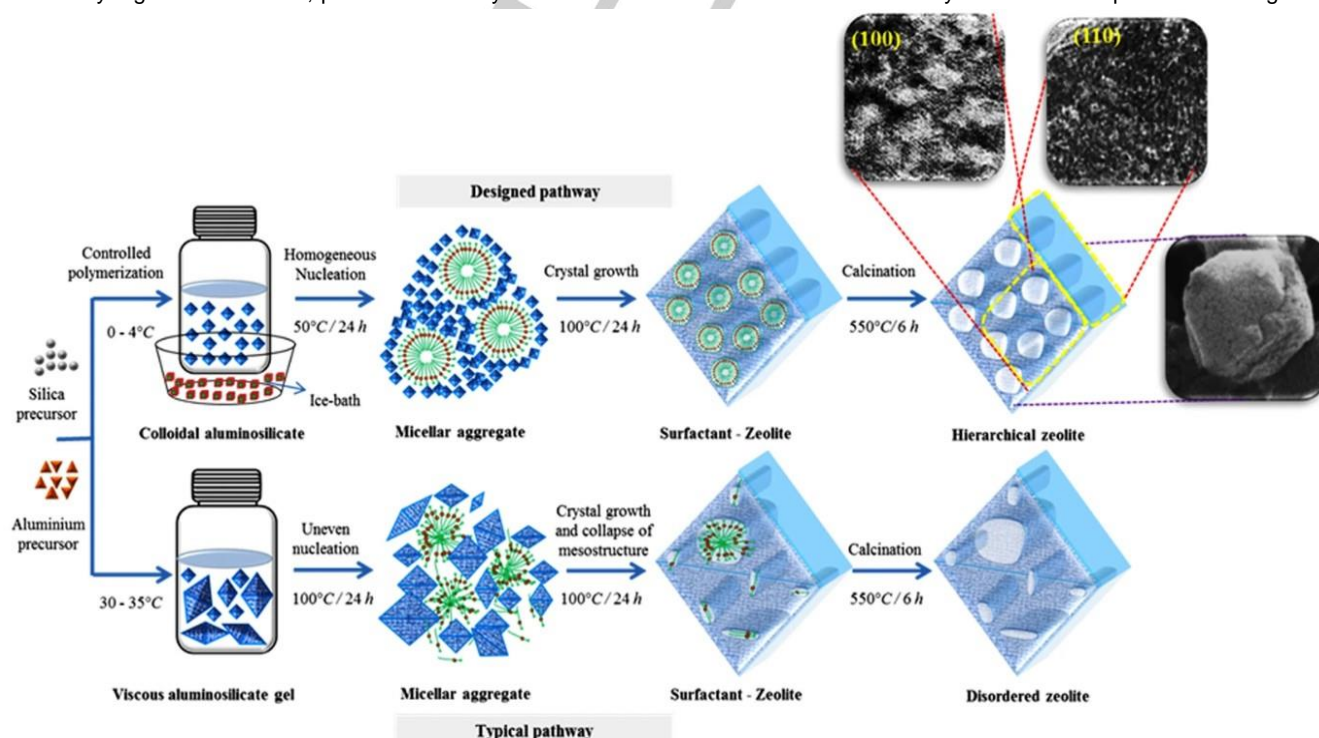

Figure 15. Proposed mechanism for the synthesis of hierarchical FAU-type zeolites.[288]

modifier that inhibits the crystal growth in one dimension, however, additive-free methods are a new point of interest from an economic and ecological point of view. This includes synthesis through kinetic regulation of the crystallization process, which will be discussed later. For more detailed information about layer-like FAU-type zeolites, the interested reader is referred to the review of Reiprich et al.[282]

Continuing on nanosheets, different synthesis strategies can be followed. An important distinction that is made among such strategies is the presence or absence of SDA. In this aspect, a first strategy from Yutthalekha et al. worked with the organosilane TPOAC as SDA.[290] Herein, the route to prepare the faujasite zeolite with the nanosheet-assembled structure, as well as the role of synthetic parameters on the characteristics and properties are systematically investigated. In the formed material, the mesopores originate from the interstitial pores between the nanosheet assemblies. Although the use of SDA's is known to be environmentally unfriendly, this research focused on a greener synthesis by recycling the waste mother-liquid, which effectively reduced environmental pollution.
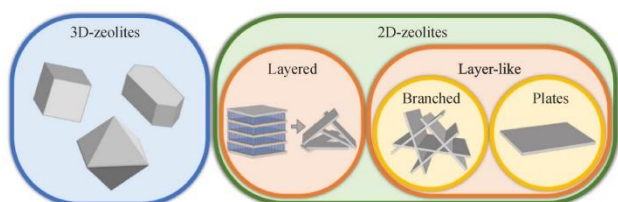

Figure 16. Schematic overview of proposed classification terms for zeolites with 2D-morphology.[282] Reproduced with permission of Springer Nature.

Next to previous template-assisted method, nanosheets can also be synthesized in absence of such templates. Here the focus lies on kinetic regulation of the crystallization process wherein synthesis conditions are controlled to obtain the desired zeolite structure or morphology. Such an additive-free method was for instance used by Jia et al. who synthesized a zeolite nanosheet with intergrown structure which held a honeycomb-like structure with abundant mesopores of 10 nm in diameter, wherein the mesopores are the result of the internal space between the zeolite nanosheets.[291] Next to these honeycomb-like structures, HCL structures are another unique type of intergrown structures that were synthesized by Liu et al. in an additive-free system (Figure 17). This group investigated the structure evolution by regulating the reaction conditions, which followed a nucleation and then skeleton crystal growth model. Here it seems that the viscosity of the synthesis gel tends to be an important factor when steering the synthesis towards nanosheet structures. An increase in viscosity can lead to the limitation of vortexing effects, which causes the supply of solutes to the growing crystal to be only possible by diffusion. As a result, the solutes-limited environment changed the growth mechanism of the crystals, making their edges and corners grow faster prior to the planes.[292] A similar concept was employed by the group of Wang et al. for the synthesis of zeolite nanoparticles and nanosheets. This group hydrothermally produced various types of microporous zeolite crystals with varying degrees of mesoporosity.[293] Following parameters were examined during synthesis: (I) water removal during reflux, (II) aging temperature, and (III) aging time. Water removal led to an increased viscosity of the synthesis gel, which can induce constrained mass transport. In this way, nanocrystals were formed under the most constrained mass transport conditions since removing water and continued heating result in supersaturation that promotes nucleation. The formed nanocrystals then packed together which created mesopores with a broad pore size distribution (2-100 nm). In addition to these nanocrystals, an interpenetrating packing of nanosheets with small pore size distribution (2 – 20 nm) was also formed under less stringent synthesis conditions. Unfortunately, the mesoporous materials were not completely composed of FAU, but were rather a mix of FAU and EMT phases.[293]

Zeolite Y
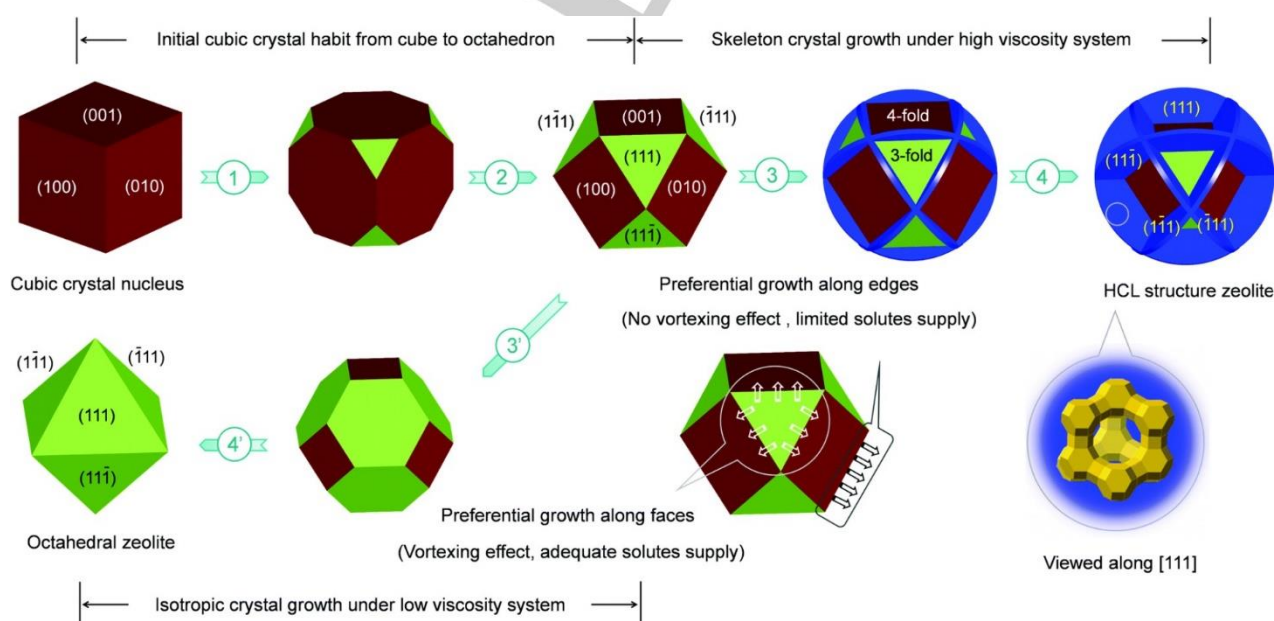
Figure 17. Comparative illustration of the evolving mechanisms of HCL-NaX with HCL structure according to the nucleation and skeleton crystal growth model and octahedral structure zeolite based on a common cubic crystal habit from cube to octahedron.[292] Reproduced with permission of The Royal Society of Chemistry.

Top-down methods

Dealumination

Recent literature regarding the dealumination of zeolite Y used an acid treatment as dealumination technique. Herein, the severity of the treatment is an important parameter that will result in zeolites with different physical properties. A mild acid treatment was employed by Feng et al. who made use of different NH_4HF_2 solutions. This acid ionizes into positive H^+ and negative F^- at a very slow rate, which avoids a sudden increase of the concentration of H^+ and F^-. Therefore, it can be concluded that the dealumination is more sustained and mild, and that the crystallinity of hierarchical Y zeolites is higher compared to zeolites that underwent more severe treatments with for instance HCl/NH_4F or HF/NH_4F.[294] Pagis et al. used a severe dealumination for the synthesis of hollow Y zeolite single crystals. Such hollow structures could be a possible solution for the often observed ineffectiveness of zeolites in catalysis. It has been seen that up to 50 % of the internal volume of bulk crystals is not used in the reaction.[295] Therefore, creating a cavity in the bulk crystal can count as a secondary level of porosity which makes these hollow Y zeolites part of the hierarchical zeolites. In this work, three main modification steps were applied on conventional NaY crystals, which are shown in Figure 18: (I) substantial dealumination of the zeolite framework by $SiCl_4$, (II) acid leaching with a 0.1 M HCl solution, and (III) a selective dissolution of the crystal core in the presence of protective aluminum species (e.g. sodium aluminate). This last step creates an Al-rich surface which protects the outer parts of the crystals from desilication. In contrast to earlier reported literature related to hollow Y zeolites, this work synthesized hollow Y zeolites with much higher Si/Al ratios which makes them stable against harsh conditions. From a practical point of view, the mild dealuminated zeolites have been tested for the adsorption of toluene, where a high adsorption capacity was measured at higher pressures due to a large number of mesopores. The hollow Y zeolites have been used as bifunctional catalysts in the hydroisomerization of n-hexadecane after being mixed with a Pt-supported alumina binder. It was seen that the use of hollow zeolites caused a higher turnover frequency compared to their bulk analogs.[294–296]

The problem with conventional dealumination treatments is the time- and energy-consuming synthesis procedure. To cope with this issue, Abdulridha et al. performed a so called microwave-assisted chelation (MWAC) for the preparation of mesoporous zeolites materials. Herein, ethylenediaminetetraacetic acid (EDTA) was used as chelation agent to remove Al from the zeolite framework by complexation. Furthermore, this process was assisted by microwave-irradiation, which intensified the complexation reaction. This can be explained by (i) an improvement of the thermal dispersion of EDTA in the zeolite framework, (ii) good microwave absorption of framework Al compared to framework Si, which accelerates the selective interaction between framework Al and EDTA, and (iii) the relatively low bond energy of the Al-O in comparison with that of the Si-O. In the end, this method proved to be able to complete the synthesis of mesoporous zeolitic materials within a treatment time of 1 minute at both 50 °C and 100 °C, while structural parameters were comparable to those of mesoporous zeolitic materials that were synthesized by a conventional hydrothermal treatment of 6 hours at 100 °C. In addition, the material proved to have suitable acidity to catalyze the catalytic cracking of 1,3,5-

triisopropylbenzene (TIPB) with high and stable activity (stable conversion of ≥ 97 %). This proves that the MWAC method is a time- (and cost-) effective method, which may be classified as environmentally friendly and sustainable.[297]
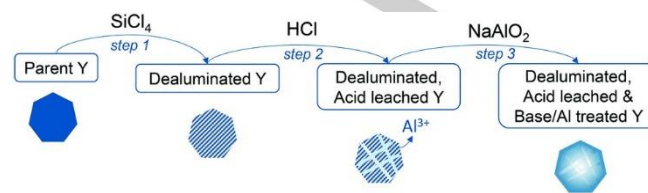
Figure 18. Schematic illustration of the fabrication of hollow Y zeolite by a three-step process.[294–296] Reproduced with permission of The Royal Society of Chemistry.

Desilication

Like previously mentioned, a dealumination step may be required previous to desilication to remove protective Al species. Starting with a publication from Li et al., this group performed such an alkaline treatment that was preceded by two dealumination steps: (I) a steam treatment and (II) an acid treatment (e.g. fluorosilicic acid, HCl). By consequence, Al was partially removed from the framework, after which the zeolite crystal was healed by the migration of Si into the framework. The actual desilication was done in a NaOH solution (0.6 M and 1.0 M) and was needed to eliminate Si debris. This last step, the desilication, is an essential process to introduce the intracrystalline mesoporosity. The resulting hierarchical zeolite Y exhibited remarkably higher catalytic activity than the conventional zeolite in the cracking reaction of TIPB. This can be attributed to the combination of high crystallinity, large external surfaces, and appropriate acid properties.[298]

To further explore the role of NaOH, its concentration and the treatment time in a desilication process, several studies were executed. Graça et al. concluded that an increase of the NaOH concentration up to 0.2 M, which is a common NaOH concentration for desilication purposes, increased the mesoporous volume (from 0.043 to 0.087 cm^3 g^{-1}) and external surface area (from 48 to 58 m^2 g^{-1}), while microporosity and crystallinity are preserved compared to the untreated zeolite.[299] Additionally, Oruji et al. used a higher concentration of 0.5 M NaOH in a conventional alkaline treatment (1 hour, 30 °C), which was comparable to the previous method from Graça et al.[300] Moreover, this group applied ultrasound energy during the desilication which accelerated the movement of OH^- ions. This proved to be beneficial for selectively extracting Si from the zeolite structure. In this aspect, a material yield of approximately 75 wt% was observed. Further, it should be noted that an increasing treatment time resulted in a decreased relative crystallinity. However, ultrasonic irradiation had a positive impact on the preservation of the micropore structure and formation of mesopores. Additionally, the obtained mesopores turned out to be well interconnected and provided easy access to the active sites. They possessed moderate acidity and led to a decreased coke formation rate, increasing catalytic stability and activity.[300] In accordance with Oruji, et al., Zhang et al. made use of ultrasound energy as well. In this study, a conventional hydrothermal desilication treatment was compared with an ultrasound-assisted desilication after a chemical dealumination with EDTA or citric acid. It was concluded that the ultrasound-

assisted method is as effective as the hydrothermal treatment with respect to mesopore formation and acid properties. However, the ultrasound-assisted method proved to be more efficient since the treatment-time was reduced by 6-fold, which makes it more energy and time-efficient compared to a conventional hydrothermal treatment.[301]

Next to NaOH as desilication agent, other alkaline solutions can be used as well. Van-Dúnem et al. tested three bases in combination with cetyltrimethylammonium bromide (CTAB) as SDA: (I) NaOH, (II) NH₄OH and (III) tetrapropylammonium hydroxide (TPAOH). The development of larger porosity was clearly dependent on the used bases. The first commonly used base, namely NaOH, created mesoporosity that corresponds mainly to pore widths higher than 10 nm. The other bases mainly created a large pore volume, with pores in the range 4 – 10 nm, and to a lesser extend to pores larger than 10 nm. The effect of different bases was seen in terms of the Fe-complex immobilization characteristics which could possibly show important consequences on the catalytic behavior and recycling.[302]

Like in previous work from Van-Dúnem et al., where different bases were tested, different mesoporogens can also influence the outcome of hierachical Y zeolites.[302] Van-Dúnem et al. and Al-Ani et al. both used CTAB to assist in their desilication approach.[302–304] Al-Ani et al. suggested that 12-MR zeolites (FAU, *BEA, MOR, LTL), which are accessible by the surfactant, facilitate the formation of regular mesopores during the desilication.[304] More in detail, Sachse et al. proposed a mechanism that explains the role of CTAB in a desilication procedure. When FAU zeolite is subjected to a mild alkaline treatment, the base initiates the hydrolysis of the Si–O bonds generating negatively charged defect sites which attract CTA⁺. As the reaction proceeds, micelles agglomerate within the individual zeolite crystals and steer silica fragments to reassemble around these micelles, creating a system of ordered mesopores. In this surfactant-templating treatment, partial dissolution of the zeolite is avoided by treating the zeolite in a surfactant solution of mild alkalinity. This induces mesostructuring of the crystalline zeolite structure. This is in contrast to recrystallization strategies where strong alkaline solutions are used to partially dissolve the zeolite, after which a surfactant is added to assemble dissolved silica species into a mesoporous amorphous phase. The surface-templating method proved to be much more controllable.[285]
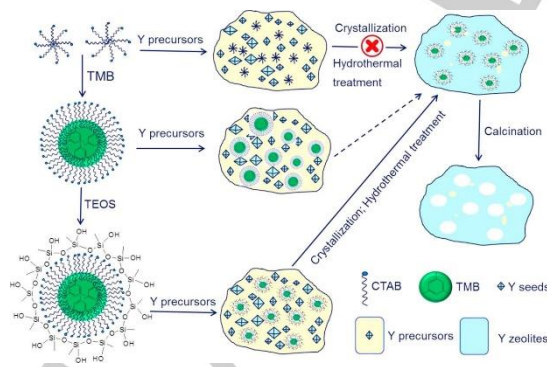
Figure 19. Possible route for the synthesis of mesoporous Y zeolite.[305] Reproduced with permission of Elsevier.

Next to CTAB, other mesoporogens include dimethylhexadecyl[3-(trimethoxysilyl)propyl]ammonium chloride (TPHAC) and dimethyloctadecyl[3-(trimethoxysilyl)propyl]ammonium chloride (TPOAC). Both are quite similar in structure since they contain both organosilane and quaternary ammonium groups. The only difference between TPHAC and TPOAC is the length of the carbon tail on the ammonium group, which includes 16 and 18 carbon atoms, respectively. Starting with Ji et al., this group executed a sequential acid wash and alkaline treatment in the presence of TPHAC. The role of the SDA in the creation of mesopores can be explained as follows. In a first step, CH₃OH, which was released after hydrolysis from TPHAC, was able to partially break framework Si-O-Al bonds into Si-OH and Al-OH. Thereafter, the Al-OH species were removed from the framework through coordination with Si-(OH)₂, whereas the other Si-OH from TPHAC was incorporated into the zeolite framework. Consequently, mesopores were created after the anchored surfactants self-assembled into micelles within the zeolite crystal.[306] The same mechanism was valid for TPOAC, which was used by the group of Li et al. in a comparable desilication process.[307] In the end, both methods obtained materials that exhibited higher microporous surface areas, external surface areas and well-preserved crystallinity compared to standard NaY zeolites.

Bottom-up methods

Soft templating

When looking at bottom-up approaches, hierarchical zeolite Y is mostly synthesized in the presence of a mesoporogen, although, there exist template-free procedures as well. Examples of possible templates include CTAB, octadecyltrimethylammonium bromide (TMODAB) and TPOAC. The first template CTAB was employed in a study from Zhou et al. where it was first self-assembled with tetraethyl orthosilicate (TEOS) to form SiO₂-CTAB micelles (Figure 19). Subsequently, the micelles swelled after 1,3,5-trimelthybenzene (TMB) was added to increase their size to mesopore size. The zeolite precursors then condensed on the micelle by forming Si-O-Si and Si-O-Al bonds with SiO₂ on the micelle surface. After a crystallization period and hydrothermal treatment, a mesostructured material with (semi)-crystalline walls was obtained.[305]

Regarding such materials with (semi)-crystalline walls, the group of Mehlhorn et al. proved that the final crystallinity strongly depended on the applied NaOH/Si ratio. In an hydrothermal synthesis in presence of TMODAB, it was shown that two main material types were formed. The first type was an ordered mesoporous material with zeolite walls and zeolite nanodomains (0.0625 < NaOH/Si < 0.10). These materials would be interesting for applications that require large mesopore volumes (up to 0.411 cm³ g⁻¹) and high acidity. The second material included ordered mesoporous structures with amorphous walls and zeolite nanodomains (0.125 < NaOH/Si < 0.25), which could possibly be interesting for applications that require large macropore volume (0.754 cm³ g⁻¹) and mild acidity. An increase in NaOH/Si ratio thus showed to result in a decreased size of the zeolite nanodomains, increased mesopore volume, decreased acidity and a decrease of micropore volume.[308]

The final mesoporogen, namely TPOAC, has been previously discussed in the desilication of zeolite Y, however, this molecule can also be useful in bottom-up approaches. This is done by Venkatesan et al.[309] and Lv et al.[310] Venkatesan et al. started

from a seed gel in combination with TPOAC as amphiphilic organosilane. Herein, the crystallization started with a long nucleation period, followed by rapid crystal growth. The formed hierarchical Y zeolite possessed a narrow pore size distribution (3-4 nm), high external surface area (110 m² g⁻¹), high BET surface area (764 m² g⁻¹) and a total pore volume of 0.41 cm³ g⁻¹. Additionally, the external surface contained highly accessible and strong acid sites.[309] In accordance to this work, Lv et al. also studied a rapid hydrothermal synthesis method with two different TPOAC concentrations. However, here microwave irradiation was used to shorten the synthesis time and improve production efficiency. This microwave irradiation caused frequent turning of polar molecules so that electromagnetic energy is converted into heat energy due to friction between the molecules. In the end, it was seen that a higher TPOAC concentration increased the total pore volume from 0.42 to 0.54 cm³ g⁻¹, wherein the mesopore volume slightly increased (from 0.10 to 0.28 cm³ g⁻¹) at the expense of micropore volume (from 0.32 to 0.26 cm³ g⁻¹).[310] Moreover, a high specific surface area of 810 m² g⁻¹ was observed, which was higher compared to a specific surface area of 764 m² g⁻¹ in the first study, where no microwaves were used. Both methods thus proved to be appropriate for synthesizing outstanding hierarchical zeolite Y.

Template free

In contrast to previous template-assisted bottom up approaches, Travkina et al. managed to successfully synthesize a highly crystalline zeolite Y with a micro-meso-macroporous structure without using any templates. This method is based on the selective crystallization into the integral cluster crystals of the preliminarily molded granules, containing crystals of the zeolite and a porous binder matrix. More in detail, the meso- and macropores were located between the separate crystals and the amorphous binder material while the micropores were in the zeolite crystal itself (Figure 20). The material revealed high activity in the multicomponent reaction of propanol with formaldehyde and ammonia towards 3,5-dimethylpyridine with a selectivity of 95 %.[311]
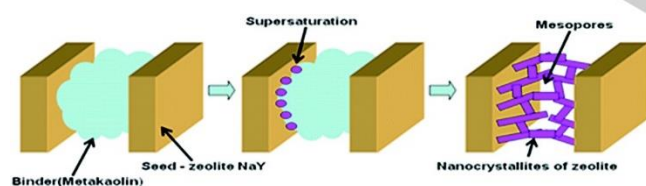

Figure 20. The mechanism of formation of a hierarchical porous structure in meso-Y(60).[311] Reproduced with permission of Springer Nature.

Nanozeolites and their assembly

Regarding zeolite Y nano-assemblies, two noteworthy works have been published that both use a template-free strategy and thus focus on kinetic regulation of the crystallization process. The first work by Ferdov et al. synthesized zeolite Y nanosheet assemblies by repetitive branching of hierarchically arranged FAU nanolayers. Since no morphology modifiers were used, kinetic control of the synthesis conditions was applied instead to induce co-crystallization of FAU- and EMT-type zeolites. The branching resulted from recrystallization of the zeolite nanoparticles which was followed by the formation of submicron faceted crystals.

These crystals served as nutrient for the final nanosheet structures. Such three-dimensional intergrown nanosheets can be interesting for low-cost and environmental friendly applications.[312] Similar to those three-dimensional intergrown nanosheets, a more exotic type of nanostructures, named as "flowerlike hierarchical Y zeolites", can be synthesized as well. Such materials were synthesized in a template-free system by Du et al. who followed a hydrothermal procedure wherein primary nanocrystals self-assembled into loose aggregates. The inner crystals were difficult to grow because of the confined spaces, while the outer crystals were able to grow further to form oriented sheet "petals", as can be seen in Figure 21. A potential application of such structures includes, for instance, pre-cracking of bulky reactants in Fluid Catalytic Cracking (FCC).[313]
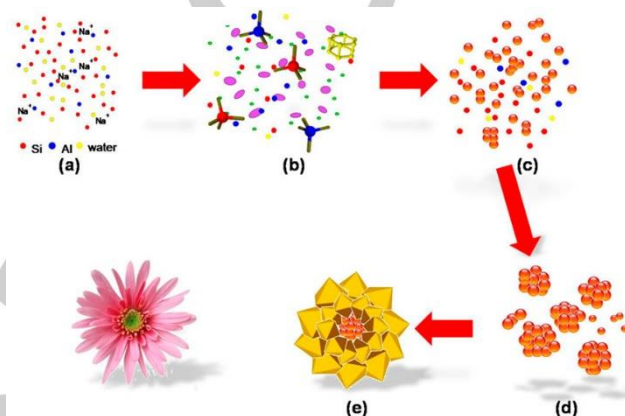
Figure 21. Proposed forming process of the flowerlike Y zeolite. Reproduced (adapted) with permission.[313] Copyright 2018 American Chemical Society.

Ultra Stable Y zeolite (USY)

Top-down methods

Dealumination
Ultra stable Y zeolites (USY) are also zeolites with FAU topology, however, these commercial USY series have been previously modified by one or more steam and/or acid treatments. This results in zeolites with a disrupted crystal morphology that have more cracks and voids as the degree of dealumination increases.[314] Further dealumination can be performed to create: (I) less Brønsted acid sites, (II) silanol nests, which can be used for impregnation of Lewis acid ions, or (III) a higher Si/Al ratio, which results in a more (steam)stable structure.[18]

A first dealumination study was performed by Pande et al. and used mineral acids such as H_3PO_4 and H_2SO_4 to steer the properties of the parent USY zeolite. In order to obtain the optimal selectivity and yield in the conversion of fructose to 5-hydroxymethylfurfural (5-HMF), the treatment needed to reduce the acidity, as well as increase the mesopore volume compared to the parent USY. The best performing hierarchical USY was obtained by treating the parent USY in an aqueous H_3PO_4 solution (10 wt%) for 2 hours at 100 °C as aging step, followed by an additional hour of stirring. This optimal combination of conditions resulted in (I) the presence of Brønsted and Lewis acid sites with moderate acidity, (II) moderate dealumination of EFAl and framework Al as well, (III) formation of new Al-O-P bonds, (IV) the formation of mesopores.[315] However, the possibility exists that the mesopores are not interconnected due to the rather random

action of the dealumination. To cope with this issue, Mi et al. developed a method that ensured interconnected mesopores after the dealumination process. This was achieved by introducing catalytic amounts of boron in the initial NaY framework, after which a steam treatment was applied as dealumination strategy. This promoted the hydrolysis of Si-O-Al and Si-O-B bonds, which resulted in the release of boron from the framework. NMR and DSC measurements indicated that this extra-framework boron further promotes framework destruction around the B-sites. In this aspect, the formation of interconnected mesopores was enhanced, which resulted in a relative increase in mesopore volume of 46 %, compared to the boron-free USY zeolite. This hierarchical USY was tested as a cracking catalyst for 2,2,4-trimethylpentane (iso-octane) and TIPB wherein it showed a higher catalytic activity, as well as a 2.1 % increase in gasoline yield.[316]

As was mentioned earlier, dealumination can also be used to create silanol nests wherein Lewis acid ions (e.g. Sn, Hf) can be immobilized. This was done in multiple works from Zhu et al. in which Sn was impregnated.[317,318] However, since the focus of these methods is more on the impregnation of Lewis acid ions than on the creation of mesopores, the interested reader is referred to literature for further details.

Desilication

Among literature concerning the desilication of USY zeolites, there exist many similar synthesis strategies under which the use of a mesoporogen is a well-known aspect. An overview of different templates that are qualified to assist in a desilication process is given in a first study from Verboekend et al. Herein, the molecular criteria for the selection of such molecules are investigated.[319] To find out which mesoporogen could tailor the intracrystalline mesopore structure and prevent realumination and amorphization, a broad screening of 18 different SDA's (anionic-, non-ionic- and cationic surfactants) was performed. The most effective mesoporogen tend to be positively charged and contained approximately 10-20 carbon atoms. Their impact on the desilication process depends on their charge, size, type and concentration of the mesoporogen. In what follows, three noteworthy mesoporogens are discussed. Starting with tetrapropylammonium cation (TPA$^+$), this quaternary ammonia was studied by Verboekend et al. It was shown that TPA$^+$ provided the largest preservation of the intrinsic zeolite properties within the mesoporous zeolite. Furthermore, a material yield of 56 % was obtained after the desilication in presence of 0.2 M TPA$^+$.[319]

A second mesoporogen is a cetyltrimethylammonium cation (CTA$^+$). This is different from TPA+ since it contains 3 methyl groups and one hexadecyl group, whereas TPA+ contains 4 shorter propyl chains. Verboekend et al. noticed that CTA+ is responsible for the introduction of mesoporosity, as well as for the preservation of intrinsic zeolite properties with a facilitated reassembly of leached species. However, even in the presence of CTA$^+$, not all leached species were reassembled since a material yield of only 50 % was observed.[320] The same template was employed by Silva et al. to assist in a desilication process with NaOH, which was followed by a hydrothermal treatment (20 hours at 150 °C) . This work studied the effect of the concentration of NaOH and CTA$^+$ on textural, chemical and morphological

characteristics. It turned out that NaOH had the greatest influence on textural properties, whereas CTA$^+$ functioned as a protective agent which prevented amorphization and desilication, leading to a material yield of 97.6 %. This protective effect of CTA$^+$ could be explained by the positively charged cation that hinders the attack of negatively charged hydroxyl-groups (OH$^-$).[321]

A third template, namely tetrabutylammonium hydroxide (TBAOH), functions both as desilication agent and mesoporogen. It was studied by Gackowski et al. who looked at the effect of TBAOH in a NaOH solution. Therefore, 3 desilication experiments were performed in 3 different solutions: (I) NaOH, (II) TBAOH, and (III) a NaOH/TBAOH mixture.[322] Best results were obtained with the NaOH/TBAOH mixture since approximately 50 % of Si was extracted without losing crystallinity and zeolite microporosity. Additionally, there was an increase in mesopore volume (from 0.20 to 0.89 cm^3 g^{-1}), BET surface area (from 802 to 826 m^2 g^{-1}), and Brønsted and Lewis acid sites.[322] Furthermore, it was shown that a 10-70 mol% TBAOH in NaOH was optimal regarding crystallinity, acidity, porosity, and catalytic properties of the resulting mesoporous zeolite. From an economic point of view, a 10 mol% TBAOH was chosen to be most interesting, especially when a potential scale up is considered.[323] In addition to the use of NaOH/TBAOH solutions, an ammonia treatment was carried out on USY zeolite as well. This was investigated from an economic point of view, since an ammonia treatment can be a promising inexpensive route. It was shown that this resulted in a partial loss of crystallinity, coupled with a loss of long-distance zeolite ordering. However, a short-range zeolite ordering was largely preserved.[324] Use of ammonia, especially on Al-poor USY zeolites had been reported before, including very advanced material and pore characterization, to be a successful mild method to open the structure through desilication with preservation of crystalline and catalytic activity domains. Moreover, the material is immediately in their acid form upon calcination. Such treatments with NH$_4$OH tend to show high material yields of up to 94 wt%.[325,326] Finally, Gackowski et al. also studied the effect of the desilication temperature on the outcome of the hierarchical USY zeolites.[323] Apparently, a temperature of 80 °C seemed to be optimal since this implied the formation of a new kind of hydroxyls with extremely high acidity (located in supercages).[327] From a practical point of view, all the hierarchical USY zeolites that were synthesized by this group were tested in the isomerization of α-pinene, which is an interesting test model to monitor improved site accessibility and acid strength (variation).[328] Here it was shown that the desilicated zeolites had an increased activity.[322–324,327]

To finish, USY zeolites can also be used as a catalyst in hydroconversion reactions. Therefore, hierarchical Brønsted acid USY zeolite, which can catalyze isomerization and cracking reactions, can be used as support for NiMo phases which can catalyze hydrogenation reactions. Such zeolites were synthesized by Ren et al.[329] and Zhang et al.[330] Both research groups employed a dealumination and desilication to synthesize a hierarchical USY support. Ren et al. performed a dealumination using steam and NH$_4$F as dealumination agents, whereas Zhang et al. employed (NH$_4$)$_2$SiF$_6$. Both methods were then followed by a desilication in NaOH. Comparison of characterization data from both methods leads to the conclusion that the method from Ren et al. gave the highest micropore surface area (376 versus 196

m² g⁻¹), micropore volume (0.20 versus 0.09 cm³ g⁻¹) and mesopore volume (0.40 versus 0.29 cm³ g⁻¹) compared to the hierarchical USY supports from Zhang et al. A comparison in catalytic performance between the parent USY and a hierarchical USY as Brønsted acid support in hydrocracking of naphthalene showed that both zeolites had a similar hydrogenation activity, however, the hierarchical support possessed a higher ring-opening ability.[329] Therefore, these modified zeolites are potentially interesting for the upgrading of FCC diesel oil[329] or waste cooking oil[330] through hydrodeoxygenation, hydroisomerization and/or hydrocracking reactions.

4.3. Beta

Zeolites with *BEA topology contain a crystal structure with a partially disordered framework. Therefore, the *BEA topology is often denoted with an asterisk as *BEA. This type of framework contains three-dimensional channels of 12 membered rings with following dimensions: (0.66 x 0.67 nm) along the [100] plane, and (0.56 x 0.56 nm) along the [001] plane.[331] Among zeolites with a *BEA framework, different materials can be distinguished (e.g. beta, Tschernichite, CIT-6, etc). However, following paragraphs mainly discuss the hierarchization of beta materials.

Top-down methods

Dealumination
Zeolites with *BEA topology can be dealuminated for two main reasons: (I) to create mesoporosity in addition to the microporous crystal structure, and (II) to create silanol nests which can be used to incorporate basic sites in the zeolite framework. However, only the first purpose will be discussed extensively since the focus of the second dealumination is more on the incorporation of basic sites instead of creating mesopores.

Dealumination of *BEA zeolites has been extensively investigated. In general, related works mainly focused on the use of different acids, which can be mineral acids (e.g. HNO_3[332–334]) or organic acids, and other synthesis parameters (e.g., temperature, treatment time, acid concentration). A first research was published by Zhao et al. and discussed the dealumination of Al-rich *BEA zeolites in a HNO_3 solution. Herein, the HNO_3 concentration varied between 4–15 %, whereas the temperature during dealumination varied between 50 – 100 °C. Subsequently, an acid HCl wash was executed to remove deposited EFAl. It was shown that a hierarchical beta zeolite with a Si/Al ratio of 22 was an excellent catalyst in the conversion of 2,5-dimethylfuran (2,5-DMF) to p-xylene yielding a 97 % p-xylene yield at 99 % DMF conversion.[332]

In contrast, Suárez et al. used HF/NH_4F as dealumination agent. Herein, the influence of the HF concentration was investigated, as well as the treatment temperature and treatment time. It was shown that the crystallinity was higher than 80 % as long as the HF concentration was lower than 0.5 M. Moreover, the treatment was best performed at temperatures and durations lower than 40 °C and 30 min, respectively. The acidic solution tends to slowly modify the crystal structure, leaving behind a highly corroded and porous sponge-like crystal structure in which the zeolite structure is retained. Next to these desired sponge-like crystals, it should be mentioned that a relatively low material yield between 30 and 60 % was observed. The HF/NH_4F treatment resulted in a higher

Brønsted/Lewis acid sites ratio, which proved to cause a lower activity in the isomerization/disproportionation reaction of m-xylene.[335]

Comparable to Suárez et al., Venkatesha et al. also investigated the influence of the concentration of the dealumination agent, however, in this work phenoldisulfonic acid (PDSA) was used. A concentration between 0.1-1 M was used during the synthesis of hierarchical *BEA zeolite, which was used for the condensation of glycerol with acetone to form glycerol acetals. Two products were formed when an untreated zeolite *BEA was used: the corresponding dioxalane (87 % selectivity) and dioxane (13 % selectivity). Applying an acid treatment with PDSA increased the selectivity towards dioxalane, which could rise to 100 % when a 1 M PDSA solution was used. This high selectivity was attributed to a decreased acidity, but also an increase in pore volume proved to be a significant factor since this increase in spatial environment facilitated the sterically demanding rearrangement of dioxane to dioxalane.[12]

Next to previous mineral acids as dealumination agent, organic acids can be used as well. This was done by several research groups.[336–338] Starting with Kowalska-Kuś et al., this group performed an acid treatment with citric acid, which was preceded by an alkaline treatment using a NaOH solution. The outcome was a hierarchical beta zeolite with superior catalytic performance. Applications included the ketalization of glycerol with acetone, forming solketal, with a conversion and selectivity up to 90 % and 98 % respectively.[336] Furthermore, the group of Li et al. performed subsequent dealumination and realumination using organic acids such as oxalic acid, DL-malic acid and DL-tartaric acid. All three acids showed different realumination abilities, where tartaric acid had the highest. Alternatively, the hierarchical beta zeolite that was formed after treatment with malic acid exhibited the best performance in the esterification of acetic acid with sec-butyl alcohol. This result was attributed to the quantity and density of medium and strong Brønsted acid sites, and to the enhanced aluminum gradient.[337] Regarding the realumination, the same research group published a study in which solid AlF_3 was used as realumination agent.[338] Herein, the structure, texture property, and acidity of the final hierarchical beta zeolite can be adjusted by changing the used amount of AlF_3. It was concluded that realumination occurred between 1.5–3 wt% AlF_3, whereas only dealumination happened when higher or lower amounts of AlF_3 were used.

Desilication
Desilication procedures can be roughly divided into three groups: (I) desilication combined with an acid wash, (II) template-free desilication, and (III) template-assisted desilication. The first group thus includes desilication procedures wherein an acid wash was used before or after desilication to make the zeolite framework more susceptible to desilication or to remove EFAl, respectively.

A first study that belongs to the first group was published by Leng et al. Herein, a beta zeolite was first desilicated in 0.2 M NaOH, after which it was refluxed in a 12 M HNO_3 solution, followed by an acid wash in 0.2 M HNO_3. After incorporating Ti into the framework, this hierarchical Ti/beta zeolite was tested in the oxidative desulfurization (ODS) of dibenzothiophene (DBT) and

4,6-dimethyldibenzothiophene (4,6-DMDBT). It was shown that the hierarchical Ti/beta zeolite, which preparation method included an acid wash after the desilication, showed enhanced activity compared to hierarchical Ti-Beta that was formed by direct dealumination or desilication.[339] A similar preparation method was employed by Jin et al. who also used a combination of an alkaline- an acid treatment. First, a pre-etching step was performed in a 0.2 M NaOH solution. Subsequently, an additional alkaline treatment, as well as a first acid treatment, was performed in respectively 0.2 M NaOH and 0.2 M HCl, which was repeated for three times. Overall, this procedure produced hierarchical pore structures with a regular pore size distribution and with material yields ranging from 40 to 60 wt%. When the alkaline-acid treatment was compared to an alkaline treatment, it was concluded that the acidic properties were comparable. However, an alkaline-acid treatment narrowed the pore size distribution, leading to enhanced catalytic performance with respect to selective production of linear alkylbenzenes, whereas an only alkaline treatment broadened the pore size distribution.[340]

The second group of desilication strategies includes template-free alkaline treatments and has been employed by several groups. In general, most research groups employ a 0.2 M NaOH solution as desilication agent,[341–345] while the effect of other synthesis parameters was explored. For instance, Dos Santos et al. investigated the influence of temperature and treatment time on the synthesis outcome. It was concluded that the optimal duration (10 - 240 min) of the alkaline treatment at 65 °C depends on the initial Si/Al ratio of the zeolite. For a high Si/Al ratio of 73 it was seen that these conditions are too drastic to develop mesoporosity with preservation of microporosity. In contrast, a Si/Al ratio of 40 was a better precursor.[341]

Continuing on template-free desilication, this strategy was also used for the synthesis of hollow beta zeolites. This was published in a study from Morgado et al., wherein different parameters were examined that could affect the desilication of nanometric beta zeolite crystals: (I) nature of the zeolite (crystal size, composition), (II) alkalinity, (III) temperature, and (IV) the amount of added Al. It was shown that alkalinity, temperature and the composition of the zeolite had the biggest effect on the morphology and properties of the hollow beta zeolites. Moreover, the addition of sodium aluminate during synthesis proved to protect the surface from desilication and favor dissolution at the center of the crystals, which in the end created the hollow structure.[346]

To finish, this paragraph discusses the third group of desilication strategies wherein mesoporogens are used to assist in the alkaline treatment. Starting with Fernandez et al., this research group performed a screening of various cationic tetraalkylammonium salts and organic amines for their potential contribution in a desilication process. This work attempted to figure out a structure – property relationship between the structure of the mesoporogen and the average mesopore size. Furthermore, the as synthesized hierarchical beta zeolites were tested in the acid catalyzed isomerization of α-pinene where an improved catalytic conversion was noticed compared to the parent beta zeolite.[347] A first mesoporogen, namely tetramethylammonium hydroxide (TMAOH), was employed by Bi et al. in combination with NaOH. The resulting hierarchical beta zeolites were used in the catalytic fast pyrolysis of Kraft lignin and showed a higher cracking activity compared to parent beta. This

was mainly attributed to the preserved acidity and larger mesopores, which ensured the entry of bulkier reactant molecules.[348] Similar mesoporogens with different alkyl chain-lengths (e.g. TEAOH, TPAOH, TBAOH), were used by several research groups.[346,349–352] As such, Werner et al.[349] and Morgado et al.[346] performed a desilication with tetraethylammonium hydroxide/bromide (TEAOH, TEABr). The first group reported no loss of microporosity and crystallinity, as well as a higher activity in the epoxidation of cyclooctene.[349] These results were also obtained by the second group who obtained an improved crystallinity and thermal stability in the synthesis of hollow beta zeolite nanocrystals.[346] Tetrapropylammonium hydroxide/bromide (TPAOH, TPABr) was used by multiple groups[350–352], as is the case for tetrabutylammonium hydroxide/bromide (TBAOH, TBABr)[353,354] and cetyltrimethylammonium hydroxide/bromide (CTAOH, CTABr).[355–357] Although there is a subtle difference in structure, the overall outcome after use of these mesoporogens was similar.

Dissolution-recrystallization

In the recrystallization of beta zeolites, NaOH is a common alkaline agent that is used by several groups, possibly in presence of an organic template (e.g. TPA+).[358] Starting with Zhang et al., this group synthesized hierarchical beta zeolites by performing a desilication in different NaOH concentrations (0.2 and 0.3 M). Catalytic tests in the conversion of benzyl alcohol with mesitylene showed that a concentration of 0.2 M is optimal in order to preserve sufficient acidity and crystallinity during synthesis. The formation of mesopores was explained by a sequential hierarchical structure formation and recrystallization mechanism. First, NaOH creates mesopores by extracting Si from the zeolite framework. Subsequently, the synthesis shows characteristics of a bottom-up approach that favors crystallization of the zeolites and recovers the defects in the zeolite framework. In the end, a material yield of about 65 wt% could be observed.[359]

In contrast to NaOH as desilication agent, Escola et al. used an ammonia/TEAOH solution in a hydrothermal treatment to rearrange the broad pore size distribution of parent hierarchical beta zeolites to a single mesopore size. A uniform mesopore size of 400 nm was successfully created and proved to be beneficial in the acylation of veratrole showing a high TOF.[360]

To finish, the group from Cho et al. performed a final recrystallization step on a post-synthetic Sn/Beta in the presence of NH4F and TEABr. The fluoride ions induced partial dissolution of the zeolite crystal, after which a rearrangement of different types of silanol defects took place in the presence of TEABr. Eventually, two material types were formed: a 3D-ordered-mesoporous imprinted catalyst, as well as a nano-crystalline Sn/Beta catalyst. Both materials showed an improved hydrophobicity and mass transport, which were beneficial in reactions that involve bulky molecules such as lactose.[361]

Bottom-up methods

Soft templating

In following paragraph, several bottom-up approaches are discussed that make use of a mesoporogen in their hydrothermal synthesis procedure. There exist various strategies that are simply based on a change of soft template as well as on a variation of the synthesis parameters. A first research was performed by Caldeira et al. who started their synthesis with a pre-
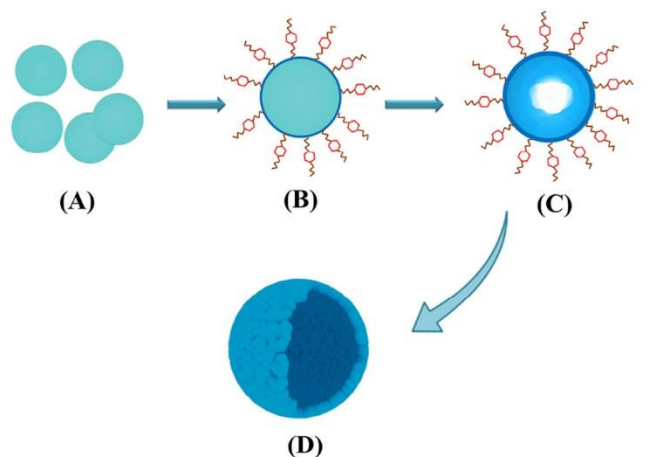
crystallization step to induce the formation of protozeolitic nano-units. Further on, these nano-units were subjected to two separate methods. The first method employed CTAB to assist in the reorganization of the nanounits, which in the end showed a narrow mesopore size distribution, high acid strength, and stable tetrahedral Al species. The second method used a silanation agent such as phenylaminopropyltrimehoxysilane (PHAPTMS), which was grafted to the outer part of the nano-units to avoid total merge during the crystallization process. This resulted in a hierarchical beta zeolite with a rather high mesopore area and external surface area, and consequently in an improved accessibility. The synthesized zeolites were evaluated in the catalytic cracking of high density polyethylene (HDPE), where the accessibility to the active sites and the acid strength seemed to influence the catalytic performance and product selectivity, respectively.[362]

As was the case for FAU zeolites, hierarchical *BEA zeolites can exist in the form of hollow zeolites. Following two groups attempted to hydrothermally synthesize this type of structures, all by using a specific mesoporogen, for instance a cationic quaternary ammonium surfactant[363] or pentacyclic lactams.[364] The first group from Zheng et al. performed a one-step hydrothermal method wherein the cationic quaternary ammonium surfactant was able to interact with anionic aluminosilicate species to induce the formation of hollow beta zeolites. The synthesis followed a surface-to-core crystallization process, which is visually represented in Figure 22. In this process, surface nanoparticles of the amorphous quasi-spheres underwent faster nucleation compared to the interior. In this aspect, a large inner cavity is created, as well as a hierarchical structure, which facilitates access to the acid sites.[363] A similar method from Zhao et al. used pentacyclic lactams as another type of hollow-directing agents. These are cost-effective and recyclable which makes them attractive in terms of environmental aspects. Hollow beta zeolites have been tested in the alkylation of benzene and benzyl alcohol with isobutylene[364] and mesitylene,[363] respectively.

Other research groups tried to implement Sn or Ni in the hierarchical beta zeolite. Zhang et al. used polydiallyldimethylammonium chloride (PDADMAC) as a mesoporogen in the hydrothermal synthesis of hierarchical beta. The hierarchical Sn/beta was tested in the conversion of sugars towards intermediates for producing alkyl lactate and showed higher TOF (almost double), as well as product selectivity up to 86 % (compared to 75 % for the conventional Sn/beta).[365] An analogous method was employed by Wang et al. where the hierarchical beta support was synthesized with another type of mesoporgen, often categorized under the name "gemini-type bifunctional multi quaternary ammonium surfactants".[366] Although such templates are complex, they prove to be effective in the synthesis of combined micro-mesoporous zeolites. This was shown in a first study from Zhang et al. Herein, $C_{18-6-diphe}$ was used in a dual-template hydrothermal approach, which resulted in the simultaneous generation of micro- and mesopores. The formed mesopore walls showed a zeolite-like micropore framework that possessed high hydrothermal stability.[367] An analogous method was used by Wang et al. who applied a one-pot dual-template strategy using a $C_{12-6-12}$ gemini-surfactant in combination with TEAOH as SDA.[368] The effect of the gemini-surfactant was unraveled on a molecular level by Castro et al. who

made use of advanced characterization techniques such as SAXS, NMR, etc.[369]

$\text{SDA: } N(CH_3)_2\text{-}C_6H_{12}\text{-}N^+(CH_3)_2\text{-}CH_2\text{-}\hexagon\text{-}CH_2\text{-}N^+(CH_3)_2\text{-}C_6H_{12}\text{-}N(CH_3)_2[Cl^-]_2$

Figure 22. Schematic representation of the formation process of hollow beta zeolite with hierarchical meso/micropores.[363] Reproduced with permission of Elsevier.

Hard templating

In a first work, Soltanali et al. investigated the hydrothermal synthesis of hierarchical beta zeolites with three hard templates: (I) carbon nanotubes, (II) carbon nanofibers, and (III) graphene oxide. Next to the hard template, an additional SDA (e.g. TEAOH) was used as well for each sample. Graphene oxide proved to be most effective as hard template regarding the final mesoporosity and pore size. An increased mesoporosity (from 0.16 to 0.19 cm³ g⁻¹, compared to template-free synthesized beta) proved to increase the catalyst lifetime and catalytic performance in methanol-to-olefins (MTO) reactions.[370] A second and, to our knowledge, last work employing hard templates was conducted by Yu et al. Herein, white carbon black was used as hard template in addition to PDADMAC as soft template. Nano-mesoporous beta molecular sieves were hydrothermally produced with large specific surface area, appropriate surface acidity and high chemical & thermal stability.[371]

Template free

In contrast to previous template-assisted hydrothermal synthesis procedures, two studies have been found that manage to synthesize hierarchical beta zeolites without using any templates.[372,373] Considering the first, Zhao et al. executed the crystallization of high Si hierarchical beta zeolites by kinetic regulation of the crystallization process. They worked under low water conditions which facilitated nucleation and crystal growth and ensured that the fusion of individual nanocrystallites inside the particle is restrained. The formed catalyst was tested in the methanol-to-propylene (MTP) reaction in which a longer catalyst lifetime was noticed. This could be explained by a slower coking rate, which was a consequence of the improved utilization of the interior acid sites, and the enhanced molecular diffusion.[372]

Nanozeolites and their assembly

Nanostructured beta zeolites can be synthesized in multiple ways. A first method was proposed by Xiong et al. who performed an

aerosol-assisted hydrothermal method in NaF medium in presence of TEAOH. Hierarchical beta zeolites with Si/Al ratios ranging from 44 to 392 were synthesized, wherein the Si/Al ratio determined the final morphology. Synthesis gels with a rather low Si/Al ratio tend to form nano-aggregates with interparticle mesopores (mesopore volume 0.21 cm³ g⁻¹), whereas higher Si/Al ratios (e.g. 150) resulted in nano-plate like zeolites with intracrystalline mesopores (mesopore volume 0.28 cm³ g⁻¹).[374]

In another study, Huang et al. hydrothermally formed hierarchical beta zeolites composed of uniform nanocrystals which had high pore volume (0.67 cm³ g⁻¹) and high external surface area (349 m² g⁻¹). Therefore, a layered silicate precursor (H-kanemite) was used as silica source, which exhibits a huge number of silanols that easily dissoluted in alkaline media. By consequence, silica fragments were formed that were subsequently reassembled, with Al species to construct the framework of nanosized beta crystals. Further assembly of these nanocrystals was assisted by TEAOH as SDA and eventually formed self-sustaining macrosized zeolitic aggregates with intracrystal microporosity, but also extremely high mesopore volumes and external surface areas.[375] The same SDA was applied in a procedure from Luo et al. wherein a micro zone synchronous crystallization method was performed by a steam-assisted conversion. This method was free of zeolite seeds or mineralizing agents, although, a small amount of TEAOH was used to successfully construct a self-sustaining plate-like nanosized aggregation with a high surface area and pore volume up to 631.09 m² g⁻¹ and 0.7 cm³ g⁻¹, respectively.[376] In accordance to Huang et al., Zhang et al. also used an SDA in the in situ assembly of nanoparticles. This time, a tailored polyquaternium surfactant is used without hydrophobic tail. Despite the fact that this surfactant had no hydrophobic tail, the synthesis proved to be successful since the catalyst showed an improved resistance against deactivation in the alkylation of benzene with propene.[377]

In another work, Chaida-Chenni et al. investigated two procedures. The first method included a direct hydrothermal method in which an assembly of nanocrystals of preformed beta seeds was formed. Herein, a pluronic P123 triblock copolymer was used as template during the assembly, which finally resulted in physical mixtures of beta nanoparticles with mesoporous SBA-15 phases.[378] Next to P123, it is also possible to employ CTAB as mesoporogen, which was the case in a work from Al-Eid et al. where an analogous method was employed in a one-pot synthesis.[379] The second method from Chaida-Chenni et al., however, executed an acidification of the beta seeds solution, without the use of an organic template. This method provided the best structured beta nanoparticles.[378]

To finish, several works are given that aimed to synthesize hierarchical *BEA nanosponges.[380–383] Therefore, Kim et al.[380] and Shin et al.[381] employed gemini-surfactants in the hydrothermal synthesis of these structures. Nanosponge zeolites can be seen as randomly interconnected ultrathin beta nanocrystals with intercrystalline mesopores. Such structures tend to perform well in catalytic tests, as there is the cycloaddition of dimethylfuran with ethylene,[380] or the tetrahydropyranylation of alcohols.[381] An enhanced catalytic activity was reported compared to commercial beta zeolite, which was attributed to facile diffusion and high accessibility of acid sites in nanosponge beta zeolites.

5. Conclusion and perspective

This review shows and confirms the great potential of synthesizing hierarchical zeolites and their use in a variety of (industrially relevant) catalytic applications. An improved performance is seen both in the activity and/or product selectivity of the zeolite and/or in a decreased deactivation rate. This can be attributed to several effects that come along with the hierarchization procedure and the obtained zeolite structure. Most affected parameters are for instance total surface area, micro- and mesopore surface area, micro- and mesopore volume, acidity, crystallinity and pore diameter. Several works discussed in this review largely attributed the better performance to an increase in mesopore surface area and volume, compared to that of the parent zeolite, and the report exemplifies this with catalytic results for several reaction types. In this aspect, site accessibility increased, diffusion limitation decreased or even disappeared so that mass transport to the active sites is more efficient. However, in many cases the hierarchization also impacts the acidity of the zeolite as well. This is due to a change in Si/Al ratio or different position of Al in or out the framework. In this aspect, and depending on the targeted reaction, a higher (either strength or number of) acidity can increase the activity at the active sites so that the zeolite appears to have a higher overall activity. Other acid types are also created upon hierarchization on top of the Brønsted acid sites, such as in particular Lewis acid sites, which may be better/worse for the catalysis. One note is important: most papers rely for their conclusions of the catalytic effect on simple conversion in time plots, whereas very detailed kinetic analyses are often missing, as well as selectivity vs. conversion plots measured at various contact times. Direct links between mesoporosity effects and reaction rates should therefore be concluded with caution, though there is no doubt that hierarchization has substantial impact on catalysis.

The processes that are used to create hierarchical zeolites can be divided in two main approaches: (I) a top-down approach, and (II) a bottom-up approach. The first is based on the action of an acid- or alkaline treatment on an already synthesized zeolite to perform a dealumination or desilication respectively. Such treatments are relatively straightforward and are suitable to be employed on an industrial scale. The second strategy is based on the direct synthesis, possibly in assistance of a mesoporogen, of a crystal structure containing inter- or intracrystalline mesopores. Both methods have clear advantages and drawbacks. Starting with a top-down treatment, the major advantage of this method is its simplicity. However, it is difficult to control the mesopore formation process since the attack of the acid and/or base is rather random. As a result, the mesopores that are created are potentially enclosed in the framework without any connection to the external surface or micropores or show low connectivity. Another drawback is the loss of material as a consequence of the partial dissolution of the zeolite framework. Although not per se a show stopper for the academic research, high loss of material, irrespective of the beauty or catalytic property of the porous material, will restrict its use in applications. It is therefore strongly advised always to report the numbers and show progress in this context as well. Furthermore, an increase in mesoporosity is often coupled to a decrease in microporosity and crystallinity. This obviously should be limited since the micropores are responsible for the structure selectivity effect that is characteristic of zeolitic catalysts, and often also for the strong zeolite-typical acidity (if

required). In contrast, the construction of the hierarchical zeolite framework in bottom-up approaches is more controllable, but often more tedious and expensive. Herein, parameters such as aging time, crystallization time, composition of the synthesis gel, temperature, stirring speed, addition of an SDA or mesoporogen can be altered in order to steer the synthesis towards a well-defined mesoporous zeolite. The use of an SDA and/or mesoporogen is helpful in the synthesis of micropores and mesopores, respectively. However, besides cost, the expensive templates can also be toxic for the environment MTT. In addition, such templates need to be burned off before the catalyst can be used, which releases CO_2 and volatile (toxic) compounds to the atmosphere. Sometimes, such template oxidation creates an exotherm that can destroy the (porous) structure of the zeolite. Here, researcher are trying other means such as the use of ozone, that oxidizes at much lower temperature. Washing and re-use of templates is also an option, but this is not systematically studied, and likely not always possible with the current procedures and molecule types used today.

Different synthesis approaches can also be used to produce nanozeolites. In recent years, the assembly of nanozeolitic units was studied further. These assemblies show great promise as they can mitigate some of the drawbacks of normal nanozeolites, such as poor stability and difficult manipulations, during catalytic reactions.

The extensive overview given in this review has shown that for most zeolite topologies variants on both approaches can be used to create a hierarchical pore system. Instead of formulating a general statement regarding the best hierarchization strategy, it should be mentioned that the appropriate strategy largely depends on the morphology and topology of the parent zeolite. Moreover, the applied strategy depends on the targeted properties of the final zeolite. In this aspect, a hierarchical zeolite that needs high acidity will be processed by a different treatment than a hierarchical zeolite wherein the acidity is of less importance compared to, for instance, its mesopore volume. Nevertheless, Figure 23 attempts an overview of the effect of different hierarchization procedures on the final characteristics of the zeolite, and shows the results for the most important topologies. Here the fraction of mesoporosity is selected as a measure, as hierarchization is about improving porosity, though its optimal value depends on the optimal balance between reaction rate of the catalysis and molecular pore transport. The mesopore fraction is plotted against the relative acidity (against the reference material), as a measure of the improvement of the amount of catalytically active sites in the final mesopore material. This is done for each discussed topology (except MTT) and is based on data found in literature. Note that acid strength is not included because these values are less reported systematically and the results are more difficult to compare among the different groups due to (slightly) different procedures used for their measurements. Although no clear trend can be observed, the figure can be a very helpful tool to determine the appropriate hierarchization strategy in order to obtain a zeolite with the desired properties for a certain application. It is apparent that with regard to TON, almost only top-down methods were explored in the last years, whereas no bottom-up syntheses have been reported recently. Yet, zeolites like ZSM-22 are interesting zeolites, e.g. for diesel dewaxing and hydroisomerization. For FER, both methods have been used. Improvement in acidity level can be realized with both methods,

whereas the highest mesoporosity is achieved with bottom-up syntheses, viz. 45 in the Figure 23. This is in contrast with the hierarchization of MOR, where particularly top-down methods are more successful to introduce high mesoporosity, as illustrated by the examples 261 and 265. For FAU topology, classically more top-down methods are studied. The whole spectrum of acidity and porosity combinations can be achieved, using different methods, and very nice procedures exist to realize both high porosity and high acidity values, e.g. examples 322 and 323. ZSM-5 is the most studied topology for its major utilization in catalysis in various reactions types such as alkylation and (hydro)cracking. Although the majority of the mesoporization research is done with bottom-up methods, the best results showing both high acidity and porosity were achieved with top-down methods, viz. 68, 78 and 80. Hierarchical *BEA materials with varying mesoporosity can be obtained with both methods and comparable acidity numbers. More detailed information concerning Figure 23 and the used references can be found in Table S1 to Table S6 in the Supplementary Information, which also includes the catalytic reactions that were tested.

In recent years, a great progress in the synthesis of hierarchical zeolites has been achieved using both established but fine-tuned and new methods. However, there remain a number of challenges in the development of hierarchical zeolites.

1. Green and cost-effective synthesis of hierarchical zeolites. In order to prepare hierarchical zeolites more economically and environmentally viable for industrialization, large-scale zeolite synthesis using commercially available and eco-friendly raw materials is highly required. The industrial production of hierarchical zeolites strongly requires cost- and energy-efficient synthetic approaches. For instance, hierarchical zeolites that are synthesized via acid/base-treatment methods generally suffer from low solid product yields and decreased zeolite crystallinities, thus, increasing the product yields and crystallinities are crucial from an economical view point. Furthermore, some two-in-one soft templates could successfully direct the formation of high-quality hierarchical zeolites, however, the design and synthesis of such organic templates are labor- and cost-intensive. To date, there are many approaches creating hierarchical zeolites, however, the high synthetic cost, low product yields and crystallinities of zeolites, and addition of soft templates which are harmful to the environment or cost-intensive limit their industrialization. On the basis of existing mature synthesis methods of hierarchical zeolites, more green and cost-effective synthetic strategies for creating high-quality hierarchical zeolites are long-term goals to pursue.

Recently, template-free approaches including seed-assisted and kinetic regulation for creating hierarchical zeolites have gained more attention and success in academia.[384] Compared with template-directed and post-treatment methods, seed-assisted and kinetic regulation are emerging green methods for the formation of hierarchical zeolites, in which a balanced nucleation and growth rate is required. Classical and non-classical crystallization mechanism coexist in such seed-assisted and
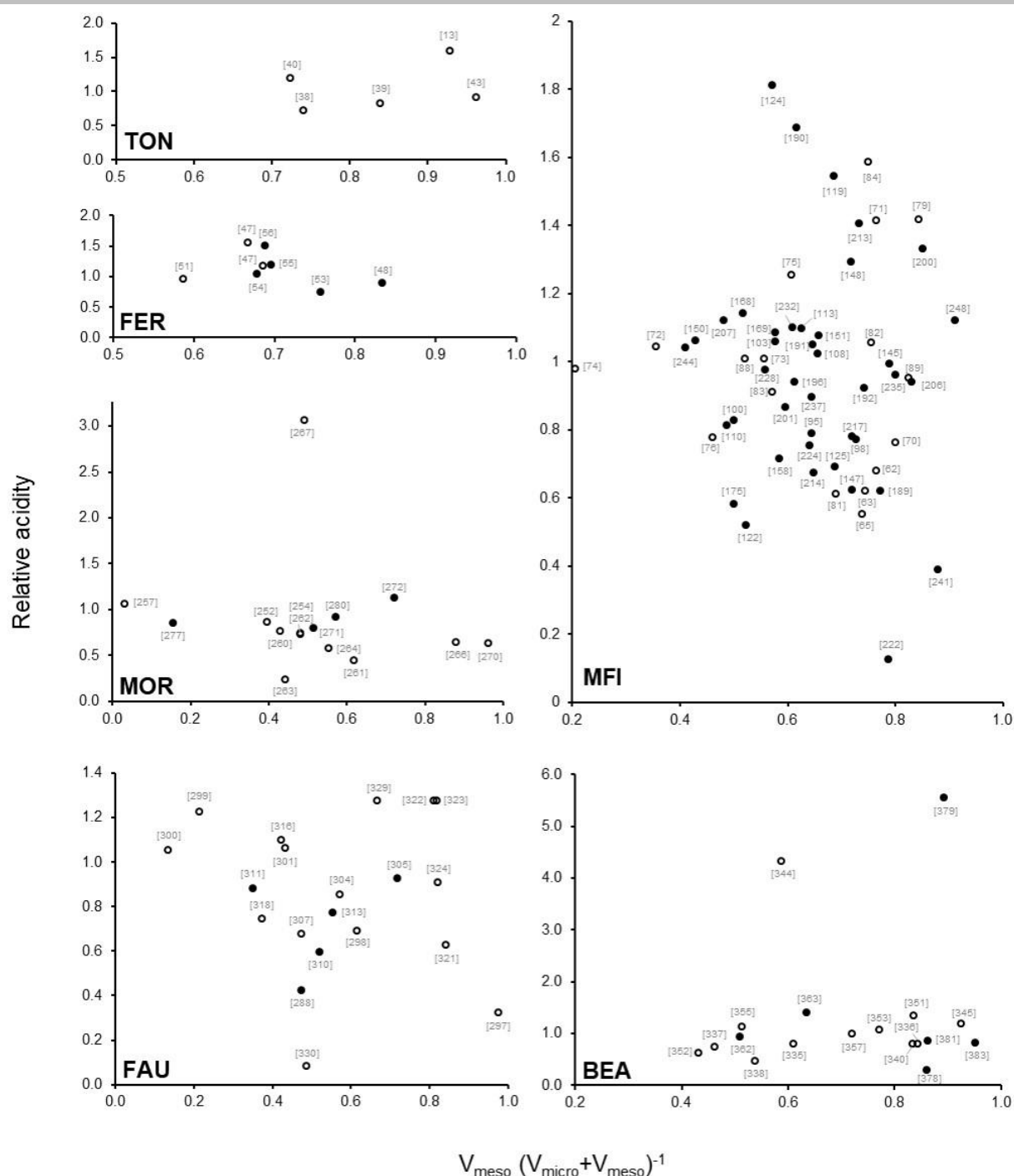
Figure 23. Overview of the effect of different hierarchization procedures on the final characteristics of each topology discussed in the review (except MTT), based on data found in literature. Open symbols represent top-down methods. Closed symbols represent bottom-up methods. More detailed information concerning this figure and the used references can be found in Table S1 to Table S6 in the Supplementary Information.

kinetic regulation processes for creating hierarchical zeolites. The adjustment on two/multi-step crystallization, addition of inorganic ions, and even concentration of precursor sources will be effective to regulate the nucleation and growth steps. Furthermore, the understanding of the formation process of hierarchical zeolites is crucial to unravel the zeolite crystallization mechanisms.

2. Fabrication of single-crystalline hierarchical zeolites. Compared with poly-crystalline hierarchical zeolites, single-crystalline hierarchical zeolites contain less grain boundaries. These grain boundaries, that are preferentially attacked by water,

may cause low hydrothermal stabilities of zeolites. In general, a specific synthetic condition is needed for the formation of hierarchical single-crystalline zeolites. For instance, nanosized crystals could aggregated to form hierarchical zeolites, in which some hierarchical zeolite products possess single-crystalline features and the others are poly-crystalline. Such aggregation process corresponds to the non-classical zeolite crystallization mechanism. A precise control on the zeolite non-classical crystallization mechanism may allow the aggregation of nanosized crystals towards an oriented-attachment manner and consequently the formation of hierarchical single-crystalline

zeolites. Fabrication of hierarchical single-crystalline zeolites and investigation of their formation mechanism remain challenges and a hot research topic in the future.

3.   Fabrication of hierarchical zeolites with interconnected pore systems or low defects. Isolated mesopores do not contribute to the improvement of mass transportation within zeolites.[385] Instead, these isolated mesopores may act as centers that gathers large amount of intermediates/products and finally lead to coke deposition, which causes decreased catalytic performance as well as decreased selectivity towards target products. In contrast, hierarchical zeolites with interconnected pore systems allow rapid diffusion of intermediates or products from the active sites before being involved in secondary events. Silanol defects play important roles in zeolite catalysis. For instance, the silanols adjacent to the active Sn hydroxyl sites in Sn-Beta promote the hydride transfer in the isomerization of glucose to fructose.[386] Tailoring silanol defects of hierarchical zeolites will be an increasingly important research topic in the future. Furthermore, the amount of defects significantly affect zeolite hydrothermal stabilities, namely, the more defects, the worse the zeolite hydrothermal stability. As no zeolite can be free of external surface defects, in this case, low defects correspond to low internal framework defects but not external surface defects. Hierarchical zeolites with interconnected and large mesoporous systems may feature low defects. This is because these interconnected and large mesopores turn to be external surfaces. In contrast, the isolated and small mesopores generate large amounts of internal framework defects. Synthesis of low-defect hierarchical zeolites endows zeolites with dramatically improved hydrothermal stabilities. Alternatively, passivation of the silanol defects via incorporation of heteroatoms has proven to be another effective approach.[387]

4.   Synthesis of hierarchical zeolites using commercially available raw materials which contain mesoporosity themselves or via 3D printing technology. Some natural and lab-synthesized silicon resources, such as diatomite and mesoporous silica possess mesoporosity/macroporosity themselves. Transformation of these resources to zeolite crystals while keeping their mesoporosity/macroporosity will be a promising strategy for the formation of hierarchical zeolites. For instance, an ordered mesoporous aluminosilicate with a completely crystalline zeolite wall structure has been synthesized using SBA-15 as silicon source.[388] In general, a low mobility of the silicon sources in the gel system are needed to suppress an extensive and fast transformation from amorphous to crystalline. Thus, a facile and slow transformation from silicon species to silica tetrahedra and finally zeolite frameworks are permitted to maintain the mesoporosity/macroporosity of raw materials. Compared with a conventional diluted gel system that generally causes high mobility of precursor sources, the dry gel synthesis, concentrated gel synthesis, or steam-assisted approach is beneficial in maintaining the mesoporosity/macroporosity of the raw resources. Taking full advantage of the mesoporosity/macroporosity of raw materials will provide opportunities for industrial production of hierarchical zeolites. 3D-printing technology is a new approach for precisely constructing materials with desirable porosities, sizes, shapes, and active site spatial arrangements. Recently, binder-free zeolite monoliths featuring hierarchical structures were obtained using 3D-printing technology.[389] Such new technology will be a good method for precise control of the proportion, connectivity, and distribution of micro-, meso-, and macro-pore systems. The molecule diffusion kinetic within various hierarchical systems significantly differs and consequently affects the catalytic performance. In this case, 3D-printing technology will be a good approach to regulate the molecule diffusion kinetic via adjusting the proportion, distribution, and connectivity of pore systems. Then, with the assistance of 3D-printing technology for tailoring hierarchical systems, a good relationship between the molecule diffusion kinetic and catalytic performance could be well established.

5.   Precise control of the aluminum distribution in hierarchical aluminosilicalite zeolites and the silicon distribution in hierarchical silicoaluminophosphate zeolites. Some soft mesoporogens possess chelation properties to chelate with Si or Al species, further controlling the Si or Al distributions. The precise control of Si distribution in SAPOs and Al distribution in aluminosilicalite zeolites remains a challenge. The Si or Al atom distributions significantly affect the catalytic performances including product selectivities and catalyst lifetimes, especially under high-temperature gas-phase catalytic processes. The organic molecules that served as mesoporogens/modifiers generally possess chelation properties because of the existence of ammonium or hydroxyl groups. The chelation between organic molecules and metal species or silica has already been reported.[390–392] Recently, aluminum-rich ZSM-5 (Si/Al = 8) zeolites were prepared via biomass-mediated supramolecular approach.[393] Silicates and aluminates are known to bind to carbohydrates in a way that diminishes their reactivity, which favors the incorporation of Al atoms into zeolite frameworks. Compared with inorganic Si/Al precursor sources, these complex may supply a "nutrient pool" providing a consecutive and slow release of Si or Al sources to nourish the nucleation/growth of hierarchical zeolites, which is favorable for the control of T atom distribution. Furthermore, this also provides in-depth molecular-level and supramolecular-level understanding of the zeolite crystallization mechanisms.

6.   Preparation of zeolite-based hierarchical core-shell catalysts that contain zeolites as core enwrapped by mesoporous materials or zeolites as shell. These zeolite-based core-shell materials have received enormous attention due to their dual functions in catalysis. Core-shell structured composites comprising zeolite crystals as cores and ordered mesoporous silica as shells presented superior performance in various catalytic process.[385,394–397] This is due to the fact that the mesoporous shells could allow providing sufficient voids for capturing reactant molecules, pre-cracking of primary bulky molecules, promoting molecule diffusion from mesopores to micropores, or preventing the active component of zeolite cores from pore blocking by heavy by-products. Furthermore, zeolite-based core-shell structures that combine both advantages may also afford improved performance in various applications, such as the application of semiconductor@zeolite in photocatalysis[398], of MOF@zeolite in adsorption[399,400], of metallic species@zeolite in tandem catalysis[401,402].

Acknowledgements

Conflict of interest

The authors declare no conflict of interest.

Keywords: Hierarchical zeolites • Mesoporous zeolites •Top-down • Bottom-up • Nanozeolites

References

[1] L. B. McCusker, D. H. Olson, C. Baerlocher, Atlas of Zeolite Framework Types, 2007.

[2] "Database of Zeolite structures," can be found under http://www.iza-structure.org/databases/, 2020.

[3] M. Dusselier, M. E. Davis, *Chem. Rev.* **2018**, *118*, 5265.

[4] K. Zhang, M. L. Ostraat, *Catal. Today* **2016**, *264*, 3.

[5] R. Bai, Y. Song, Y. Li, J. Yu, *Trends Chem.* **2019**, *1*, 601.

[6] A. Feliczak-Guzik, *Microporous Mesoporous Mater.* **2018**, *259*, 33.

[7] Y. Wei, T. E. Parmentier, K. P. De Jong, J. Zečević, *Chem. Soc. Rev.* **2015**, *44*, 7234.

[8] A. Taguchi, F. Schüth, *Microporous Mesoporous Mater.* **2005**, *77*, 1.

[9] J. Jiang, J. Yu, A. Corma, *Angew. Chemie Int. Ed.* **2010**, *49*, 3120.

[10] Y. Yan, X. Guo, Y. Zhang, Y. Tang, *Catal. Sci. Technol.* **2015**, *5*, 772.

[11] H. Qu, Y. Ma, B. Li, L. Wang, Emergent Mater. 2020, DOI 10.1007/s42247-020-00088-z.

[12] N. J. Venkatesha, Y. S. Bhat, B. S. Jai Prakash, *RSC Adv.* **2016**, *6*, 18824.

[13] A. K. Jamil, O. Muraza, M. H. Ahmed, A. Zainalabdeen, K. Muramoto, Y. Nakasaka, Z. H. Yamani, T. Yoshikawa, T. Masuda, *Microporous Mesoporous Mater.* **2018**, *260*, 30.

[14] Y. Liao, R. Zhong, M. Halluin, D. Verboekend, B. F. Sels, ACS Sustain. Chem. Eng. 2020, 8, 23, 8713.

[15] D. Verboekend, J. Pérez-ramírez, Catal. SCi. Technol. 2011, 1, 879.

[16] J. Pérez-Ramírez, C. H. Christensen, K. Egeblad, C. H. Christensen, J. C. Groen, *Chem. Soc. Rev.* **2008**, *37*, 2530.

[17] D. P. Serrano, J. M. Escola, P. Pizarro, *Chem. Soc. Rev.* **2013**, *42*, 4004.

[18] X. Jia, W. Khan, Z. Wu, J. Choi, A. C. K. Yip, *Adv. Powder Technol.* **2019**, *30*, 467.

[19] K. Li, J. Valla, J. Garcia-Martinez, *ChemCatChem* **2014**, *6*, 46.

[20] K. Möller, T. Bein, *Chem. Soc. Rev.* **2013**, *42*, 3689.

[21] E. Koohsaryan, M. Anbia, *Cuihua Xuebao/Chinese J. Catal.* **2016**, *37*, 447.

[22] V. Valtchev, S. Mintova, *MRS Bull.* **2016**, *41*, DOI 10.1557/mrs.2016.171.

[23] R. Chal, C. Gérardin, M. Bulut, S. VanDonk, *ChemCatChem* **2011**, *3*, 67.

[24] S. Van Donk, A. H. Janssen, J. H. Bitter, K. P. De Jong, *Catal. Rev. - Sci. Eng.* **2003**, *45*, 297.

[25] X. Fan, Y. Jiao, *Porous Materials for Catalysis: Toward Sustainable Synthesis and Applications of Zeolites*, Elsevier Inc., **2019**. https://doi.org/10.1016/B978-0-12-814681-1.00005-9

[26] I. I. Ivanova, E. E. Knyazeva, *Chem. Soc. Rev.* **2013**, *42*, 3671.

[27] C. Dai, A. Zhang, M. Liu, X. Guo, C. Song, *Adv. Funct. Mater.* **2015**, *25*, 7479.

[28] K. Na, G. A. Somorjai, *Catal. Letters* **2015**, *145*, 193.

[29] K. Na, M. Choi, R. Ryoo, *Microporous Mesoporous Mater.* **2013**, *166*, 3.

[30] Q. Li, D. Creaser, J. Sterte, *Chem. Mater.* **2002**, *14*, 1319.

[31] S. Mintova, J. P. Gilson, V. Valtchev, *Nanoscale* **2013**, *5*, 6693.

[32] K. Möller, T. Bein, *Microporous Mesoporous Mater.* **2011**, *143*, 253.

[33] O. Muraza, I. A. Bakare, T. Tago, H. Konno, T. Taniguchi, A. M. Al-Amer, Z. H. Yamani, Y. Nakasaka, T. Masuda, *Fuel* **2014**, *135*, 105.

[34] B. J. B. Silva, L. V. Sousa, L. R. A. Sarmento, S. L. Alencar, P. H. L. Quintela, A. O. S. Silva, *Appl. Catal. B Environ.* **2020**, *267*, 118699.

[35] M. Zhai, L. Li, Y. Ba, K. Zhu, X. Zhou, *Catal. Today* **2019**, *329*, 82.

[36] B. J. B. Silva, L. V. Sousa, L. R. A. Sarmento, R. P. Carvalho, P. H. L. Quintela, J. G. A. Pacheco, R. Fréty, A. O. S. Silva, *Microporous Mesoporous Mater.* **2019**, *290*, 109647.

[37] D. Verboekend, A. M. Chabaneix, K. Thomas, J.-P. Gilson, J. Perez-Ramirez, *CrystEngComm* **2011**, *13*, 3408.

[38] X. Wang, X. Zhang, Q. Wang, *Ind. Eng. Chem. Res.* **2019**, *58*, 8495.

[39] M. Dyballa, U. Obenaus, M. Rosenberger, A. Fischer, H. Jakob, E. Klemm, M. Hunger, *Microporous Mesoporous Mater.* **2016**, *233*, 26.

[40] P. del Campo, P. Beato, F. Rey, M. T. Navarro, U. Olsbye, K. P. Lillerud, S. Svelle, *Catal. Today* **2018**, *299*, 120.

[41] P. del Campo, U. Olsbye, K. P. Lillerud, S. Svelle, P. Beato, *Catal. Today* **2018**, *299*, 135.

[42] B. J. B. Silva, L. V. de Sousa, P. H. L. Quintela, N. R. Alencar Júnior, S. L. Alencar, P. A. M. Maciel, J. R. Santos, L. R. A. Sarmento, S. M. P. Meneghetti, A. O. S. Silva, *Mater. Lett.* **2018**, *218*, 119.

[43] H. Li, C. Liu, Y. Wang, J. Zheng, B. Fan, R. Li, *RSC Adv.* **2018**, *8*, 28909.

[44] S. Liu, J. Ren, H. Zhang, E. Lv, Y. Yang, Y. W. Li, *J. Catal.* **2016**, *335*, 11.

[45] S. Liu, L. Zhang, L. Zhang, H. Zhang, J. Ren, *New J. Chem.* **2020**, *44*, 4744.

[46] X. Wang, X. Zhang, Q. Wang, *Mater. Lett.* **2019**, *244*, 96.

[47] K. Brylewska, K. A. Tarach, W. Mozgawa, Z. Olejniczak, U. Filek, K. Góra-Marek, *J. Mol. Struct.* **2016**, *1126*, 147.

[48] V. J. Margarit, M. R. Díaz-Rey, M. T. Navarro, C. Martínez, A. Corma, *Angew. Chemie - Int. Ed.* **2018**, *57*, 3459.

[49] X. Cheng, T. Cacciaguerra, D. Minoux, J. P. Dath, F. Fajula, C. Gérardin, *Microporous Mesoporous Mater.* **2018**, *260*, 132.

[50] M. M. Pereira, A. Vieira, E. B. Pereira, L. R. M. dos Santos, Y. L. Lam, *Appl. Catal. A Gen.* **2017**, *548*, 89.

[51] E. Catizzone, A. Migliori, A. Aloise, R. Lamberti, G. Giordano, *J. Chem.* **2019**, *2019*, DOI 10.1155/2019/3084356.

[52] D. Verboekend, R. Caicedo-Realpe, A. Bonilla, M. Santiago, J.

Pérez-Ramírez, *Chem. Mater.* **2010**, *22*, 4679.

[53] A. Bolshakov, A. J. F. Van Hoof, B. Mezari, N. Kosinov, E. Hensen, *Catal. Sci. Technol.* **2019**, *9*, 6737.

[54] A. Bolshakov, R. van de Poll, T. van Bergen-Brenkman, S. C. C. Wiedemann, N. Kosinov, E. J. M. Hensen, *Appl. Catal. B Environ.* **2020**, *263*, 118356.

[55] W. Chu, X. Li, X. Zhu, S. Xie, C. Guo, S. Liu, F. Chen, L. Xu, *Microporous Mesoporous Mater.* **2017**, *240*, 189.

[56] W. Liu, H. Hu, M. Ke, Y. Liu, L. Zhang, C. Xia, Q. Wang, *ChemistrySelect* **2019**, *4*, 9972.

[57] P. Wuamprakhon, C. Wattanakit, C. Warakulwit, T. Yutthalekha, W. Wannapakdee, S. Ittisanronnachai, J. Limtrakul, *Microporous Mesoporous Mater.* **2016**, *219*, 1.

[58] S. K. Saxena, N. Viswanadham, A. H. Al-Muhtaseb, *J. Ind. Eng. Chem.* **2014**, *20*, 2876.

[59] Z. Wu, Y. Wang, *Curr. Org. Chem.* **2014**, *18*, 1305.

[60] J. C. Groen, J. A. Moulijn, J. Pérez-Ramírez, *J. Mater. Chem.* **2006**, *16*, 2121.

[61] S. Yang, C. Yu, L. Yu, S. Miao, M. Zou, C. Jin, D. Zhang, L. Xu, S. Huang, *Angew. Chemie - Int. Ed.* **2017**, *56*, 12553.

[62] F. Wang, X. Chu, P. Zhao, F. Zhu, Q. Li, F. Wu, G. Xiao, *Fuel* **2020**, *262*, 116538.

[63] Y. Fang, F. Yang, X. He, X. Zhu, *Front. Chem. Sci. Eng.* **2019**, *13*, 543.

[64] J. Li, M. Liu, X. Guo, S. Zeng, S. Xu, Y. Wei, Z. Liu, C. Song, *Ind. Eng. Chem. Res.* **2018**, *57*, 15375.

[65] J. Li, M. Liu, X. Guo, S. Xu, Y. Wei, Z. Liu, C. Song, *ACS Appl. Mater. Interfaces* **2017**, *9*, 26096.

[66] J. C. Groen, L. A. . Peffer, J. . Moulijn, J. Perez-Ramirez, *Colloids Surfaces A Physicochem. Eng. Asp.* **2004**, *241*, 53.

[67] D. Verboekend, J. Pérez-Ramírez, *Catal. Sci. Technol.* **2011**, *1*, 879.

[68] Y. Ji, H. Yang, W. Yan, *Catalysts* **2017**, *7*, 367.

[69] D. Verboekend, S. Mitchell, M. Milina, J. C. Groen, J. Pérez-Ramírez, *J. Phys. Chem. C* **2011**, *115*, 14193.

[70] W. Wan, T. Fu, R. Qi, J. Shao, Z. Li, *Ind. Eng. Chem. Res.* **2016**, *55*, 13040.

[71] H. Smail, M. Rehan, K. Shareef, Z. Ramli, A.-S. Nizami, J. Gardy, *ChemEngineering* **2019**, *3*, 35.

[72] R. Feng, X. Yan, X. Hu, Y. Wang, Z. Li, K. Hou, J. Lin, *J. Porous Mater.* **2018**, *25*, 1743.

[73] R. Khoshbin, R. Karimzadeh, *Adv. Powder Technol.* **2017**, *28*, 1888.

[74] W. Feng, X. Gao, C. Ding, Y. Jia, J. Wang, K. Zhang, P. Liu, *Appl. Organomet. Chem.* **2017**, *31*, 1.

[75] L. Zhang, M. Ke, Z. Song, Y. Liu, W. Shan, Q. Wang, C. Xia, C. Li, C. He, *Catalysts* **2018**, *8*, 298.

[76] F. Gorzin, J. Towfighi Darian, F. Yaripour, S. M. Mousavi, *RSC Adv.* **2018**, *8*, 41131.

[77] Y. Xu, W. Lai, Y. Dong, Z. Chen, X. Yi, W. Fang, *CrystEngComm* **2018**, *20*, 5625.

[78] T. Fu, R. Qi, X. Wang, W. Wan, Z. Li, *Microporous Mesoporous Mater.* **2017**, *250*, 43.

[79] T. Fu, R. Qi, W. Wan, J. Shao, J. Z. Wen, Z. Li, *ChemCatChem* **2017**, *9*, 4212.

[80] Y. Xu, J. Wang, G. Ma, J. Lin, M. Ding, *ACS Sustain. Chem. Eng.* **2019**, *7*, 18125.

[81] X. Niu, F. Feng, G. Yuan, X. Zhang, Q. Wang, *Nanomaterials* **2019**, *9*, 362.

[82] J. Lin, T. Yang, C. Lin, J. Sun, *Catal. Commun.* **2018**, *115*, 82.

[83] Y. Jiao, L. Forster, S. Xu, H. Chen, J. Han, X. Liu, Y. Zhou, J. Liu, J. Zhang, J. Yu, C. D'Agostino, X. Fan, *Angew. Chemie* **2020**, *116023*

[84] Z. Ma, T. Fu, Y. Wang, J. Shao, Q. Ma, C. Zhang, L. Cui, Z. Li, *Ind. Eng. Chem. Res.* **2019**, *58*, 2146.

[85] T. Fu, Z. Ma, Y. Wang, J. Shao, Q. Ma, C. Zhang, L. Cui, Z. Li, *Fuel Process. Technol.* **2019**, *194*, 106122.

[86] X. L. Luo, F. Pei, W. Wang, H. ming Qian, K. K. Miao, Z. Pan, Y. S. Chen, G. D. Feng, *Microporous Mesoporous Mater.* **2018**, *262*, 148.

[87] Y. Shi, E. Xing, Y. Cao, M. Liu, K. Wu, M. Yang, Y. Wu, *Chem. Eng. Sci.* **2017**, *166*, 262.

[88] Y. Zhang, M. Li, E. Xing, Y. Luo, X. Shu, *RSC Adv.* **2018**, *8*, 37842.

[89] M. Rahmani, M. Taghizadeh, *React. Kinet. Mech. Catal.* **2017**, *122*, 409.

[90] F. Subhan, S. Aslam, Z. Yan, Z. Liu, U. J. Etim, A. Wadood, R. Ullah, *Chem. Eng. J.* **2018**, *354*, 706.

[91] B. Rogéria, Z. Olesia, L. Benoît, **2019**, 6.

[92] J. Lin, M. O. Cichocka, F. Peng, T. Yang, J. Sun, *Chem. - A Eur. J.* **2018**, *24*, 14974.

[93] J. Zhou, J. Teng, L. Ren, Y. Wang, Z. Liu, W. Liu, W. Yang, Z. Xie, *J. Catal.* **2016**, *340*, 166.

[94] Y. Zhang, X. Han, S. Che, *Chem. Commun.* **2019**, *55*, 810.

[95] L. Meng, X. Zhu, W. Wannapakdee, R. Pestman, M. G. Goesten, L. Gao, A. J. F. van Hoof, E. J. M. Hensen, *J. Catal.* **2018**, *361*, 135.

[96] Y. Zhang, X. Shen, Z. Gong, L. Han, H. Sun, S. Che, *Chem. - A Eur. J.* **2019**, *25*, 738.

[97] Q. Tian, Z. Liu, Y. Zhu, X. Dong, Y. Saih, J. M. Basset, M. Sun, W. Xu, L. Zhu, D. Zhang, J. Huang, X. Meng, F. S. Xiao, Y. Han, *Adv. Funct. Mater.* **2016**, *26*, 1881.

[98] M. Sadrara, M. Khanmohammadi Khorrami, A. Bagheri Garmarudi, *React. Kinet. Mech. Catal.* **2019**, *128*, 1111.

[99] Y. Shen, F. Wang, Z. Han, X. Zhang, *J. Chem. Technol. Biotechnol.* **2018**, *93*, 1347.

[100] L. Meng, B. Mezari, M. G. Goesten, E. J. M. Hensen, *Chem. Mater.* **2017**, *29*, 4091.

[101] W. Wannapakdee, L. Meng, A. J. F. van Hoof, A. Bolshakov, C. Wattanakit, E. J. M. Hensen, *Eur. J. Inorg. Chem.* **2019**, *2019*, 2493.

[102] L. Meng, B. Mezari, M. G. Goesten, W. Wannapakdee, R. Pestman, L. Gao, J. Wiesfeld, E. J. M. Hensen, *Catal. Sci. Technol.* **2017**, *7*, 4520.

[103] M. Zhou, F. Wang, W. Xiao, L. Gao, G. Xiao, *React. Kinet. Mech. Catal.* **2016**, *119*, 699.

[104] M. Yang, B. Wang, F. Hu, X. Mi, H. Liu, H. Liu, X. Gao, C. Xu, *Mater. Lett.* **2018**, *222*, 153.

[105] H. Zhu, E. Abou-Hamad, Y. Chen, Y. Saih, W. Liu, A. Kumar Samal, J. M. Basset, *Langmuir* **2016**, *32*, 2085.

[106] Y. Wang, Z. Chen, L. Dong, C. Chen, Y. Wang, J. Zhang, W. Qian, M. Hong, *Nanoscale* **2019**, *11*, 16667.

[107] Y. Shen, Z. Han, H. Li, H. Li, G. Wang, F. Wang, X. Zhang, *CrystEngComm* **2018**, *20*, 6319.

[108] L. Xing, Z. Wei, Z. Wen, X. Zhu, *Pet. Sci. Technol.* **2017**, *35*, 2235.

[109] Y. Wang, D. Liu, *Chem. Lett.* **2016**, *45*, 1012.

[110] Q. Liu, D. Wen, Y. Yang, Z. Fei, Z. Zhang, X. Chen, J. Tang, M. Cui, X. Qiao, *Appl. Surf. Sci.* **2018**, *435*, 945.

[111] G. Song, W. Chen, P. Dang, Y. Wang, F. Li, R. Soc. Open Sci. 2018, 5, 181691.

[112] G. Song, D. Xue, J. Xue, F. Li, *Microporous Mesoporous Mater.* **2017**, *248*, 192.

[113] Y. Gao, G. Wu, F. Ma, C. Liu, F. Jiang, Y. Wang, A. Wang, *Microporous Mesoporous Mater.* **2016**, *226*, 251.

[114] D. Guo, C. Shi, H. Zhao, R. Chen, S. Chen, P. Sun, T. Chen, *Microporous Mesoporous Mater.* **2020**, *293*, 109821.

[115] R. Liu, S. Lin, L. Shi, H. Gao, M. Lv, K. Tan, R. Wang, *Microporous Mesoporous Mater.* **2019**, *285*, 120.

[116] K. Miyake, Y. Hirota, Y. Uchida, N. Nishiyama, *J. Porous Mater.* **2016**, *23*, 1395.

[117] X. Niu, Y. Sun, Z. Lei, G. Qin, C. Yang, *Prog. Nat. Sci. Mater. Int.* **2020**, *30*, 35.

[118] R. Sabarish, G. Unnikrishnan, *J. Porous Mater.* **2020**, *27*, 691.

[119] H. Tian, Z. Zhang, H. Chang, X. Ma, *J. Energy Chem.* **2017**, *26*, 574.

[120] X. Chen, R. Jiang, Z. Zhou, X. Wang, J. Dispers. Sci. Technol. 2019, DOI 10.1080/01932691.2019.1703735.

[121] R. Sabarish, G. Unnikrishnan, *SN Appl. Sci.* **2019**, *1*, 1.

[122] P. Noor, M. Khanmohammadi, B. Roozbehani, F. Yaripour, A. Bagheri Garmarudi, *J. Energy Chem.* **2018**, *27*, 582.

[123] L. Jin, T. Xie, S. Liu, Y. Li, H. Hu, *Catal. Commun.* **2016**, *75*, 32.

[124] R. Feng, X. Wang, J. Lin, Z. Li, K. Hou, X. Yan, X. Hu, Z. Yan, M. J. Rood, *Microporous Mesoporous Mater.* **2018**, *270*, 57.

[125] Q. Che, M. Yang, X. Wang, Q. Yang, Y. Chen, X. Chen, W. Chen, J. Hu, K. Zeng, H. Yang, H. Chen, *Bioresour. Technol.* **2019**, *289*, 121729.

[126] R. Sabarish, G. Unnikrishnan, *Powder Technol.* **2017**, *320*, 412.

[127] J. Jiang, S. Ji, C. Duanmu, Y. Pan, J. Wu, M. Wu, J. Chen, *Particuology* **2017**, *33*, 55.

[128] Q. Zhang, A. Mayoral, O. Terasaki, Q. Zhang, B. Ma, C. Zhao, G. Yang, J. Yu, *J. Am. Chem. Soc.* **2019**, 3772.

[129] C. J. H. Jacobsen, C. Madsen, J. Houzvicka, I. Schmidt, A. Carlsson, *J. Am. Chem. Soc.* **2000**, *122*, 7116.

[130] I. Schmidt, A. Boisen, E. Gustavsson, K. Ståhl, S. Pehrson, S. Dahl, A. Carlsson, C. J. H. Jacobsen, *Chem. Mater.* **2001**, *13*, 4416.

[131] A. H. Janssen, I. Schmidt, C. J. H. Jacobsen, A. J. Koster, K. P. de Jong, *Microporous Mesoporous Mater.* **2003**, *65*, 59.

[132] S. S. Kim, J. Shah, T. J. Pinnavaia, *Chem. Mater.* **2003**, *15*, 1664.

[133] A. Sakthivel, S. J. Huang, W. H. Chen, Z. H. Lan, K. H. Chen, T. W. Kim, R. Ryoo, A. S. T. Chiang, S. Bin Liu, *Chem. Mater.* **2004**, *16*, 3168.

[134] Y. Tao, H. Kanoh, K. Kaneko, *J. Am. Chem. Soc.* **2003**, *125*, 6044.

[135] K. Zhu, K. Egeblad, C. H. Christensen, *Eur. J. Inorg. Chem.* **2007**, 3955.

[136] X. Wang, G. Li, W. Wang, C. Jin, Y. Chen, *Microporous Mesoporous Mater.* **2011**, *142*, 494.

[137] Ó. De La Iglesia, J. L. Sánchez, J. Coronas, *Mater. Lett.* **2011**, *65*, 3124.

[138] H. Katsuki, S. Furuta, T. Watari, S. Komarneni, *Microporous Mesoporous Mater.* **2005**, *86*, 145.

[139] H. Zhu, Z. Liu, Y. Wang, D. Kong, X. Yuan, Z. Xie, *Chem. Mater.* **2008**, *20*, 1134.

[140] B. T. Holland, L. Abrams, A. Stein, *J. Am. Chem. Soc.* **1999**, *121*, 4308.

[141] L. Xu, S. Wu, J. Guan, H. Wang, Y. Ma, K. Song, H. Xu, H. Xing, C. Xu, Z. Wang, Q. Kan, *Catal. Commun.* **2008**, *9*, 1272.

[142] Y. J. Lee, J. S. Lee, Y. S. Park, K. B. Yoon, *Adv. Mater.* **2001**, *13*, 1259.

[143] J. B. Koo, N. Jiang, S. Saravanamurugan, M. Bejblová, Z. Musilová, J. Čejka, S. E. Park, *J. Catal.* **2010**, *276*, 327.

[144] S. Han, Z. Wang, L. Meng, N. Jiang, *Mater. Chem. Phys.* **2016**, *177*, 112.

[145] S. Zhao, W. D. Wang, L. Wang, W. Schwieger, W. Wang, J. Huang, *ACS Catal.* **2020**, *10*, 1185.

[146] C. Zhang, H. Chen, X. Zhang, Q. Wang, *Mater. Lett.* **2017**, *197*, 111.

[147] C. Flores, N. Batalha, V. V. Ordomsky, V. L. Zholobenko, W. Baaziz, N. R. Marcilio, A. Y. Khodakov, *ChemCatChem* **2018**, *10*, 2291.

[148] Y. Y. Chen, C. J. Chang, H. V. Lee, J. C. Juan, Y. C. Lin, *Ind. Eng. Chem. Res.* **2019**, *58*, 7948.

[149] S. Soltanali, Z. Hajjar, F. Bahadoran, *Mater. Res. Express* **2019**, *6*, DOI 10.1088/2053-1591/ab29d7.

[150] S. Soltanali, J. Towfighi Darian, *Mater. Res. Express* **2019**, *6*, DOI 10.1088/2053-1591/ab13e6.

[151] Y. Qiu, L. Wang, X. Zhang, G. Liu, *RSC Adv.* **2015**, *5*, 78238.

[152] L. Vafi, R. Karimzadeh, *J. Nat. Gas Sci. Eng.* **2016**, *32*, 1.

[153] Z. Liu, D. Wu, S. Ren, X. Chen, M. Qiu, G. Liu, G. Zeng, Y. Sun, *RSC Adv.* **2016**, *6*, 15816.

[154] J. O. Abildstrøm, M. Kegnæs, G. Hytoft, J. Mielby, S. Kegnæs, *Microporous Mesoporous Mater.* **2016**, *225*, 232.

[155] T. Hu, J. Liu, C. Cao, W. Song, *Cuihua Xuebao/Chinese J. Catal.* **2017**, *38*, 872.

[156] P. Liu, L. N. Jin, C. Jin, J. N. Zhang, S. W. Bian, *Microporous Mesoporous Mater.* **2018**, *262*, 217.

[157] Z. Peng, L. H. Chen, M. H. Sun, H. Zhao, Z. Wang, Y. Li, L. Y. Li, J. Zhou, Z. C. Liu, B. L. Su, *Inorg. Chem. Front.* **2018**, *5*, 2829.

[158] M. Krishnamurthy, K. Msm, C. Kanakkampalayam Krishnan, *Microporous Mesoporous Mater.* **2016**, *221*, 23.

[159] M. Zhang, X. Liu, Z. Yan, *Mater. Lett.* **2016**, *164*, 543.

[160] Y. Zang, X. Dong, D. Ping, J. Geng, H. Dang, *Catal. Commun.* **2018**, *113*, 51.

[161] H. Chen, X. Shi, F. Zhou, H. Ma, K. Qiao, X. Lu, J. Fu, H. Huang, *Catal. Commun.* **2018**, *110*, 102.

[162] B. Zhang, X. Li, Q. Wu, C. Zhang, Y. Yu, M. Lan, X. Wei, Z. Ying, T. Liu, G. Liang, F. Zhao, *Green Chem.* **2016**, *18*, 3315.

[163] G. V. Brião, S. L. Jahn, E. L. Foletto, G. L. Dotto, *J. Colloid Interface Sci.* **2017**, *508*, 313.

[164] F. C. Drumm, J. S. de Oliveira, E. L. Foletto, G. L. Dotto, E. M. Moraes Flores, M. S. Peters Enders, E. I. Müller, S. L. Janh, *Chem. Eng. Commun.* **2018**, *205*, 445.

[165] A. Khamkeaw, M. Phisalaphong, B. Jongsomjit, K. Y. A. Lin, A. C. K. Yip, *J. Hazard. Mater.* **2020**, *384*, 121161.

[166] X. Ma, G. Li, J. Tao, P. Li, H. Zheng, S. Li, Y. Xu, *Chem. - A Eur. J.* **2018**, *24*, 2980.

[167] E. S. Gomes, D. A. G. Aranda, M. M. Pereira, B. Louis, *Microporous Mesoporous Mater.* **2018**, *263*, 251.

[168] L. Huang, F. Qin, Z. Huang, Y. Zhuang, J. Ma, H. Xu, W. Shen, *Ind. Eng. Chem. Res.* **2016**, *55*, 7318.

[169] S. Zhuang, Z. Hu, L. Huang, F. Qin, Z. Huang, C. Sun, W. Shen, H. Xu, *Catal. Commun.* **2018**, *114*, 28.

[170] X. Jia, D. Jiang, D. C. W. Tsang, J. Choi, A. C. K. Yip, *Microporous Mesoporous Mater.* **2019**, *276*, 147.

[171] X. He, T. Ge, Z. Hua, J. Zhou, J. Lv, J. Zhou, Z. Liu, J. Shi, *ACS*

Appl. Mater. Interfaces **2016**, *8*, 7118.

[172] T. Ge, Z. Hua, X. He, J. Lv, H. Chen, L. Zhang, H. Yao, Z. Liu, C. Lin, J. Shi, *Chem. - A Eur. J.* **2016**, *22*, 7895.

[173] H. Guo, T. Ge, J. Lv, C. Du, J. Zhou, Z. Liu, Z. Hua, *Eur. J. Inorg. Chem.* **2019**, *2019*, 51.

[174] M. Rilyanti, R. R. Mukti, G. T. M. Kadja, M. Ogura, H. Nur, E. P. Ng, Ismunandar, *Microporous Mesoporous Mater.* **2016**, *230*, 30.

[175] M. S. M. Kamil, K. K. Cheralathan, *J. Porous Mater.* **2020**, *27*, 587.

[176] Y. Jia, J. Wang, K. Zhang, G. Chen, Y. Yang, S. Liu, C. Ding, Y. Meng, P. Liu, *Powder Technol.* **2018**, *328*, 415.

[177] F. Wei, Q. Zhang, H. Wu, C. Cao, W. Song, *Sci. China Chem.* **2017**, *60*, 1588.

[178] Y. Zhang, P. Lu, Y. Yuan, L. Xu, H. Guo, X. Zhang, L. Xu, *CrystEngComm* **2017**, *19*, 4713.

[179] D. Hartanto, R. Kurniawati, A. B. Pambudi, W. P. Utomo, W. L. Leaw, H. Nur, *Solid State Sci.* **2019**, *87*, 150.

[180] Z. Ye, Y. Zhao, H. Zhang, Y. Zhang, Y. Tang, *Chem. - A Eur. J.* **2020**, DOI 10.1002/chem.201904807.

[181] X. Zhou, Y. Chen, T. Ge, Z. Hua, H. Chen, J. Shi, *Sci. Bull.* **2017**, *62*, 1018.

[182] G. T. M. Kadja, R. R. Mukti, Z. Liu, M. Rilyanti, Ismunandar, I. N. Marsih, M. Ogura, T. Wakihara, T. Okubo, *Microporous Mesoporous Mater.* **2016**, *226*, 344.

[183] T. Zhao, Y. Wang, C. Sun, A. Zhao, C. Wang, X. Zhang, J. Zhao, Z. Wang, J. Lu, S. Wu, W. Liu, *Microporous Mesoporous Mater.* **2020**, *292*, 109731.

[184] Y. Wang, J. Song, N. C. Baxter, G. T. Kuo, S. Wang, *J. Catal.* **2017**, *349*, 53.

[185] D. Wu, X. Yu, X. Chen, G. Yu, K. Zhang, M. Qiu, W. Xue, C. Yang, Z. Liu, Y. Sun, *ChemSusChem* **2019**, *12*, 3871.

[186] Y. Zhang, S. Che, *Chem. - A Eur. J.* **2019**, *25*, 6196.

[187] N. Wang, W. Qian, K. Shen, C. Su, F. Wei, *Chem. Commun.* **2016**, *52*, 2011.

[188] S. Mintova, J. Grand, V. Valtchev, *Comptes Rendus Chim.* **2016**, *19*, 183.

[189] J. Zhao, Y. Wang, C. Sun, A. Zhao, C. Wang, X. Zhang, Z. Wang, T. Zhao, W. Liu, J. Lu, S. Wu, *React. Kinet. Mech. Catal.* **2019**, *128*, 1079.

[190] Z. Wang, Y. Wang, C. Sun, A. Zhao, C. Wang, X. Zhang, J. Zhao, T. Zhao, W. Liu, J. Lu, S. Wu, *Trans. Tianjin Univ.* **2019**, DOI 10.1007/s12209-019-00223-w.

[191] H. Chen, Y. Wang, F. Meng, C. Sun, H. Li, Z. Wang, F. Gao, X. Wang, S. Wang, *Microporous Mesoporous Mater.* **2017**, *244*, 301.

[192] H. Chen, Y. Wang, F. Meng, H. Li, S. Wang, C. Sun, S. Wang, X. Wang, *RSC Adv.* **2016**, *6*, 76642.

[193] H. Chen, Y. Wang, C. Sun, X. Wang, C. Wang, *Catal. Commun.* **2018**, *112*, 10.

[194] L. Shi, N. Li, L. Wang, R. Liu, S. Lin, J. Liu, R. Wang, Y. Li, *Microporous Mesoporous Mater.* **2018**, *258*, 178.

[195] H. Li, Y. Wang, F. Meng, F. Gao, C. Sun, C. Fan, X. Wang, S. Wang, *RSC Adv.* **2017**, *7*, 25605.

[196] H. Zhang, Y. Zhao, H. Zhang, P. Wang, Z. Shi, J. Mao, Y. Zhang, Y. Tang, *Chem. - A Eur. J.* **2016**, *22*, 7141.

[197] H. Zhang, H. Zhang, Y. Zhao, Z. Shi, Y. Zhang, Y. Tang, *Chem. Mater.* **2017**, *29*, 9247.

[198] K. Shen, N. Wang, X. Chen, Z. Chen, Y. Li, J. Chen, W. Qian, F. Wei, *Catal. Sci. Technol.* **2017**, *7*, 5143.

[199] H. Zhang, L. Wang, D. Zhang, X. Meng, F. S. Xiao, *Microporous Mesoporous Mater.* **2016**, *233*, 133.

[200] R. Beerthuis, L. Huang, N. R. Shiju, G. Rothenberg, W. Shen, H. Xu, *ChemCatChem* **2018**, *10*, 211.

[201] T. Xue, S. Li, H. Wu, P. Wu, M. He, *Ind. Eng. Chem. Res.* **2017**, *56*, 13535.

[202] M. Li, I. N. Oduro, Y. Zhou, Y. Huang, Y. Fang, *Microporous Mesoporous Mater.* **2016**, *221*, 108.

[203] J. Ahmadpour, M. Taghizadeh, *Synth. React. Inorganic, Met. Nano-Metal Chem.* **2016**, *46*, 1133.

[204] Q. Liu, P. He, X. Qian, Z. Fei, Z. Zhang, X. Chen, J. Tang, M. Cui, X. Qiao, Y. Shi, *Energy & Fuels* **2017**, *31*, 13933.

[205] X. Qian, G. Bai, P. He, Z. Fei, Q. Liu, Z. Zhang, X. Chen, J. Tang, M. Cui, X. Qiao, *Ind. Eng. Chem. Res.* **2018**, *57*, 16875.

[206] H. Li, Y. Wang, C. Fan, C. Sun, X. Wang, C. Wang, X. Zhang, S. Wang, *Appl. Catal. A Gen.* **2018**, *551*, 34.

[207] Y. Jia, J. Wang, K. Zhang, W. Feng, S. Liu, C. Ding, P. Liu, *Microporous Mesoporous Mater.* **2017**, *247*, 103.

[208] H. Chen, X. Shi, J. Liu, K. Jie, Z. Zhang, X. Hu, Y. Zhu, X. Lu, J. Fu, H. Huang, S. Dai, *J. Mater. Chem. A* **2018**, *6*, 21178.

[209] D. P. Serrano, J. M. Escola, R. Sanz, R. A. Garcia, A. Peral, I. Moreno, M. Linares, *New J. Chem.* **2016**, *40*, 4206.

[210] G. Song, W. Chen, P. Dang, S. Yang, Y. Zhang, Y. Wang, R. Xiao, R. Ma, F. Li, *Nanoscale Res. Lett.* **2018**, *13*, 364.

[211] X. Shen, W. Mao, Y. Ma, D. Xu, P. Wu, O. Terasaki, L. Han, S. Che, *Angew. Chemie - Int. Ed.* **2018**, *57*, 724.

[212] J. Ding, J. Hu, T. Xue, Y. Wang, H. Wu, P. Wu, M. He, *RSC Adv.* **2016**, *6*, 38671.

[213] R. Barakov, N. Shcherban, P. Yaremov, I. Bezverkhyy, A. Baranchikov, V. Trachevskii, V. Tsyrina, V. Ilyin, *Microporous Mesoporous Mater.* **2017**, *237*, 90.

[214] Y. Wang, C. Fan, H. Li, X. Wang, F. Meng, C. Sun, L. Sun, *Trans. Tianjin Univ.* **2019**, *25*, 9.

[215] X. Dong, S. Shaikh, J. R. Vittenet, J. Wang, Z. Liu, K. D. Bhatte, O. Ali, W. Xu, I. Osorio, Y. Saih, J. M. Basset, S. A. Ali, Y. Han, *ACS Sustain. Chem. Eng.* **2018**, *6*, 15832.

[216] C. Shang, Z. Wu, W. D. Wu, X. D. Chen, *ACS Appl. Mater. Interfaces* **2019**, *11*, 16693.

[217] H. Li, Y. Wang, F. Meng, H. Chen, C. Sun, S. Wang, *RSC Adv.* **2016**, *6*, 99129.

[218] K. A. Sashkina, Z. Qi, W. Wu, A. B. Ayupov, A. I. Lysikov, E. V. Parkhomchuk, *Microporous Mesoporous Mater.* **2017**, *244*, 93.

[219] S. K. Saxena, N. Viswanadham, *Appl. Mater. Today* **2016**, *5*, 25.

[220] L. Shi, J. Wang, N. Li, S. Lin, *J. Alloys Compd.* **2017**, *695*, 2488.

[221] T. Xue, H. Liu, Y. Zhang, H. Wu, P. Wu, M. He, *Microporous Mesoporous Mater.* **2017**, *242*, 190.

[222] C. Fan, Y. Wang, H. Li, X. Wang, C. Sun, X. Zhang, C. Wang, S. Wang, *New J. Chem.* **2018**, *42*, 17043.

[223] K. Moukahhal, T. J. Daou, L. Josien, H. Nouali, J. Toufaily, T. Hamieh, A. Galarneau, B. Lebeau, *Microporous Mesoporous Mater.* **2019**, *288*, 109565.

[224] X. Yan, B. Liu, J. Huang, Y. Wu, H. Chen, H. Xi, *Ind. Eng. Chem. Res.* **2019**, *58*, 2924.

[225] P. Y. Chao, C. H. Hsu, A. Loganathan, H. P. Lin, *J. Am. Ceram. Soc.* **2018**, *101*, 3719.

[226] X. Zhang, C. Wang, Chem. Soc. Rev. 2011, 40, 94.

[227] B. Liu, Z. Chen, J. Huang, H. Chen, Y. Fang, *Microporous*

Mesoporous Mater. **2019**, *273*, 235.

[228] C. Li, Y. Ren, J. Gou, B. Liu, H. Xi, *Appl. Surf. Sci.* **2017**, *392*, 785.

[229] R. Wei, H. Yang, J. A. Scott, K. F. Aguey-Zinsou, D. Zhang, *Appl. Mater. Today* **2018**, *11*, 22.

[230] Y. Kim, K. Kim, R. Ryoo, *Chem. Mater.* **2017**, *29*, 1752.

[231] Y. Shang, W. Wang, Y. Zhai, Y. Song, X. Zhao, T. Ma, J. Wei, Y. Gong, *Microporous Mesoporous Mater.* **2019**, *276*, 173.

[232] H. Chen, W. Shang, C. Yang, B. Liu, C. Dai, J. Zhang, Q. Hao, M. Sun, X. Ma, *Ind. Eng. Chem. Res.* **2019**, *58*, 1580.

[233] P. Gong, B. Li, X. Kong, J. Liu, S. Zuo, *Appl. Surf. Sci.* **2017**, *423*, 433.

[234] G. Liu, Y. Tian, B. Zhang, L. Wang, X. Zhang, *J. Hazard. Mater.* **2019**, *367*, 568.

[235] Y. Tian, B. Zhang, H. Liang, X. Hou, L. Wang, X. Zhang, G. Liu, *Appl. Catal. A Gen.* **2019**, *572*, 24.

[236] J. jia Xiao, H. Li, G. bin Zhu, *Adv. Powder Technol.* **2016**, *27*, 1396.

[237] Z. Qin, L. Pinard, M. A. Benghalem, T. J. Daou, G. Melinte, O. Ersen, S. Asahina, J. P. Gilson, V. Valtchev, *Chem. Mater.* **2019**, *31*, 4639.

[238] J. Přech, K. N. Bozhilov, J. El Fallah, N. Barrier, V. Valtchev, *Microporous Mesoporous Mater.* **2019**, *280*, 297.

[239] Q. Wu, M. Li, Y. Huang, Y. Fang, *Microporous Mesoporous Mater.* **2016**, *226*, 284.

[240] S. W. Han, J. Kim, R. Ryoo, *Microporous Mesoporous Mater.* **2017**, *240*, 123.

[241] N. Simone, W. A. Carvalho, D. Mandelli, R. Ryoo, *J. Mol. Catal. A Chem.* **2016**, *422*, 115.

[242] Y. Zhang, P. Luo, H. Xu, L. Han, P. Wu, H. Sun, S. Che, *Chem. - A Eur. J.* **2018**, *24*, 19300.

[243] Y. Shen, H. Li, X. Zhang, X. Wang, G. Lv, *Nanoscale* **2020**, *12*, 5824.

[244] J. Zheng, H. Zhang, Y. Liu, G. Wang, Q. Kong, M. Pan, H. Tian, R. Li, *Catal. Letters* **2016**, *146*, 1457.

[245] H. Zhang, G. Wang, J. Zheng, Q. Kong, M. Pan, B. Li, R. Li, *Chem. Lett.* **2016**, *45*, 481.

[246] G. Li, H. Huang, B. Yu, Y. Wang, J. Tao, Y. Wei, S. Li, Z. Liu, Y. Xu, R. Xu, *Chem. Sci.* **2016**, *7*, 1582.

[247] B. Peng, H. Zou, L. He, P. Wang, Z. Shi, L. Zhu, R. Wang, Z. Zhang, *CrystEngComm* **2017**, *19*, 7088.

[248] R. Qi, T. Fu, W. Wan, Z. Li, *Fuel Process. Technol.* **2017**, *155*, 191.

[249] J. Shao, T. Fu, Z. Ma, C. Zhang, H. Li, L. Cui, Z. Li, *Catal. Sci. Technol.* **2019**, *9*, 6647.

[250] H. Issa, N. Chaouati, J. Toufaily, T. Hamieh, A. Sachse, L. Pinard, *ChemCatChem* **2019**, *11*, 4581.

[251] International Zeolite Association (IZA), "MOR: Framework Type," can be found under https://europe.iza-structure.org/IZA-SC/framework.php?STC=MOR, **n.d.**

[252] P. Tamizhdurai, A. Ramesh, P. S. Krishnan, S. Narayanan, K. Shanthi, S. Sivasanker, Microporous Mesoporous Mater. 2019, 287, 192.

[253] S. K. Wahono, D. J. Prasetyo, T. H. Jatmiko, D. Pratiwi, A. Suwanto, Hernawan, K. Vasilev, in AIP Conf. Proc., American Institute Of Physics Inc., 2019.

[254] G. Nasser, T. Kurniawan, K. Miyake, A. Galadima, Y. Hirota, N. Nishiyama, O. Muraza, *J. Nat. Gas Sci. Eng.* **2016**, *28*, 566.

[255] S. K. Saxena, N. Viswanadham, A. H. Al-Muhtaseb, *J. Porous Mater.* **2016**, *23*, 1671.

[256] Z. V. Rahbari, M. Khosravan, A. N. Kharat, *Bull. Chem. Soc. Ethiop.* **2017**, *31*, 281.

[257] A. A. C. Reule, J. A. Sawada, N. Semagina, J. Catal. 2017, 349, 98.

[258] J. Zhang, C. Rao, H. Peng, C. Peng, L. Zhang, X. Xu, W. Liu, Z. Wang, N. Zhang, X. Wang, *Chem. Eng. J.* **2018**, DOI 10.1016/j.cej.2017.10.017.

[259] M. Popova, H. Lazarova, Y. Kalvachev, T. Todorova, Á. Szegedi, P. Shestakova, G. Mali, V. D. B. C. Dasireddy, B. Likozar, *Catal. Commun.* **2017**, *100*, 10.

[260] H. Issa, J. Toufaily, T. Hamieh, J. D. Comparot, A. Sachse, L. Pinard, *J. Catal.* **2019**, *374*, 409.

[261] O. S. Travkina, A. N. Khazipova, I. N. Pavlova, A. F. Akhmetov, B. I. Kutepov, L. S. Galyautdinova, *Int. Res. J. Pure Appl. Chem.* **2018**, *17*, 1.

[262] J. Pastvova, D. Kaucky, J. Moravkova, J. Rathousky, S. Sklenak, M. Vorokhta, L. Brabec, R. Pilar, I. Jakubec, E. Tabor, P. Klein, P. Sazama, *ACS Catal.* **2017**, *7*, 5781.

[263] Z. Huang, J. Zhang, Q. Han, X. Zhang, P. Lu, L. Xu, Y. Yuan, L. Xu, *Appl. Catal. A Gen.* **2019**, *572*, 80.

[264] N. Chaouati, A. Soualah, I. Hussein, J. D. Comparot, L. Pinard, *Appl. Catal. A Gen.* **2016**, *526*, 95.

[265] S. T. Tsai, P. Y. Chao, P. H. Chao, K. J. Du, M. J. Fang, S. Bin Liu, T. C. Tsai, Catal. Today 2016, 259, 423.

[266] H. Issa, J. Toufaily, T. Hamieh, A. Sachse, L. Pinard, Appl. Catal. A Gen. 2019, 583, 117139.

[267] W. Wang, X. Gao, R. Feng, Q. Yang, T. Zhang, J. Zhang, Q. Zhang, Y. Han, Y. Tan, *Catalysts* **2019**, *9*, 628.

[268] Wojciechowska, Król, Bajda, Mozgawa, *Materials (Basel).* **2019**, *12*, 3271.

[269] Y. H. Lee, W. Y. Kim, H. Park, Y. H. Choi, J. S. Lee, *ChemCatChem* **2016**, *8*, 2996.

[270] O. A. Ponomareva, A. A. Mal'tseva, A. A. Maerle, L. I. Rodionova, V. S. Pavlov, I. V. Dobryakova, M. V. Belova, I. I. Ivanova, *Pet. Chem.* **2016**, *56*, 253.

[271] B. P. S. Santos, N. C. Almeida, I. S. Santos, M. de F. V. Marques, L. D. Fernandes, *Catal. Letters* **2018**, *148*, 1870.

[272] H. Sheng, H. Qian, H. Zhang, P. Zhao, H. Ma, W. Ying, Microporous Mesoporous Mater. 2020, 295,109950.

[273] G. Dai, W. Hao, H. Xiao, J. Ma, R. Li, *Chem. Phys. Lett.* **2017**, *686*, 111.

[274] A. Bolshakov, D. E. Romero Hidalgo, A. J. F. van Hoof, N. Kosinov, E. J. M. Hensen, *ChemCatChem* **2019**, *11*, 2803.

[275] B. K. Singh, Y. Kim, S. Bin Baek, A. Meena, S. Sultan, J. H. Kwak, K. S. Kim, J. Ind. Eng. Chem. 2018, 57, 363.

[276] B. Velaga, R. P. Parde, J. Soni, N. R. Peela, *Microporous Mesoporous Mater.* **2019**, *287*, 18.

[277] X. Wang, R. Li, C. Yu, L. Zhang, C. Xu, H. Zhou, Microporous Mesoporous Mater. 2019, 274, 227.

[278] M. Liu, W. Jia, J. Li, Y. Wang, S. Ma, H. Chen, Z. Zhu, *Catal. Letters* **2016**, *146*, 249.

[279] K. Lu, J. Huang, L. Ren, C. Li, Y. Guan, B. Hu, H. Xu, J. Jiang, Y. Ma, P. Wu, Angew. Chemie Int. Ed. 2020, 59, 6258.

[280] O. S. Travkina, M. R. Agliullin, R. Z. Kuvatova, I. N. Pavlova, N. Narender, B. I. Kutepov, *J. Porous Mater.* **2019**, *26*, 995.

[281] "FAU: Framework Type," can be found under https://europe.iza-structure.org/IZA-SC/framework.php?STC=FAU, **n.d.**

[282] B. Reiprich, T. Weissenberger, W. Schwieger, A. Inayat, *Front.*

Chem. Sci. Eng. **2020**, DOI 10.1007/s11705-019-1883-3.

[283] D. Verboekend, N. Nuttens, R. Locus, J. Van Aelst, P. Verolme, J. C. Groen, J. Pérez-Ramírez, B. F. Sels, *Chem. Soc. Rev.* **2016**, *45*, 3331.

[284] R. Zhang, S. Xu, D. Raja, N. B. Khusni, J. Liu, J. Zhang, S. Abdulridha, H. Xiang, S. Jiang, Y. Guan, Y. Jiao, X. Fan, *Microporous Mesoporous Mater.* **2019**, *278*, 297.

[285] A. Sachse, A. Grau-Atienza, E. O. Jardim, N. Linares, M. Thommes, J. García-Martínez, *Cryst. Growth Des.* **2017**, *17*, 4289.

[286] A. Al-Ani, R. J. Darton, S. Sneddon, V. Zholobenko, *ACS Appl. Nano Mater.* **2018**, *1*, 310.

[287] J. M. Gómez, E. Díez, A. Rodríguez, M. Calvo, *Microporous Mesoporous Mater.* **2018**, *270*, 220.

[288] R. K. Parsapur, P. Selvam, Sci. Rep. 2018, 8, 16291.

[289] E. Koohsaryan, M. Anbia, *Mater. Lett.* **2019**, *236*, 390.

[290] T. Yutthalekha, C. Wattanakit, C. Warakulwit, W. Wannapakdee, K. Rodponthukwaji, T. Witoon, J. Limtrakul, *J. Clean. Prod.* **2017**, *142*, 1244.

[291] X. Jia, L. Han, Y. Ma, S. Che, *Sci. China Mater.* **2018**, *61*, 1095.

[292] L. Liu, H. Wang, Z. Wang, L. Zhu, L. Huang, L. Yu, J. Fan, Y. Yao, S. Liu, J. Zou, X. Zeng, *Chem. Commun.* **2018**, *54*, 9821.

[293] B. Wang, P. K. Dutta, *Microporous Mesoporous Mater.* **2017**, *239*, 195.

[294] A. Feng, Y. Yu, L. Mi, Y. Cao, Y. Yu, L. Song, *Microporous Mesoporous Mater.* **2019**, *280*, 211.

[295] C. Pagis, C. Bouchy, M. Dodin, R. Martinez Franco, D. Farrusseng, A. Tuel, *Oil Gas Sci. Technol. – Rev. d'IFP Energies Nouv.* **2019**, *74*, 38.

[296] C. Pagis, A. R. Morgado Prates, N. Bats, A. Tuel, D. Farrusseng, *CrystEngComm* **2018**, *20*, 1564.

[297] S. Abdulridha, Y. Jiao, S. Xu, R. Zhang, A. A. Garforth, X. Fan, *Front. Chem.* **2020**, *8*, 482.

[298] W. Li, J. Zheng, Y. Luo, C. Tu, Y. Zhang, Z. Da, *Energy & Fuels* **2017**, *31*, 3804.

[299] I. Graça, M. C. Bacariza, A. Fernandes, D. Chadwick, *Appl. Catal. B Environ.* **2018**, *224*, 660.

[300] S. Oruji, R. Khoshbin, R. Karimzadeh, *Fuel Process. Technol.* **2018**, *176*, 283.

[301] R. Zhang, P. Zhong, H. Arandiyan, Y. Guan, J. Liu, N. Wang, Y. Jiao, X. Fan, *Front. Chem. Sci. Eng.* **2020**, *14*, 275.

[302] V. Van-Dúnem, A. P. Carvalho, L. M. D. R. S. Martins, A. Martins, *ChemCatChem* **2018**, *10*, 4058.

[303] A. Al-Ani, C. Freitas, V. Zholobenko, Microporous Mesoporous Mater. 2020, 293, 109805.

[304] A. Al-Ani, J. J. C. Haslam, N. E. Mordvinova, O. I. Lebedev, A. Vicente, C. Fernandez, V. Zholobenko, *Nanoscale Adv.* **2019**, *1*, 2029.

[305] W. Zhou, Y. Zhou, Q. Wei, S. Ding, S. Jiang, Q. Zhang, M. Liu, *Chem. Eng. J.* **2017**, *330*, 605.

[306] D. Ji, H. Liu, X. Wang, H. Liu, X. Gao, C. Xu, S. Wei, *Mater. Chem. Phys.* **2017**, *196*, 284.

[307] W. Li, J. Zheng, Y. Luo, C. Tu, L. Han, Z. Da, *ChemistrySelect* **2017**, *2*, 3872.

[308] D. Mehlhorn, J. Rodriguez, T. Cacciaguerra, R.-D. Andrei, C. Cammarano, F. Guenneau, A. Gedeon, B. Coasne, M. Thommes, D. Minoux, C. Aquino, J.-P. Dath, F. Fajula, A. Galarneau, *Langmuir* **2018**, *34*, 11414.

[309] C. Venkatesan, H. Park, J. Kim, S. Lee, R. Ryoo, *Microporous Mesoporous Mater.* **2019**, *288*, DOI 10.1016/j.micromeso.2019.109579.

[310] P. Lv, L. Yan, L. Liu, Y. Liu, M. Wang, W. Bao, F. Li, *Ind. Eng. Chem. Res.* **2019**, *58*, 21817.

[311] O. S. Travkina, M. R. Agliullin, N. A. Filippova, A. N. Khazipova, I. G. Danilova, N. G. Grigor'Eva, N. Narender, M. L. Pavlov, B. I. Kutepov, *RSC Adv.* **2017**, *7*, 32581.

[312] S. Ferdov, *Microporous Mesoporous Mater.* **2017**, *242*, 59.

[313] Y. Du, Q. Kong, Z. Gao, Z. Wang, J. Zheng, B. Qin, W. Li, R. Li, *Ind. Eng. Chem. Res.* **2018**, *57*, 7395.

[314] P. Levecque, D. W. Gammon, P. Jacobs, D. De Vos, B. Sels, *Green Chem.* **2010**, *12*, 828.

[315] A. Pande, P. Niphadkar, K. Pandare, V. Bokade, *Energy & Fuels* **2018**, *32*, 3783.

[316] S. Mi, T. Wei, J. Sun, P. Liu, X. Li, Q. Zheng, K. Gong, X. Liu, X. Gao, B. Wang, H. Zhao, H. Liu, B. Shen, *J. Catal.* **2017**, *347*, 116.

[317] Z. Zhu, H. Xu, J. Jiang, P. Wu, *J. Phys. Chem. C* **2016**, *120*, 23613.

[318] Z. Zhu, H. Xu, J. Jiang, X. Liu, J. Ding, P. Wu, Appl. Catal. A Gen. 2016, 519, 155.

[319] D. Verboekend, G. Vilé, J. Pérez-Ramírez, *Cryst. Growth Des.* **2012**, *12*, 3123.

[320] D. Verboekend, G. Vilé, J. Pérez-Ramírez, *Cryst. Growth Des.* **2012**, *12*, 3123.

[321] J. Silva, E. Ferracine, D. Cardoso, *Appl. Sci.* **2018**, *8*, 1299.

[322] M. Gackowski, K. Tarach, Kuterasiński, J. Podobiński, S. Jarczewski, P. Kuśtrowski, J. Datka, *Microporous Mesoporous Mater.* **2018**, *263*, 282.

[323] M. Gackowski, K. Tarach, Ł. Kuterasiński, J. Podobiński, B. Sulikowski, J. Datka, *Microporous Mesoporous Mater.* **2019**, *281*, 134.

[324] M. Gackowski, Ł. Kuterasiński, J. Podobiński, B. Sulikowski, J. Datka, *Spectrochim. Acta - Part A Mol. Biomol. Spectrosc.* **2018**, *193*, 440.

[325] J. Van Aelst, D. Verboekend, A. Philippaerts, N. Nuttens, M. Kurttepeli, E. Gobechiya, M. Haouas, S. P. Sree, J. F. M. Denayer, J. A. Martens, C. E. A. Kirschhock, F. Taulelle, S. Bals, G. V. Baron, P. A. Jacobs, B. F. Sels, *Adv. Funct. Mater.* **2015**, *25*, 7130.

[326] J. Van Aelst, M. Haouas, E. Gobechiya, K. Houthoofd, A. Philippaerts, S. P. Sree, C. E. A. Kirschhock, P. Jacobs, J. A. Martens, B. F. Sels, F. Taulelle, *J. Phys. Chem. C* **2014**, *118*, 22573.

[327] M. Gackowski, Ł. Kuterasiński, J. Podobiński, J. Datka, *ChemPhysChem* **2018**, *19*, 3372.

[328] N. Nuttens, D. Verboekend, A. Deneyer, J. Van Aelst, B. F. Sels, *ChemSusChem* **2015**, *8*, 1197.

[329] S. Ren, B. Meng, X. Sui, H. Duan, X. Gao, H. Zhang, P. Zeng, Q. Guo, B. Shen, *Ind. Eng. Chem. Res.* **2019**, *58*, 7886.

[330] Z. Zhang, Q. Wang, H. Chen, X. Zhang, *Catalysts* **2017**, *7*, 281.

[331] "*BEA: Framework Type," can be found under https://europe.iza-structure.org/IZA-SC/framework.php?STC=BEA, **n.d.**

[332] R. Zhao, Z. Zhao, S. Li, A.-N. Parvulescu, U. Müller, W. Zhang, *ChemSusChem* **2018**, *11*, 3803.

[333] J. X. Liu, N. He, C. Y. Liu, G. R. Wang, Q. Xin, H. C. Guo, *RSC Adv.* **2018**, *8*, 9731.

[334] Y. Wang, R. Otomo, T. Tatsumi, T. Yokoi, *Catal. Surv. from Asia* **2016**, *20*, 1.

[335] N. Suárez, J. Pérez-Pariente, C. Márquez-Álvarez, M. Grande Casas, A. Mayoral, A. Moreno, Microporous Mesoporous Mater. 2019, 284, 296.

[336] J. Kowalska-Kuś, A. Held, K. Nowińska, *ChemCatChem* **2020**, *12*, 510.

[337] J. Li, H. Liu, T. An, Y. Yue, X. Bao, *RSC Adv.* **2017**, *7*, 33714.

[338] J. Li, H. Liu, F. Li, T. An, X. Bao, *Ind. Eng. Chem. Res.* **2018**, *57*, 10876.

[339] K. Leng, X. Li, G. Ye, Y. Du, Y. Sun, W. Xu, *Catal. Sci. Technol.* **2016**, *6*, 7615.

[340] Y. Jin, L. Zhang, J. Liu, S. Zhang, S. Sun, S. Asaoka, K. Fujimoto, Microporous Mesoporous Mater. 2017, 248, 7.

[341] L. R. M. Dos Santos, M. A. P. Da Silva, S. C. De Menezes, L. S. Chinelatto, Y. L. Lam, Microporous Mesoporous Mater. 2016, 226, 260.

[342] Y. M. Kim, J. Jeong, S. Ryu, H. W. Lee, J. S. Jung, M. Z. Siddiqui, S. C. Jung, J. K. Jeon, J. Jae, Y. K. Park, Energy Convers. Manag. 2019, 195, 727.

[343] K. Zhang, S. Fernandez, J. A. Lawrence, M. L. Ostraat, *ACS Omega* **2018**, *3*, 18935.

[344] M. H. M. Ahmed, O. Muraza, A. K. Jamil, E. N. Shafei, Z. H. Yamani, K.-H. Choi, *Energy & Fuels* **2017**, *31*, 5482.

[345] P. Lanzafame, S. Perathoner, G. Centi, E. Heracleous, E. F. Iliopoulou, K. S. Triantafyllidis, A. A. Lappas, *ChemCatChem* **2017**, *9*, 1632.

[346] A. R. Morgado Prates, T. Chetot, L. Burel, C. Pagis, R. Martinez-Franco, M. Dodin, D. Farrusseng, A. Tuel, J. Solid State Chem. 2020, 281, 121033.

[347] S. Fernandez, M. L. Ostraat, J. A. Lawrence, K. Zhang, *Microporous Mesoporous Mater.* **2018**, *263*, 201.

[348] Y. Bi, X. Lei, G. Xu, H. Chen, J. Hu, *Catalysts* **2018**, *8*, 82.

[349] A. Werner, P. Bludovsky, C. Selzer, U. Koch, L. Giebeler, S. Oswald, S. Kaskel, *ChemCatChem* **2017**, *9*, 3860.

[350] K. Zhang, S. Fernandez, S. Kobaslija, T. Pilyugina, J. O'Brien, J. A. Lawrence, M. L. Ostraat, *Ind. Eng. Chem. Res.* **2016**, *55*, 8567.

[351] Y.-S. Kim, K.-S. Cho, Y.-K. Lee, *Catalysts* **2020**, *10*, 47.

[352] M. A. Sanhoob, U. Khalil, E. N. Shafei, K. H. Choi, T. Yokoi, O. Muraza, Fuel 2020, 263, 116624.

[353] H. Sammoury, J. Toufaily, K. Cherry, T. Hamieh, Y. Pouilloux, L. Pinard, Appl. Catal. A Gen. 2018, 551, 1.

[354] H. Sammoury, J. Toufaily, K. Cherry, T. Hamieh, Y. Pouilloux, L. Pinard, Appl. Catal. A Gen. 2018, 551, 1.

[355] N. Suárez, J. Pérez-Pariente, F. Mondragón, A. Moreno, *Microporous Mesoporous Mater.* **2019**, *280*, 144.

[356] N. Suárez, M. A. Arribas, A. Moreno, A. Martínez, Catal. Sci. Technol. 2020, 10, 1073.

[357] D. H. Morawala, A. K. Dalai, K. C. Maheria, Catal. Letters 2019, 150, 1049.

[358] E. Dib, H. El Siblani, S. M. Kunjir, A. Vicente, N. Nuttens, D. Verboekend, B. F. Sels, C. Fernandez, *Cryst. Growth Des.* **2018**, *18*, 2010.

[359] K. Zhang, S. Fernandez, J. T. O'Brien, T. Pilyugina, S. Kobaslija, M. L. Ostraat, *Catal. Today* **2018**, *316*, 26.

[360] J. M. Escola, D. P. Serrano, R. Sanz, R. A. Garcia, A. Peral, I. Moreno, M. Linares, *Catal. Today* **2018**, *304*, 89.

[361] H. J. Cho, N. S. Gould, V. Vattipalli, S. Sabnis, W. Chaikittisilp, T. Okubo, B. Xu, W. Fan, Microporous Mesoporous Mater. 2019, 278, 387.

[362] V. P. S. Caldeira, A. Peral, M. Linares, A. S. Araujo, R. A. Garcia-Muñoz, D. P. Serrano, *Appl. Catal. A Gen.* **2017**, *531*, 187.

[363] K. Zheng, B. Liu, J. Huang, K. Zhang, F. Li, H. Xi, Inorg. Chem. Commun. 2019, 107,107468.

[364] D. Zhao, Y. Wang, W. Chu, X. Wang, X. Zhu, X. Li, S. Xie, H. Wang, S. Liu, L. Xu, *J. Mater. Chem. A* **2019**, *7*, 10795.

[365] J. Zhang, L. Wang, G. Wang, F. Chen, J. Zhu, C. Wang, C. Bian, S. Pan, F.-S. Xiao, *ACS Sustain. Chem. Eng.* **2017**, *5*, 3123.

[366] S. Wang, B. He, R. Tian, C. Sun, R. Dai, X. Li, X. Wu, X. An, X. Xie, Mol. Catal. 2018, 453, 64.

[367] K. Zhang, Z. Liu, M. Wang, X. Yan, C. Li, H. Xi, *New J. Chem.* **2017**, *41*, 3950.

[368] S. Wang, Z. Zheng, B. He, C. Sun, X. Li, X. Wu, X. An, X. Xie, *Appl. Organomet. Chem.* **2018**, *32*, e4145.

[369] M. Castro, P. Losch, W. Park, M. Haouas, F. Taulelle, C. Loerbroks, G. Brabants, E. Breynaert, C. E. A. Kirschhock, R. Ryoo, W. Schmidt, *Chem. Mater.* **2018**, *30*, 2676.

[370] S. Soltanali, J. T. Darian, *Microporous Mesoporous Mater.* **2019**, 286, 169.

[371] L. Yu, P. Han, H. Jin, H. Wei, W. Liu, L. Ma, C. Xu, *Process Saf. Environ. Prot.* **2019**, 129, 63

[372] X. Zhao, L. Wang, P. Guo, N. Yan, T. Sun, S. Lin, X. Guo, P. Tian, Z. Liu, *Catal. Sci. Technol.* **2018**, *8*, 2966.

[373] Y. Yue, X. Guo, T. Liu, H. Liu, T. Wang, P. Yuan, H. Zhu, Z. Bai, X. Bao, *Microporous Mesoporous Mater.* **2019**, 293, 109772

[374] G. Xiong, M. Feng, J. Liu, Q. Meng, L. Liu, H. Guo, *RSC Adv.* **2019**, *9*, 3653.

[375] G. Huang, P. Ji, H. Xu, J. G. Jiang, L. Chen, P. Wu, *Microporous Mesoporous Mater.* **2017**, *248*, 30.

[376] Y. Luo, M. Li, X. Lv, Q. Huang, X. Chen, *Microporous Mesoporous Mater.* **2019**, 293, 109675

[377] K. Zhang, Z. Liu, X. Yan, X. Hao, M. Wang, C. Li, H. Xi, *Langmuir* **2017**, *33*, 14396.

[378] F. Z. Chaida-Chenni, F. Belhadj, M. S. Grande Casas, C. Márquez-Álvarez, R. Hamacha, A. Bengueddach, J. Pérez-Pariente, *Appl. Catal. A Gen.* **2018**, DOI 10.1016/j.apcata.2018.10.005.

[379] M. Al-Eid, L. Ding, Q. Saleem, H. Badairy, H. Sitepu, A. Al-Malki, *Microporous Mesoporous Mater.* **2019**, *279*, 99.

[380] T. W. Kim, S. Y. Kim, J. C. Kim, Y. Kim, R. Ryoo, C. U. Kim, *Appl. Catal. B Environ.* **2016**, *185*, 100.

[381] H. S. Shin, M. Opanasenko, C. P. Cabello, R. Ryoo, J. Čejka, *Appl. Catal. A Gen.* **2017**, 537, 24

[382] L. El Hanache, B. Lebeau, H. Nouali, J. Toufaily, T. Hamieh, T. J. Daou, *J. Hazard. Mater.* **2019**, 364, 206.

[383] O. Veselý, M. Shamzhy, M. Mazur, P. Eliášová, *Catal. Today* **2019**, 345, 97

[384] R. Bai, Y. Song, Y. Li, J. Yu, *Trends Chem.* **2019**, *1*, 601.

[385] W. Schwieger, A. G. Machoke, T. Weissenberger, A. Inayat, T. Selvam, M. Klumpp, A. Inayat, *Chem. Soc. Rev.* **2016**, *45*, 3353.

[386] N. Rai, S. Caratzoulas, D. G. Vlachos, *ACS Catal.* **2013**, *3*, 2294.

[387] J. Grand, S. N. Talapaneni, A. Vicente, C. Fernandez, E. Dib, H. A. Aleksandrov, G. N. Vayssilov, R. Retoux, P. Boullay, J. P. Gilson, V. Valtchev, S. Mintova, *Nat. Mater.* **2017**, *16*, 1010.

[388] Y. Fang, H. Hu, *J. Am. Chem. Soc.* **2006**, *128*, 10636.

[389] S. Wang, P. Bai, M. Sun, W. Liu, D. Li, W. Wu, W. Yan, J. Shang, J. Yu, *Adv. Sci.* **2019**, *6*, 1901317.

[390]   T. M. Davis, M. A. Snyder, J. E. Krohn, M. Tsapatsis, *Chem. Mater.*
         2006, *18*, 5814.

[391]   M. S. Taylor, E. N. Jacobsen, *J. Am. Chem. Soc.* **2003**, *125*, 11204.

[392]   J. K. Myers, E. N. Jacobsen, *J. Chem. Soc., Perkin Trans. 1* **1998**,
         120, 8959.

[393]   M. M. Pereira, E. S. Gomes, A. V. Silva, A. B. Pinar, M. G. Willinger,
         S. Shanmugam, C. Chizallet, G. Laugel, P. Losch, B. Louis, *Chem.
         Sci.* **2018**, *9*, 6532.

[394]   X. Qian, J. Du, B. Li, M. Si, Y. Yang, Y. Hu, G. Niu, Y. Zhang, H. Xu,
         B. Tu, Y. Tang, D. Zhao, *Chem. Sci.* **2011**, *2*, 2006.

[395]   H. Peng, L. Xu, H. Wu, Z. Wang, Y. Liu, X. Li, M. He, P. Wu,
         Microporous Mesoporous Mater. **2012**, *153*, 8.

[396]   M. Enterría, F. Suárez-García, A. Martínez-Alonso, J. M. D. Tascón,
         Microporous Mesoporous Mater. **2014**, *190*, 156.

[397]   X. Qian, R. Che, A. M. Asiri, X. F. Qian, B. Li, Y. Y. Hu, G. X. Niu,]
         D Yahong, H. Zhang, R. C. Che, Y. Tang, D. S. Su, D. Y. Zhao,
         Chem. Eur. J. **2012**, *18*, 931.

[398]   J. Liu, H. Lin, Y. He, Y. Dong, E. Rose, G. Y. Menzembere, *J.
         Clean. Prod.* **2020**, *260*, 121047.

[399]   B. Han, A. Chakraborty, *Microporous Mesoporous Mater.* **2019**, *288*,
         109590.

[400]   Q. Al-Naddaf, H. Thakkar, F. Rezaei, *ACS Appl. Mater. Interfaces*
         2018, *10*, 29656.

[401]   T. Qiu, L. Wang, S. Lv, B. Sun, Y. Zhang, Z. Liu, W. Yang, J. Li,
         Fuel **2017**, *203*, 811.

[402]   Z. Di, T. Zhao, X. Feng, M. Luo, *Catal. Letters* **2019**, *149*, 441.

Entry for the Table of Contents

This review presents a practical overview of the most recent literature on synthesis of hierarchical zeolites for most relevant (10- and 12-membered ring) zeolite topologies. Several fine tuning efforts of established and novel synthesis methods are discussed. The review ends with remaining challenges and points of attention and our personal view for future synthesis research to obtain the most sustainable and catalytically active hierarchical zeolites.

Supporting Information

Synthesis of Hierarchical Zeolites for Industrial Applications: a Critical Review

Dorien Kerstens, Brent Smeyers, Jonathan Van Waeyenberg, Qiang Zhang, Jihong Yu and Bert F. Sels*

Table S1. Supporting information for the TON scatter plot

Reference	Type of method	$V_{meso} (V_{micro}+V_{meso})^{-1}$ [a]	Relative acidity[b]	Catalyst code	Catalytic testing
[13]	Top-down	0.93	1.59	FT2-1	Steam assisted catalytic cracking of *n*-hexane
[38]	Top-down	0.74	0.73	430 ATC	Hydroisomerization of *n*-dodecane
[39]	Top-down	0.84	0.83	P1	MTO
[40]	Top-down	0.72	1.19	c-ZSM-22-ats1-HCl	-
[43]	Top-down	0.96	0.92	H-ZSM-22-0.5	Hydroisomerization of *n*-hexane

[a] Data corresponds to the synthesized hierarchical zeolite
[b] Relative acidity is defined as (Acidity$_{hierarchical zeolite}$ acidity$^{-1}_{parent zeolite}$) wherein the acidity represents the total acidity of the zeolite (Brønsted + Lewis)

Table S2. Supporting information for the FER scatter plot

Reference	Type of method	$V_{meso} (V_{micro}+V_{meso})^{-1}$ [a]	Relative acidity[b]	Catalyst code	Catalytic testing
[47]	Top-down	0.69	1.17	FER/9/P	Dehydration of ethanol
[47]	Top-down	0.67	1.56	FER/23/P	Dehydration of ethanol
[48]	Nano	0.83	0.89	N-FER(15)-120	Oligomerization of 1-pentene
[51]	Top-down	0.59	0.96	D1	Dehydration of methanol
[53]	Bottom-up	0.76	0.75	FER-0.15	Dehydration–isomerization of 1-butanol
[54]	Bottom-up	0.68	1.04	FER-0.05	Isomerization of fatty acids
[55]	Nano	0.7	1.2	S1	Isomerization of 1-butene
[56]	Nano	0.69	1.5	S2	Isomerization of 1-butene

[a] Data corresponds to the synthesized hierarchical zeolite
[b] Relative acidity is defined as (Acidity$_{hierarchical zeolite}$ acidity$^{-1}_{parent zeolite}$) wherein the acidity represents the total acidity of the zeolite (Brønsted + Lewis)

Table S3. Supporting information for the MFI scatter plot

Reference	Type of method	$V_{meso} (V_{micro}+V_{meso})^{-1}$ [a]	Relative acidity[b]	Catalyst code	Catalytic testing
[62]	Top-down	0.76	0.68	3 h 450 °C/0.3M NaOH/HZSM-5	Glycerol-to-aromatics (GTA)
[63]	Top-down	0.74	0.62	SAZ0.2	MTA
[65]	Top-down	0.74	0.55	HZ-F6-AT	MTP
[70]	Top-down	0.8	0.76	NZ5-0.5	MTH
[71]	Top-down	0.76	1.41	ZSM-5-CT	Friedel-Crafts acylation of anisole and propionic anhydride to *p*-methoxypropiophenone
[72]	Top-down	0.35	1.04	Z5-ACE	Cracking of *n*-heptane
[73]	Top-down	0.56	1.01	UAT-20	Cracking of light naphtha
[74]	Top-down	0.21	0.98	ZSM-5/NH3·H2O	MTA
[75]	Top-down	0.61	1.25	ATHZ5-Cs	Oligomerization of butene
[76]	Top-down	0.46	0.78	DeSi-NaAlO2-TPA0.4-AW	MTP
[79]	Top-down	0.84	1.42	MH-Z5	MTG
[81]	Top-down	0.69	0.61	hZSM-5	Hydrodeoxygenation of guaiacol to cycloalkanes
[82]	Top-down	0.76	1.06	ZSM-5-120(2h)-160(24h)	self-etherification of benzyl alcohol
[83]	Top-down	0.57	0.91	ZSM-5-P-0.1-6	Cracking of n-octane and cumene
[84]	Top-down	0.75	1.59	HS900-30	MTH
[88]	Top-down	0.52	1.01	T-16 h	MTP
[89]	Top-down	0.82	0.95	DRZ-Opt	MTP
[95]	Bottom-up	0.65	0.79	MFI(C16MP, DEA)	MTH
[98]	Bottom-up	0.73	0.77	ZSM-5/0.7D/T	MTG
[100]	Bottom-up	0.5	0.83	CTAOH-ZSM-5	MTH
[103]	Bottom-up	0.58	1.06	(CNT) HZSM-5	MTA
[108]	Bottom-up	0.66	1.03	NK-Z5	MTA
[110]	Bottom-up	0.49	0.81	HP-ZSM-5-140	Chloromethane to light-olefins
[113]	Bottom-up	0.63	1.1	S-NZ5-5	MTA
[119]	Bottom-up	0.69	1.55	IHS	MTA
[122]	Bottom-up	0.52	0.52	ZSM-5(S)	MTG

[124]	Bottom-up	0.57	1.81	ZSM-5-T3	MTP
[125]	Bottom-up	0.69	0.69	ZSM-ST	Catalytic pyrolysis of biomass
[145]	Bottom-up	0.79	1	h-ZSM-5(Carbon-B)	Dehydration of ethanol, benzylation of substituted aromatics with benzyl alcohol
[147]	Bottom-up	0.72	0.62	CoCNT(10–20)/ZSM-5	Fischer-Tropsch
[148]	Bottom-up	0.72	1.29	GaCNT-HZ	MTA
[150]	Bottom-up	0.43	1.06	ZSM-5/GO	MTO
[151]	Bottom-up	0.66	1.08	SAC-20	Cracking of *n*-decane
[158]	Bottom-up	0.59	0.71	MesoZSM	Esterification of benzyl alcohol with hexanoic acid
[168]	Bottom-up	0.52	1.14	HP-ZSM-5	Dehydration of glycerol to acrolein
[169]	Bottom-up	0.58	1.09	Z5-us-60	MTP
[175]	Bottom-up	0.5	0.58	ZSM-Al	Benzylation of mesitylene with benzyl alcohol
[189]	Bottom-up	0.77	0.62	ZSM-5-4C	MTG
[190]	Bottom-up	0.62	1.69	HZ5-423 K-5d-3C	Alkylation of toluene with methanol
[191]	Bottom-up	0.65	1.05	S-ZSM-5-0.19	MTP
[192]	Bottom-up	0.74	0.92	N-ZSM-5	MTP
[196]	Bottom-up	0.61	0.94	Z5-0.1C	MTP
[200]	Bottom-up	0.85	1.33	Hier-ZSM-5-10%	Dehydration of glycerol to acrolein
[201]	Bottom-up	0.59	0.87	HZA-40-1.5-H	Cracking of low density polyethylene
[206]	Bottom-up	0.83	0.94	MZ-4	MTP
[207]	Bottom-up	0.48	1.12	NSHZ	MTA
[213]	Bottom-up	0.73	1.41	Sample 18	-
[214]	Bottom-up	0.65	0.67	AHN-0.008	MTG
[217]	Bottom-up	0.72	0.78	NA-2	MTP
[222]	Bottom-up	0.79	0.13	ZSM-5-0.065	MTG
[224]	Bottom-up	0.64	0.75	HZSM-5/1	Alkylation of mesitylene with benzyl alcohol
[228]	Bottom-up	0.56	0.98	MLMFI	Aldol condensation of benzaldehyde.
[232]	Bottom-up	0.61	1.1	BLZ5_30	MTP
[235]	Bottom-up	0.8	0.96	DZN-2	Cracking of *n*-decane

[237]	Bottom-up	0.65	0.89	ZF	Ethanol-to-hydrocarbons (ETH)
[241]	Bottom-up	0.88	0.39	MFI-UL-100	Etherification of glycerol with *tert*-butyl alcohol
[244]	Bottom-up	0.41	1.04	NZSM-5	Cracking of isopropylbenzene and *n*-octane
[248]	Bottom-up	0.91	1.12	Z100-2	MTH

[a] Data corresponds to the synthesized hierarchical zeolite
[b] Relative acidity is defined as (Acidity$_{hierarchical\ zeolite}$ acidity$^{-1}_{parent\ zeolite}$) wherein the acidity represents the total acidity of the zeolite (Brønsted + Lewis)
MTH, MTG, MTP, MTA stands for methanol-to-hydrocarbons, gasoline, propylene, aromatics, respectively.

Table S4. Supporting information for the MOR scatter plot

Reference	Type of method	$V_{meso} (V_{micro}+V_{meso})^{-1}$ [a]	Relative acidity[b]	Catalyst code	Catalytic testing
[252]	Top-down	0.4	0.87	Mordenite_40	Isomerization of *n*-pentane, *n*-hexane and light naphtha
[254]	Top-down	0.48	0.74	ZK-3M-6h (C)	Dimethyl ether to olefins
[257]	Top-down	0.03	1.07	H-MOR 15.4	Carbonylation of dimethyl ether
[260]	Top-down	0.43	0.77	PyF$_{0,50}$	Toluene disproportionation, cracking of *n*-hexane
[261]	Top-down	0.62	0.45	HMORm-0,9N	Hydroisomerisation of benzene-heptane mixture
[262]	Top-down	0.48	0.73	deAl-mm-MOR/9.5	Hydroisomerization of *n*-hexane
[263]	Top-down	0.44	0.24	HM(13)-al(0.05)-ac(4 h)	*Tert*-butylation of naphthalene with tertiary butanol
[264]	Top-down	0.55	0.58	MOR-al(0.4/85)ac	*m*-xylene transformation
[266]	Top-down	0.88	0.65	D$_{0,6}$ P$_{8250}$	Cracking of *n*-hexane, transformation of propene
[267]	Top-down	0.49	3.06	10%V2O5/deAlmm-H-MOR	Direct oxidation of dimethyl ether
[270]	Top-down	0.96	0.63	RM-3	Isobutylene production from acetone
[271]	Bottom-up	0.51	0.8	MORC-7.4	catalytic cracking of *n*-heptane
[272]	Bottom-up	0.72	1.14	HMOR- 0.2NBA	Carbonylation of dimethyl ether
[277]	Nano	0.16	0.86	PEG6000	Carbonylation of dimethyl ether
[280]	Nano	0.57	0.92	NaMOR-meso (60)	Hydroizomerization of benzene-*n*-heptane mixture

[a] Data corresponds to the synthesized hierarchical zeolite
[b] Relative acidity is defined as (Acidity$_{hierarchical zeolite}$ acidity$^{-1}_{parent zeolite}$) wherein the acidity represents the total acidity of the zeolite (Brønsted + Lewis)

Table S5. Supporting information for the FAU scatter plot

Reference	Type of method	$V_{meso} (V_{micro}+V_{meso})^{-1}$ [a]	Relative acidity[b]	Catalyst code	Catalytic testing
[288]	Bottom-up	0.47	0.43	ZH-X	Vapor phase tertiary butylation of phenol
[297]	Top-down	0.97	0.33	MZM-MW-1m-100	Catalytic dealkylation of 1,3,5-triisopropylbenzene. Catalytic aldol condensation of benzaldehyde with 1-heptanal
[298]	Top-down	0.61	0.69	AT-Y (H)-550	Catalytic cracking of 1,3,5-triisopropylbenzene (TIPB) and heavy oil
[299]	Top-down	0.21	1.23	NaY$_{0,2}$	Isomerization of glucose
[300]	Top-down	0.13	1.06	UAY-60	Catalytic cracking of middle distillate cut
[301]	Top-down	0.43	1.06	EAY-0.1-6h-S	Catalytic cracking of n-octane
[304]	Top-down	0.57	0.86	MY-1	Dealkylation of 1,3,5-triisopropylbenzene (TIPB)
[305]	Bottom-up	0.72	0.93	MY-0.5C-0.35T-2.4B	Adsorption of dibenzothiophene (DBT) and 4,6-dimethyldibenzothiophene (4,6-DMDBT)
[307]	Top-down	0.47	0.68	DeY-At-TPOACl	Catalytic cracking of 1,3,5-triisopropylbenzene (TIPB)
[310]	Bottom-up	0.52	0.6	TY2	Catalytic upgrading of coal pyrolysis gaseous tar
[311]	Bottom-up	0.35	0.88	HY-mmm(60)	Synthesis of 3,5-dimethylpyridine
[313]	Nano	0.55	0.77	YSA-13	Precracking of bulky reactant molecules
[316]	Top-down	0.42	1.1	USY$_B$	Cracking of iso-octane and 1,3,5-triisopropylbenzene (TIPB)
[318]	Top-down	0.37	0.75	Sn-Y-1	Baeyer-Villiger oxidation
[321]	Top-down	0.84	0.63	YB0.08-S0.1	-
[322]	Top-down	0.81	1.28	NaOH/TBAOH	Isomerization of α-pinene
[323]	Top-down	0.82	1.28	10%	Isomerization of α-pinene
[324]	Top-down	0.82	0.91	0.05 M NH$_3$	Isomerization of α-pinene
[329]	Top-down	0.67	1.27	USY-F-AT	Hydrocracking of naphthalene
[330]	Top-Down	0.49	0.09	8AHFS-Y	Hydroconversion of waste cooking oil

[a] Data corresponds to the synthesized hierarchical zeolite
[b] Relative acidity is defined as (Acidity$_{hierarchical\ zeolite}$ acidity$^{-1}_{parent\ zeolite}$) wherein the acidity represents the total acidity of the zeolite (Brønsted + Lewis)

Table S6. Supporting information for the *BEA scatter plot

Reference	Type of method	$V_{meso} (V_{micro}+V_{meso})^{-1}$ [a]	Relative acidity[b]	Catalyst code	Catalytic testing
[335]	Top-down	0.61	0.8	5-0.5-BC	Isomerization-disproportionation of m-xylene
[336]	Top-down	0.84	0.81	H-Beta(H)	Ketalization of glycerol with acetone
[337]	Top-down	0.46	0.74	M-Beta	Esterification of carboxylic acids
[338]	Top-down	0.54	0.47	O−F(2.0)-Beta	Esterification of sec-butanol with acetic acid
[340]	Top-down	0.83	0.79	MHB-1	Benzene alkylation with 1-dodecene
[344]	Top-down	0.59	4.33	0.2Ni-0.2Co-Dsi-BEA	Steam catalytic cracking of n-dodecane
[345]	Top-down	0.92	1.2	Des H-Beta	Hydroisomerisation and hydrocracking of n-hexadecane
[351]	Top-down	0.84	1.36	Ni2P/DS-β	Hydrocracking of pyrolysis fuel oil into benzene, toluene, and xylene (BTX)
[352]	Top-down	0.43	0.63	DT4-DeAl1	Steam cracking of green diesel (C_{12}) to BTX and olefins
[353]	Top-down	0.77	1.07	D3	Hydroisomerization of n-decane
[355]	Top-down	0.51	1.14	B-NH-6	Isomerization-disproportionation of m-xylene
[357]	Top-down	0.72	0.99	MCRK	Synthesis of n-butyl levulinate
[362]	Bottom-up	0.51	0.94	h-Beta (PHAPTMS)	Catalytic cracking of high density polyethylene
[363]	Bottom-up	0.64	1.4	HHM-Beta (120 h)	Benzylation of benzyl alcohol with mesitylene
[378]	Bottom-up	0.86	0.3	H-βNPs(24 h)-DHM	Isomerization-disproportionation of m-xylene
[379]	Bottom-up	0.89	5.55	MN-11	-
[381]	Nano	0.86	0.87	N-BEA*-110	Tetrahydropyranylation of alcohols
[383]	Nano	0.95	0.83	nsBeta	Pechmann condensation

[a] Data corresponds to the synthesized hierarchical zeolite
[b] Relative acidity is defined as (Acidity$_{hierarchical\ zeolite}$ acidity$^{-1}_{parent\ zeolite}$) wherein the acidity represents the total acidity of the zeolite (Brønsted + Lewis)